Carolina Velhinho Pereira

Degree in Biomedical Science in Histocellular Pathology

Effect of Citrus Bioactive Compounds on Targeting Human Colorectal Cancer Stem Cells

Dissertation to obtain master degree in
Biotechnology

Supervisor: Ana Teresa Serra, PhD, iBET/ITQB-UNL
Co-supervisor: Cristina Albuquerque, Senior Investigator, IPOLFG

Jury
President: Professor Doutor Pedro Miguel Ribeiro Viana Baptista
Arguer: Doutora Maria Luisa Mourato de Oliveira Marques Serralheiro
Supervisor: Doutora Ana Teresa de Carvalho Negrão Serra

FACULDADE DE CIÊNCIAS E TECNOLOGIA
UNIVERSIDADE NOVA DE LISBOA

September 2016

Carolina Velhinho Pereira

Degree in Biomedical Science in Histocellular Pathology

Effect of Citrus Bioactive Compounds on Targeting Human Colorectal Cancer Stem Cells

Dissertation to obtain master degree in
Biotechnology

Supervisor: Ana Teresa Serra, PhD, iBET/ITQB-UNL
Co-supervisor: Cristina Albuquerque, Senior Investigator, IPOLFG

Jury
President: Professor Doutor Pedro Miguel Ribeiro Viana Baptista
Arguer: Doutora Maria Luisa Mourato de Oliveira Marques Serralheiro
Supervisor: Doutora Ana Teresa de Carvalho Negrão Serra

FACULDADE DE CIÊNCIAS E TECNOLOGIA
UNIVERSIDADE NOVA DE LISBOA

September 2016

“Copyright”

Effect of Citrus Bioactive Compounds on Targeting Human Colorectal Cancer Stem Cells

Carolina Velhinho Pereira, FCT/UNL e UNL

Acknowledgments

Gostaria de expressar o maior agradecimento a todas as pessoas que contribuíram direta e indiretamente para a realização deste trabalho.

Primeiramente, quero agradecer à Dra. Teresa Serra e Dra. Cristina Albuquerque por logo na entrevista terem confiado que seria a pessoal ideal para integrar este projeto. Agradeço por ao longo de todo o período me terem orientado, aconselhado e transmitido novos conhecimentos nas mais diversas áreas. Importante também será agradecer a paciência inesgotável para me ajudarem a esclarecer as minhas "dúvidas laboratoriais". Obrigada por ao longo deste ano me terem ajudado a crescer profissionalmente e por me fazerem acreditar que um dia poderei ser uma boa investigadora!

À Dra. Catarina Duarte agradeço a oportunidade de permitir desenvolver o meu trabalho no grupo de Nutracêuticos e Libertação Controlada. Aos membros desde grupo: Joana Poejo, Maria João Pereira, Ana Nunes e Vanessa Gonçalves agradeço toda a ajuda, comentários e sugestões que deram. Ao Agostinho Alexandre e ao Luís Martins agradeço especialmente o divertimento na tentativa de causar inveja com a caça de Pokemóns durante o verão que trabalhei para a tese e não para o bronze e sem não esquecer o apoio que prestaram na preparação dos extractos de laranja. À Inês Silva, agradeço todo o conhecimento da cultura 3D que me transmitiu.

Tenho um agradecimento especial à Marlene Duarte e Patrícia Silva por todo o apoio, paciência, ensinamentos e ajuda ao longo da minha curta estadia do IPOLFG.

Agradeço às minhas colegas de tese, por todo o apoio e ajuda que proporcionaram nos momentos mais difíceis. Obrigada Lucília, Ana e Anyse! Especialmente, obrigada Joana pela ajuda incondicional nas mais diversas áreas, pois sem ti tudo teria sido mais difícil! Obrigada por todos os momentos engraçados que aliviaram toda a pressão.

À minha mãe, pai e mano agradeço todo o apoio e confiança que tiveram nas minhas decisões e por me ajudarem a construir um futuro que espero que seja promissor.

Kika, agradeço os instantes que me aliviaram nas fases mais difíceis. Obrigada por tudo!

Ao André, agradeço todos os momentos de companheirismo, ajuda, compreensão. Acima de tudo, agradeço pela paciência em ouvir as minhas angústias e por ter sempre acreditado em mim.

Abstract

Recently, there has been an increase in the interest of the application of natural extract for cancer prevention and treatment, where phenolic compounds are associated with a high effectiveness in prevention and treatment of the disease. One of the promising targets for cancer therapy is the cancer stem cells population, which has been recognized as responsible for tumor initiating, relapse and chemo-resistance.

The main goal of this thesis was to evaluate the chemotherapeutical potential of polymethoxylated flavones (PMFs) from orange peel extracts, using HT29 3D colorectal cancer model. This model was characterized in terms of stemness and self-renewal properties.

HT29 cell spheroids were characterized along the culture time showing resemblances to the *in vivo* tumors, reflecting highly rich stem population where high expression of *CD44*, *CD133* and ALDH1 biomarkers was associated to high self-renewal capacity. Moreover, this model showed partial EMT characteristics.

Orange peel extract showed anticancer potential in HT29 cell aggregates by inhibiting cell proliferation and inducing cell cycle arrest and apoptosis. Self-renewal ability was also affected with association to decreasing of the expression of stemness markers. The bioactive molecules in the extract were identified as nobiletin, sinensetin, tangeretin and scutellarein tetramethylether. Among all PMFs, tangeretin exhibited the highest capability in affecting self-renewal, inducing apoptosis and cell cycle arrest and reducing the expression of mesenchymal and stemness markers. The mixture of PMFs showed similarities with the activity of orange extract although in a less effective way, suggesting the presence of other compounds that might potentiate the effect. Additionally, orange peel extract showed to interact synergistically with 5-fluorouracil decreasing the drug dosage to inhibit HT29 cell spheroids proliferation.

Results of this thesis revealed that orange bioactive compounds, including PMFs, are able to target cancer cells with stemness and self-renewal characteristics and thus can be considered as promising natural chemotherapeutic agents for colorectal cancer treatment.

Keywords

Colorectal cancer; Cancer stem cells; Phytochemicals; Polymethoxylated flavones; Orange peel extracts; 3D cell models

Resumo

Recentemente tem surgido um crescente interesse na prevenção e tratamento do cancro através da aplicação de compostos naturais. Nomeadamente, os compostos fenólicos têm demonstrado uma elevada eficácia nestas áreas. Um dos alvos mais promissores na terapia do cancro são as células estaminais cancerígenas, sendo esta população reconhecida como responsável pelo início, recorrência e quimio-resistência dos tumores.

O objectivo deste trabalho consistiu em avaliar o potencial quimio-terapêutico das flavonas polimetoxiladas (PMFs) presentes em extractos de casca de laranja através de um modelo 3D do cancro colorectal (HT29). Este modelo foi caracterizado a nível do carácter estaminal e capacidade de autorrenovação.

O modelo celular 3D (HT29) foi caracterizado ao longo do tempo de cultura mostrando semelhanças com os tumores *in vivo*, tendo uma população rica em características estaminais. A elevada expressão dos biomarcadores estaminais CD44, CD133 e ALDH mostrou ter associação com uma elevada capacidade de autorrenovação. Ainda, este modelo mostrou características de uma transição epitelial-mesenquimal (EMT) parcial.

O extrato de casca de laranja mostrou ter potencial anticancerígeno nos agregados HT29 através da inibição da proliferação celular e indução da apoptose e paragem do ciclo celular. A capacidade de autorrenovação dos agregados HT29 foi afectada em associação com a diminuição da expressão de biomarcadores estaminais. As moléculas bioativas identificadas no extracto foram: nobiletina, sinensetina, tangeretina e tetrametil-O-escutelareína. De todas as PMFs, a tangeretina foi o composto que exibiu maior capacidade em influenciar a autorrenovação, induzir apoptose e paragem do ciclo celular e em reduzir a expressão de biomarcadores mesenquimais e estaminais. A mistura das PMFs mostrou atividade semelhante com a obtida com o extrato de laranja, embora não tão eficaz o que sugere a presença de outros compostos no extrato que poderão potenciar a atividade. Ainda, o extracto de casca de laranja mostrou interagir sinergicamente com a fármaco 5-fluorouracil, levando à diminuição da dosagem do fármaco para a inibição da proliferação dos agregados HT29.

Os resultados deste trabalho revelaram que os compostos bioativos presentes na laranja, incluindo PMFs, são capazes de exercer efeito em células cancerígenas com características estaminais e de autorrenovação podendo ser considerados como promissores agentes quimio-terapêuticos naturais para o tratamento do cancro colorectal.

Palavras-chave

Cancro colorectal; Células estaminais cancerígenas; Fitoquímicos; Flavonas polimetoxiladas; Extratos de casca de laranja; Modelos celulares em 3D

List of Contents

List of Figures

List of Tables

List of Abbreviations

Abbreviation	Full form
5-FU	5-fluorouracil
5HHMF	5-hydroxy-3,6,7,8,3′,4′-hexamethoxyflavone
5HPMF	5-hydroxy-6,7,8,3′,4′-pentamethoxyflavone
5HTMF	5-hydroxy-6,7,8,4´-tetramethoxyflavone
ALDH	Aldehyde dehydrogenase
APC	Adenomatous poliposis coli
Bcl-2	B-cell lymphoma 2
cDNA	Complementary deoxyribonucleic acid
CRC	Colorectal carcinoma
CSC	Cancer stem cell
COX-2	Cyclo-oxigenase 2
CK18	cytokeratin 18
DAD	Diode array detector
DCC	Deleted in colorectal cancer
DEPC	Diethylpyrocarbonate
DEAB	Diethylaminobenzaldehyde
DMSO	Dimethyl sulfoxide
DNA	Deoxyribonucleic acid
dNTP	Deoxynucleotide triphosphate
DTT	Dithiothreitol
EC50	Effective dose value
ECM	Extra cellular matrix
EGCG	Epigallocatechin gallate
EMT	Epythelial-mesenchymal transition
EPCAM	Epithelial cell adhesion molecule
FACS	Fluorescence activated cell sorting
FAP	Familiar adenomatous polyposis
FBS	Fetal bovine serum
GEMM	Genetically engineered mouse models
GSK3β	Glycogen synthase kinase three beta

HNPCC	Hereditary nonpolyposis colorectal cancer
LEF	Lymphoid enhancer factor
Lgr5	Leucine-rich-repeat-containing G-protein coupled receptor 5
LOH	Loss of heterozygosity
MAPK	Mitogen activated protein kinases
MCTS	Multicellular tumor spheroids
MMP-2	Metalloproteinase 2
mRNA	Messenger ribonucleic acid
N	Nobiletin
NSAIDS	Non-steroidal inflammatory drugs
OPE	Orange peel extract
PBS	Phosphate-buffered saline
PMF	Polymethoxylated flavones
PROM1	Prominin 1
RCCS	Rotary cell culture system
RNA	Ribonucleic acid
RPMI	Roswell Park Memorial Institute
RT-qPCR	Reverse transcriptase quantitative polymerase chain reaction
S	Sinensetin
Sc	Scutellarein tetramethylether
SFE	Supercritical fluid extraction
SGF	Simulated gastric fluid
SIF	Simulated intestinal fluid
T	Tangeretin
TCF	T-cell factor
TGF-β	Transforming growth factor beta
TNF	Tumor necrosis factor
TNM	Tumor-node-metastasis

1. Introduction

1.1. Colorectal Cancer

1.1.1. Epidemiology and etiology

Worldwide, cancer is the second leading cause of death in developed countries and the third in developing countries, resulting in 14.1 million new cases in 2012 [1].

According to *Ferlay et al.*, colorectal carcinoma (CRC) is the second foremost cause for cancer-related death in Europe, being the third most frequently diagnosed cancer in men (13.2% of all cancer cases) and the second in women (12.7% of all cancer cases) (Figure 1.1) [2], [3]. For the past 30 years, it has been registered an increase in incidence rate of CRC in Europe, North America, New Zealand and Australia and, a decrease in mortality rate specially in women [2], [4].

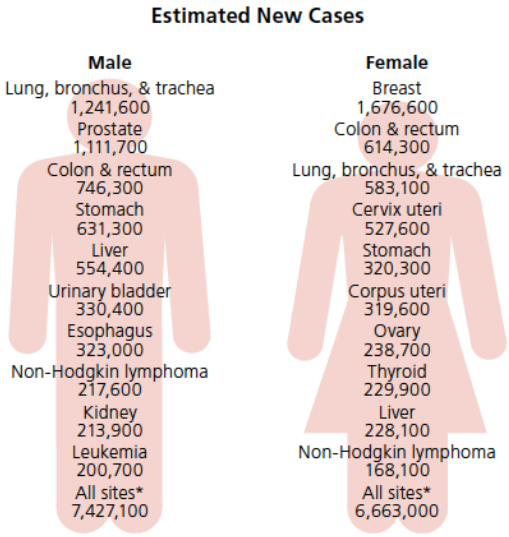

Figure 1.1 – Estimated new cancer cases worldwide in 2012 [1].

Colon cancer is a result of genetic predisposition and environmental factors consistent to developed countries lifestyle. In fact, it has been reported that a diet rich in red meat and saturated fat allied with low intake of fiber, calcium and vitamin D; obesity; sedentary lifestyle; and alcohol and tobacco consumption may lead to the development of this disease. Moreover, inflammatory diseases as Crohn's disease and ulcerative colitis increase the probability of CRC development [5], [6]. Regarding genetic predisposition, inherited CRC syndromes have been described and some are well characterized both at clinical and molecular features. The most frequent syndromes are familiar adenomatous polyposis (FAP) and hereditary nonpolyposis colorectal cancer (HNPCC), which account for 1% and 5% of all CRC cases, respectively [7]. FAP is characterized by the presence of hundreds of adenomatous polyps distributed throughout the colon and its genetic cause is a dominant autosomal mutation at *APC* gene. Lynch syndrome accounts for a subset of HNPCC and is characterized by germinal mutations in DNA mismatch repair genes (mainly *MLH1* and *MSH2*; rarely *MSH6* or *PMS2*). Another well-characterized hereditary CRC syndromes include Peutz-Jeghers

syndrome (*STK11*), juvenile polyposis (*SMAD4* and *BMPR1A*) and MUTYH-associated polyposis [7]–[9].

1.1.2. Location and characterization

Colon is a tubular organ with 1.5-1.8 m composed by 2 main portions: proximal (ascending and transverse colon) and distal (descending and sigmoid colon). It is connected to the anus through rectum [10]. Histologically, colon and rectum are constituted by: serosa (the thin out layer); *muscularis mucosae*, (responsible for the intestinal movements); submucosa (containing the nerves, blood vessels and connective tissue); and mucosa (closest to the lumen). The intestinal mucosa layer exhibits invaginations, known as crypts, which are comprised predominantly by differentiated cells (enterocytes, enteroendocrine cells and goblet cells) [11], [12]. In the bottom of the crypt is the stem cells niche, which are undifferentiated cells with self-renewal capacity and regulation of tissue repair and homeostasis. The division of these cells gives rise to progenitor cells that are capable of differentiating toward all epithelial lineages. Consequently, stem cells play a key role in regulating the maintenance of the normal colonic epithelium [12].

Colorectal carcinoma is characterized by the uncontrolled proliferation of epithelial tumor cells into the *muscularis mucosae* layer [9]. CRC development can be summarized in the adenoma-carcinoma sequence, first proposed by *Fearon et al.*. In this sequence, the normal colorectal epithelium accumulates various genetic and epigenetic mutations that result in progression to an early adenoma and latter, to an invasive carcinoma. This is a multistage slow process, which evolves in 5-10 years. (Figure 1.2) [13].

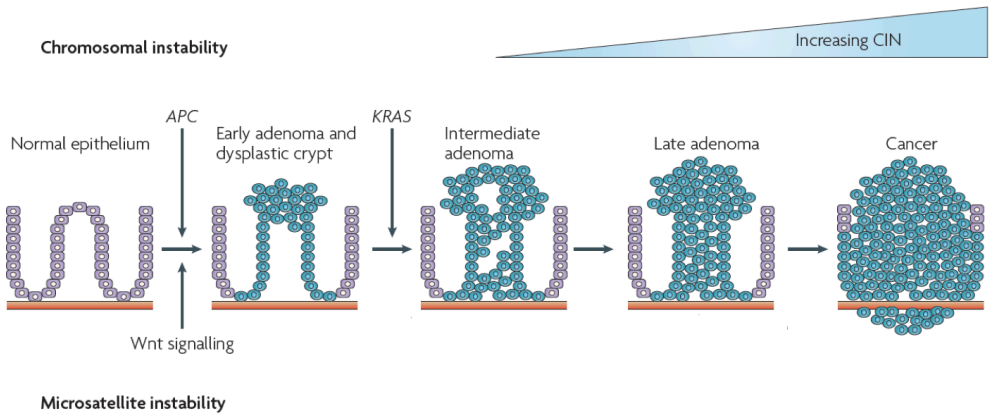

Figure 1.2 – The adenoma-carcinoma sequence: main histological and molecular alterations in each stage of sporadic colon cancer progression (adapted from [14]).

In early stage tumors, around 80% of sporadic CRC cases have loss of heterozygosity (LOH) or mutation in *APC* gene, which encodes a protein responsible for inducing degradation of β-catenin and, therefore, functions as a negative regulator of the Wnt signaling pathway. In *APC* mutated CRC cells,

β-catenin accumulates in the nucleus, activating transcription of oncogenes as c-myc and cyclin D1, and promoting cellular proliferation [8], [15]. In the progression of early to late adenoma, an activation of oncogene *KRAS* (promoting proliferation and avoiding apoptosis) occurs followed by inactivation of TGF-β pathway genes, such as *SMAD2*, *SMAD4* and the tumor suppressor *DCC* [16]. The next step in the transition from adenoma to carcinoma sequence, a bi-allelic inactivation of tumor suppressor *TP53* occurs [8], [16], [17].

1.1.3. Molecular pathways involved in carcinogenesis

Countless signaling pathways have been described to be involved in colon tumorigenesis and some of the genes involved in these pathways may be promising therapeutic targets [18]. The pathways referred in section 1.1.2 (Wnt, TFG-β, *RAS* and p53) are associated with an increased chromosomal instability characterized by LOH and chromosomal abnormalities [19]. The Wnt signaling pathway plays a key role in regulating the nuclear localization of β-catenin and maintaining the normal homeostasis in intestinal stem cells. When Wnt signaling is inactive (absence of Wnt ligand), the key effector, β-catenin is recruited by a protein complex (APC, AXIN and GSK3β) for ubiquitination and targeted for proteossomal degradation. By activating the pathway (either by presence of Wnt ligand, or mutation in the pathway genes), the protein complex cannot bind to β-catenin giving rise to a β-catenin cytoplasmic accumulation and migration into the nucleus. There, it will bind to TCF/LEF transcription factors, activating target genes transcription and increasing proliferation, differentiation, migration and adhesion of colonic cells [18], [19]. The alterations in the canonical Wnt signaling may occur in APC, AXIN2 and β-catenin proteins. In *APC* gene, molecular alterations resulting in functional loss or protein truncation drive constitutive activation of Wnt. *AXIN2* is a negative Wnt regulator and a tumor suppressor gene. This gene is frequently mutated in sporadic CRC, contributing to Wnt negative feedback and to the disruption of β-catenin destruction complex [17], [18], [20]. Furthermore, mutations in *CTNNB1* gene (encoding β-catenin) are known to block β-catenin ubiquitination and degradation. These mutations are found in approximately 48% of sporadic CRC without *APC* mutation, which suggests that mutations in *CTNNB1* may substitute APC mutations in early stage event of carcinogenesis [18], [19].

Alterations in other signaling pathways occur later in the development of CRC, namely during progression to malignant lesion, like *KRAS* mutations and *p53* loss of function (as described above). In addition, *p53* also regulates the expression of the cell cycle inhibitor *p21* [19], [21], [22].

1.1.4. Metastasizing process

The metastatic spread of tumor cells is composed of several steps where cells acquired biochemical characteristics that enable them to escape from a primary site tumor to other place in the human body where they can proliferate giving rise to a metastatic tumor [23], [24]. Figure 1.3 elucidates the molecular mechanisms that underlie the metastatic process.

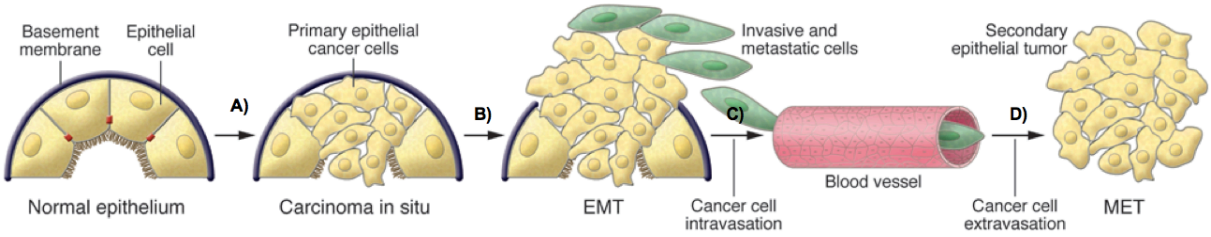

Figure 1.3 – Representative model of metastatic process: acquisition of genetic/epigenetic alterations (A); epithelial-mesenchymal transition (B); intravasation to vascular circulation(C); extravasation and mesenchymal-epithelial transition with angiogenesis originating a secondary tumor (D) (adapted from [23]).

Tumor cells can develop invasive and mesenchymal characteristics that facilitate tumor detachment and acquisition of a migratory capacity and plasticity. In the epithelial-to-mesenchymal transition (EMT) the capacity of cell-cell adhesion is lost, allowing tumor cells dissociation from the primary tumor and invasion of the surrounding extracellular matrix (ECM). EMT cells intravasate into the lumen of blood vessels invading the vascular basement membrane and extracellular matrix in the process of extravasation. Finally, these cells attach at a new location and re-initiate their proliferative programs at metastatic sites [23], [24]. In CRC, liver is the common site of metastasis, however the underlying cause of liver-specific metastasis of CRC is not yet well elucidated [24].

EMT is a biological process where the cell develops resistance to apoptosis, capacity to migrate and invade, and production of ECM components. In this process a polarized epithelial cell is transformed into a mesenchymal-like cell and, it is characterized by the degradation of the basement membrane where epithelial cells are attached. EMT is described as a transition phenomenon due to its reversibility – phenotypic plasticity allows mesenchymal cells conversion to epithelial. This is a normal process during embryogenesis and organ development (EMT type 1), although, it can be activated in the presence of inflammation (by wound healing and tissue repair – EMT type 2) and high-graded carcinomas (EMT type 3). In EMT type 3, tumor cells only progress once they can invade and metastasize, however, they may not lose all of the epithelial characteristics [23].

A variety of signaling factors regulate the metastatic process in different manners and they can be organized as described in the Table 1.1. Briefly, the changes in cell-cell adhesion is due to the loss of E-cadherin; nuclear β-catenin and the activation of other transcription factors like Snail and TCF/LEF change the apicobasal polarity and tissue architecture; moreover, in an advance stage of EMT with the expression of mesenchymal markers, there is a replacement of intermediate filament of the cell by Vimentin [25].

Table 1.1 – Classes of molecules involved in EMT [25].

Cell-cell adhesion	Cadherins, Catenins
Cell-ECM adhesion	Integrins, ECM proteins
Transcription factors	Snail, SMAD LEF, Nuclear β-catenin
Growth factors	TGF-β, Wnts
Extracellular proteases	Matrix metalloproteinases
Cytoskeletal modulators	Rho family

Wnt signaling pathway is involved not only in early stages but also in the invasive front of metastasis where the activation of Wnt signaling key effector, β-catenin, leads to the transcription of genes related to tumor aggressiveness, invasiveness, and migration [26]. Figure 1.4 shows the activation of genes responsible for i) cellular growth, ii) survival, dedifferentiation, migration and dissemination, iii) proteolysis and iv) stroma induction and angiogenesis, in response to Wnt activation [27].

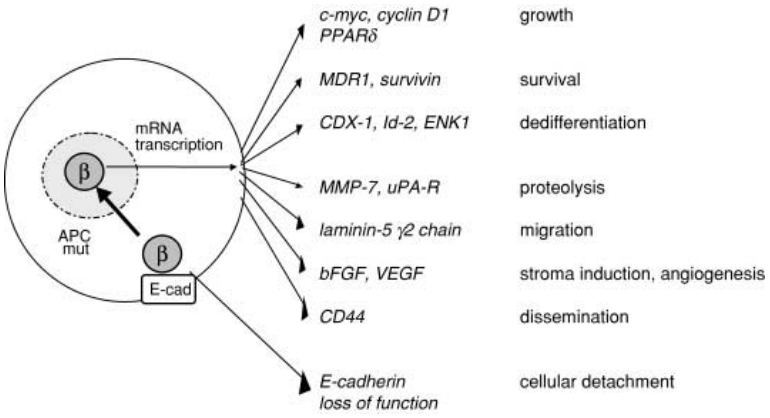

Figure 1.4 – Gene expression induced by nuclear translocation of β-catenin and its influence on the metastasizing process [27].

A crucial event in EMT is the loss of E-cadherin, the most important molecule for cell-cell adhesion, which is also regulated by β-catenin [26]. The expression of E-cadherin can be inhibited by inactivating mutations or transcriptional repression. For instance, Snail transcription factor, activated by *RAS* and TGF-β activated pathways [28], has been reported to repress E-cadherin transcription, being considered a EMT inducer [29]. In addition, Snail downregulates Muc-1 (epithelial mucin) and CK18 [28] and upregulates mesenchymal markers as Vimentin, fibronectin [30] and MMP-2 [31]. Another study also demonstrates the capacity of Snail to enhance invasive ability and immunosuppression accelerating EMT [32].

Nevertheless, loss of E-cadherin also correlates with tumor grade, and that does necessarily lead to EMT. The acquisition of a mesenchymal phenotype is also necessary [29]. However, it is important to mention that the metastasizing process is very complex and the majority of signaling pathways,

including TGF-β, Notch, Hedgehog, NF-κB, PI3K/Akt and RAS have been highlighted to have an important role in EMT process [33], [34].

1.1.5. The role of stem cells in colorectal carcinogenesis

Initially the stochastic model (Figure 1.5 A), predicted that any mutated cells could lead to proliferation and had the ability of developing a tumor [35]. Then, the cancer stem cells (CSCs) model arose (Figure 1.5 B), postulating the presence of a hierarchical structure within the tumor where cells with stemness properties and self-renewal capabilities are the responsible for tumor growth [36]. CSCs share properties with adult stem cells (section 1.1.2) as self-renewal, differentiation capacity, and homeostatic control [12]. Their role in carcinogenesis has been studied in the last years, and there are scientific evidences that this population of cell is the main responsible for tumor origin and relapse (as described in Figure 1.5).

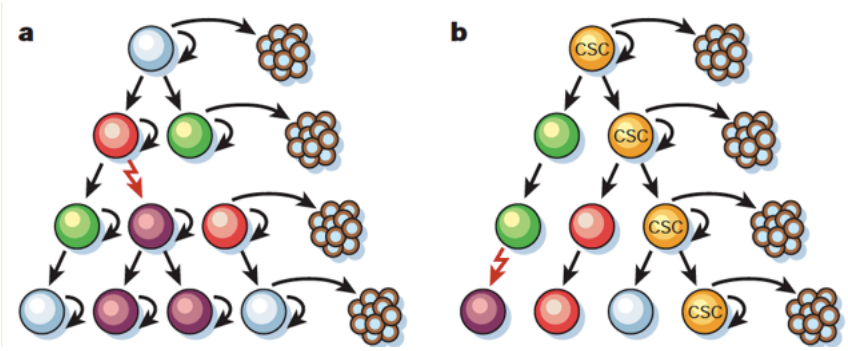

Figure 1.5 – Representative models of carcinogenesis [37]. Stochastic model – cells with different phenotypes origin tumors (A). CSCs model – cells with stemness capacity are the ones capable of tumor development (B).

CSCs model also explains the intratumoral heterogeneity originated by a single cell and, that tumor maintenance is due to the presence of stem-like niche [36]. This has been confirmed through the isolation of a subset of cells from colorectal tumors and consequent evaluation of the tumorigenic capacity when compared with the original tumor, where it was proved that CSCs are the ones with the ability of tumor growth [38]. Regardless of the concept, the microenvironment has an important role in tumor heterogeneity. Epigenetic alterations as DNA methylation, histone modifications and the presence of inflammation are the main factors for it [35].

The isolation of cell clusters with stemness properties proves the correlation between CSCs and the origin of metastasis. The CSCs isolation is based on putative stem cell markers, being the most common CD44, CD133, ALDH, and Lgr5 (Table 1.2) [11], [18], [19], [27], [39]–[41].

Table 1.2 – Putative cancer stem cell markers.

Biomarkers	Function	References
CD44 Surface glycoprotein	Cell-cell and cell-ECM interactions Apoptosis resistance mediator Hyaluronic acid receptor Dissemination	[27], [39]
CD133 Transmembrane glycoprotein	Self-renewal Tumor angiogenesis (still unclear in normal mucosa)	[11], [40]
ALDH Isoenzyme	Oxidation of aldehydes Differentiation Self-protection	[41]
Lgr5 Membrane G-protein receptor	Wnt signaling mediator Not well defined in carcinogenesis	[18], [19]

Several studies have reported tumorigenesis driven by cells positive for the biomolecules described in Table 1.2. $CD44^+$ primary tumor cells showed a significantly high colony formation and proliferative index and, moreover, this population was responsible for increasing the formation of tumor *in vivo* [39], [42]. Higher CD133 expression in CRC has been associated to tumor progression [43] specially in invasive front and metastasis [44]. *Dalerba et al.* described that the presence of CD133 associated with $CD44^+/EPCAM^{high}/ALDH^+$ phenotype showed bigger tumor growth than in the isolated $CD133^+$ cell niche [40]. Other studies confirmed CD44 as a better immature cell marker than CD133 once $CD44^+/CD133^+$ population showed higher tumorigenesis that $CD44^-/CD133^+$. However the use of both markers is important for the establishment of stemness-like niche [45], [46]. ALDH presence has been described in both normal and malignant colorectal cells and its activity increases during tumor progression. In fact, several studies revealed that increasing the number of $ALDH^+$ cells in xenografts resulted in reduced tumor formation time and, that associating with $CD44^+$ and/or $CD133^+$ cells increases dramatically the tumor initiating abilities, giving rise to a tumor with a similar profile as the primary tumor [39], [47]. Finally, normal Lgr5 expression restricted to the crypt bottom is consistent with adult colon stem cells location. However, recent data observed an increasing expression of this marker in the upper zone of the colonic crypt during dysplasia, which confirmed it as an invasive cell population. Although its role at carcinogenesis is not yet well defined, Lgr5 overexpression has been not only associated with early stages of tumorigenesis [48] but also with invasiveness and metastasis [49], and thus considered as a potential CSC marker.

All the studies summarized above, allow the conclusion that there is not only one marker for identification of CSCs but a set of cell markers that must be chosen when studying tumorigenesis driven by stem cells. Furthermore, it was proven that cells with stemness properties are entirely correlated with the progression of CRC to metastasis [38].

1.1.6. Cancer treatment and chemoprevention

The majority of CRC cases are diagnosed in a stage of advanced disease (metastatic CRC), which decreases the effectiveness of treatment and consequently the survival rate. In an early stage CRC, the survival chance is around five years and it drops dramatically to two years survival in metastatic CRC [50]. Surgery remains the only curative treatment for CRC patients, associated with the standard treatments of radio and/or chemotherapy (5-fluorouracil and leucovorin, oxaliplatin, capecitabine or irinotecan) [51]. However, metastatic CRC is generally resistant to conventional therapies [50]. In CRC with liver metastasis, the combination of three drugs (5-fluorouracil, leucovorin and oxaliplatin, also known as FOLFOX) is commonly used. Other combinations between the five drugs are also possible. The combination of 5-fluorouracil, leucovorin and irinotecan (FOLFIRI) is also applied, particularly in younger patients where shows more effectiveness. The complementation of neoadjuvant chemotherapy with antiangiogenic drugs (bevacizumab and ramucirumab) and anti-EGFR therapy (cetuximab and panitumumab) is also common [11], [51]. Therapies for primary and metastatic tumors are different, which highlights the theory that metastatic cells have a more aggressive phenotype [37]. The existence of therapeutic resistance shows that tumor biology in not yet fully understood. Most of the tumor cells are not sensitive to these treatments, leading to the possibility of tumor relapse. Chemo- and radioresistance of the tumor can be explained by the presence of CSCs, due to their plasticity. Conventional treatments may not have effect on them which results in tumor relapse. Considering the CSC model for carcinogenesis (section 1.1.5), the target goal for therapy must be this cellular population in order to prevent relapse and metastasis (Figure1.6). Therefore, more effective and specific therapeutic treatments should be developed. Identifying new molecular markers and therapeutical targets in CSCs have been highlighted as a future and promising approach for CRC treatment [50].

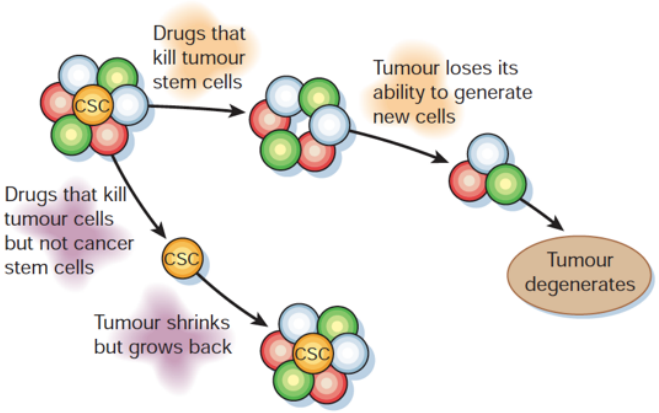

Figure 1.6 – Representative model of a novel approach on cancer treatment: CSCs have the ability of self-renewal and resistance to death allowing tumor relapse after treatment, which make them the most promising candidate for a therapy [37].

Cancer therapies that eliminate CSCs should be related to surface markers and signaling pathways present in CSCs. Defining CSCs markers as CD44, CD133, and EPCAM (a transmembrane glycoprotein, extremely express in CRC cancer cells, and whose transcription is regulated by β-

catenin) a monoclonal antibody therapy can be developed. Inhibiting these molecules, the cell signaling will be compromised and a decrease of resistance, tumor size or metastatic potential may occur [12], [52].

Interfering with signaling cascades may be a more difficult method since these pathways also have an important role in normal colorectal cells, which can affect organ development and body homeostasis. Some inhibitors of Wnt signaling have already been developed. Although none was effective, some compounds have chemopreventive effect by inhibiting the cascade: NSAIDS (like aspirin) and vitamins (A and D). These interfere mainly with β-catenin/TCF/LEF complex.[53].

Since EMT is a major step in enabling the metastatic tumor development, this is a good target for therapy. Treatments inducing cell differentiation or disruption of this process force CSCs to acquire a mature phenotype losing their self-renewal abilities and, consequently be more fragile for elimination through the traditional chemo- or radiotherapies. These treatments include: alteration of survival pathways, epigenetic therapy and microRNAs. Moreover, the microenvironment is fundamental for tumor growth especially for CSCs maintenance originating an interesting approach too [12]. An example is salinomycin, a potassium ionophore capable of inducing terminal differentiation of $CD44^+$ CSCs, thus avoiding EMT and metastasis [11].

Combination of treatments that act in different targets can give better and quick results in tumor regression. With the advances on the understanding of cancer biology, it has been discovered new mechanisms in cancer cells that may be helpful to act as therapeutical targets, as summarized in Figure 1.7 [54].

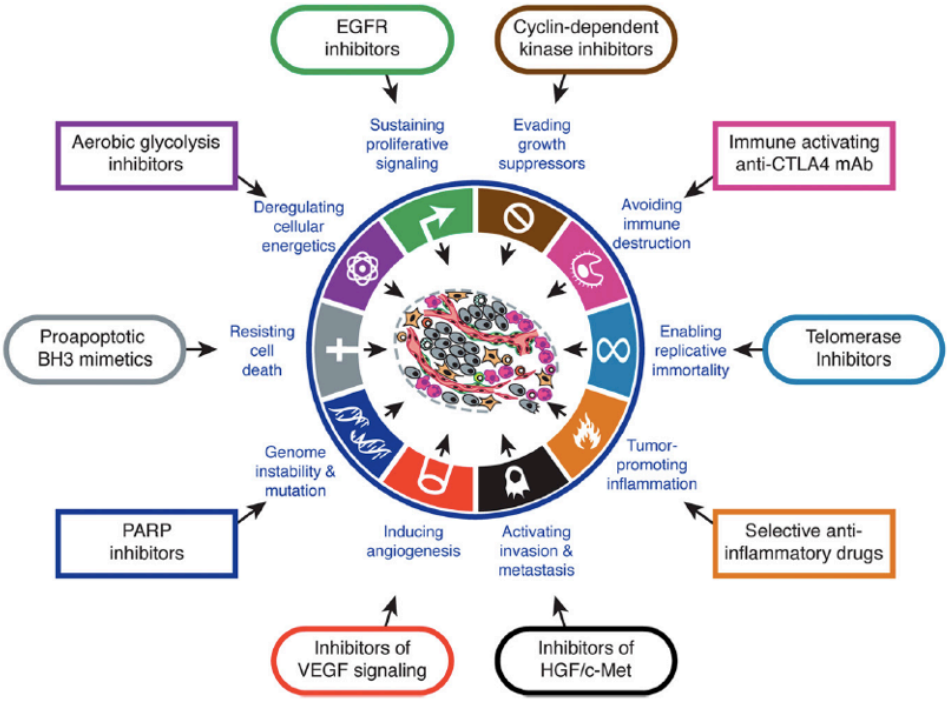

Figure 1.7 – Therapeutic targets of Hallmarks of cancer [54].

An approach that never must be forgotten is the prevention. There are three types of cancer prevention: primary, which is related to reducing possibilities of cancer development; secondary, related with early detection and screening in order to enhance treatment responsiveness and; tertiary prevention, which decreases the probabilities of recurrence and the risk of metastasizing [55]. Most of CRC cases appear in patients over 50 years, being recommended a regular screening after this age. This is frequently done through an annual identification of fecal occult blood and colonoscopy every ten years [56]. Other factor that is related with preventing CRC is a healthy lifestyle associated with a rich-dietary in fruit, vegetables and fibers [5]. In fact, natural compounds derived from plants, vegetables and fruits have been recognized as promising bioactive compounds with positive effect on CRC prevention and therapy [57].

1.2. Natural compounds and CRC

1.2.1. Phytochemicals

For the last ten years, the ingestion of natural products has been increasing worldwide with the aim to promote wellness and prevent and treat diseases. Thus, natural products have been started to be seen has chemopreventive agents, acting in all stages of carcinogenesis. These can include nutrients, vitamins, minerals, herbal medicines, probiotics, and bioactive food components. The last category has been emerging for the last years. Bioactive compounds occur naturally in low quantities in plant-derived food like fruits, vegetables and grains. The main characteristics are the association as non-essential compounds to human dietary, not causing deficiency syndromes and reducing the risk of chronic diseases as cardiovascular disease and cancer [58]. Due to their chemical structure, phytochemicals can be classified as phenolics, carotenoids, alkaloids, nitrogen-containing compounds, organosulfur, and phytosterols [59].

Phenolic compounds are the most studied class of phytochemicals. They are easily found in berries, pomegranate, plum, red grape, apple, spinach, broccoli and beets, as a secondary metabolite and being responsible for fruit color and defense mechanisms against pathogens, predators, UV-radiation, they are mainly located in the peel of these fruits/vegetables [58]. Subclassification of phenolics is shown in the Figure 1.8 and, it is based on quantity of aromatic rings in their chemical structure in association with one or more hydroxyl groups (-OH) [60]. Flavonoids are the larger category of phenolic compounds, and more than 4000 molecules are already reported. Their structures have two aromatic rings linked by three carbons from a heterocycle ring and, it is the differences in this heterocycle ring than provides different types of flavonoids (Appendix A). Flavonoids can be found in nature associated with glycosylated or esterified complexes but also in a aglycosylated form [58].

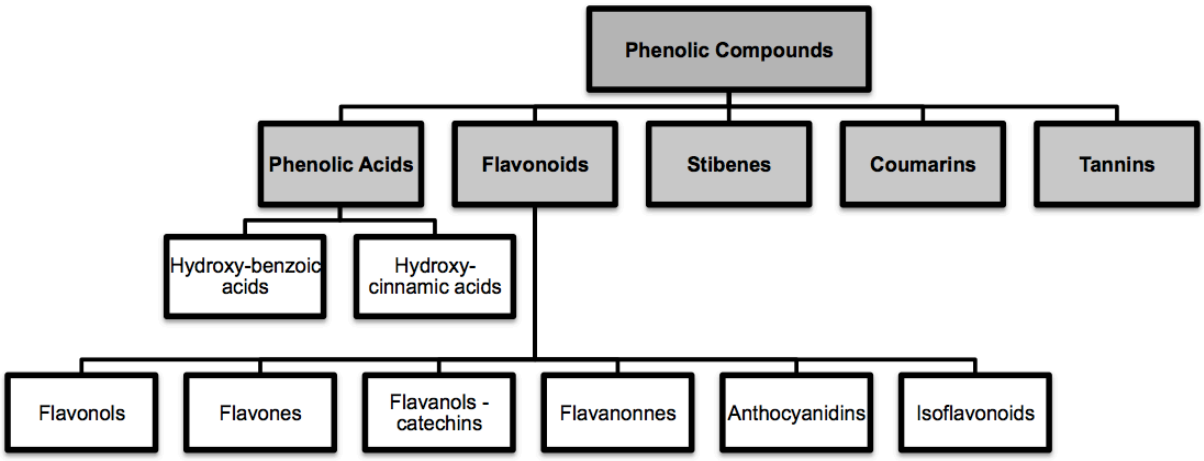

Figure 1.8 – Classification of phenolic compounds according with *Liu et al*. [61].

It has been reported that flavonoids can affect multistage carcinogenesis through several mechanisms as summarizes in Table 1.3.

Table 1.3 – Main mechanisms of chemoprevention by flavonoids in multistage carcinogenesis [59], [61], [62].

Properties	Mechanisms of action	
Antioxidant	Scavenge superoxide, hydroxy, and proxy-radicals ↓ Carcinogens cellular uptake ↓ DNA oxidation and damage	
Anticancer	↑ DNA repair ↑ Cell differentiation ↑ Tumor suppressor genes ↑ Cell-cycle arrest and apoptosis	↓ Cell proliferation ↓ Oncogene expression ↓ Transduction pathways (NF-κB, MAPK, Wnt) ↓ Enzyme metabolism (COX-2, telomerase) ↓ Angiogenesis

In the context of CRC, innumerous phenolic compounds have been reported by their effect. They have the special ability to interfere with Wnt signaling pathway: modulation of ligand-receptor interaction, expression of Wnt inhibitor gene (*wif-1*), inhibition of cytoplasmic β-catenin and β-catenin/TCF/LEF complex, reduction of nuclear β-catenin levels [63]. Some flavonoids studied in CRC field are quercetin, luteolin, apigenin, EGCG, isoquercitrin, genistein, and kaempferol [63]. These compounds are mainly found in fruit and plants [58], thus, a selective extraction of phytochemicals, might be a good strategy to originate a fruit/plant extract with high anticancer potential. Extracts from oranges, pomegranate, cherries, bamboo and tea leaves have already been reported with potential affects on carcinogenesis [64]–[69].

1.2.2. Phytochemicals from citrus

Citrus production is the bigger in fruit section worldwide, where only 34% of the fruit is processed into juice leaving a large amount of by-products, namely orange peels [70]. It is a large residue existing on agriculture that can get a new added value in industry due to its chemical and biological characteristics. The main phytochemicals present in oranges are mostly located in the peels and include flavonoids (polymethoxylated flavones), terpenoids (limonene and linalool) and volatile oils. Polymethoxylated flavones (PMFs) are particular flavonoids of interest due to their range of biological activities including anti-inflammation, anticancer, cardiovascular (antithrombotic and antiatherogenic), antipathogenic and antioxidant [69], [71]. Comparing to polyhydroxylated flavonoids (e.g. narigin, luteolin, quercetin), PMFs are more lipophilic due to the hydrophobic nature of the methoxy groups giving these compounds the ability of easy absorption in the small intestine to blood circulation [69]. The high permeability and low solubility of PMF contributes to its potential for excellent bioavailability [72].

PMFs exist almost restricted to citrus plants and particularly abundant in *Citrus sinensis* – sweet orange [72]. Its anticancer activity has been reported *in vivo* in several types of tumors: skin, colon,

prostate, lung, liver and breast [73]. *In vitro* studies also reported the antiproliferative e anticancer effect of PMFs in a large spectrum of cancer cell lines [74]. From all PMFs, tangeretin and nobiletin are reported as the most promising inhibitors of cancer cell proliferation [74]. The Table 1.4 summarizes some studies that have already reported the anticancer property of citrus flavonoids particularly in CRC.

Table 1.4 – Most common citrus flavonoids and its effect at CRC.

Flavonoids	Function	Mechanisms of action	Cancer models	Ref
5HTMF **5HPMF** **5HHMF**	Induction of apoptosis Cell cycle arrest	Apoptosis – p53 and Bax dependent; G1 – p53 and p21 dependent; G2/M – p53 and p21 independent; ↑ Caspase3	Cell-based assays	[74]–[76]
Apigenin	Inhibition of proliferation Cell cycle arrest (G2/M)	↓ TNF, $p34^{cdc2}$, cyclin B1	Cell-based assays	[77], [78]
Hesperidin	Inhibition of proliferation Induction of apoptosis	↑ Caspase3 and Bax proteins, prostaglandin biosynthesis; ↓ Bcl-2 proteins	Cell-based assays Animal models	[79]–[82]
Naringenin	Induction of apoptosis	↓ p38, cyclin D1	Cell-based assays Animal models	[83], [82], [84]
Nobiletin	Inhibition of proliferation Cell cycle arrest (G1)	↓ MMP-7, Bcl-2 protein, leptin, prostaglandin E2 biosynthesis; ↑ p53 and Bax proteins	Cell-based assays Animal models	[77], [85]–[87]
Sinensetin	Inhibition of proliferation Cell cycle arrest (S)	S phase cell arrest	Cell-based assays	[77], [88]
Tangeretin	Cell cycle arrest (G1) Inhibition of proliferation Metastasis	↑ p21 and p27; ↓ β-catenin	Cell-based assays Animal models	[77], [85], [89], [90]

Recently, studies reported that metabolites resulting of biotransformation of PMFs, specially from nobiletin and tangeretin, had higher anticancer and anti-inflammatory effects than original PMFs [91]. Using mice models fed with PMFs, PMFs metabolites from fecal and urine samples were identified, presenting these compounds a strong inhibitory effect on colon cancer cell growth than the original PMFs [91], [92].

It is important to mention that although the high anticancer potential of PMFs, there is no information regarding to the effect of citrus PMFs and its metabolites in CSCs niche.

1.3. Cancer models

According to FDA, there are five steps to follow in drug development process: i) discovery and development; ii) preclinical research; iii) clinical research (phases I, II, III and IV); iv) FDA review and; v) FDA post-market safety monitoring. Once clinical research, the so called clinical trials, refers to the studies performed in humans, it is important to first test the safety/toxicity and the dosage of the drugs in preclinical research. This is evaluated using *in vivo* (animal models) and *in vitro* (cellular models – 2D and 3D) approaches [93].

To better understand the effect of drug in cancer it is important to choose an appropriate model that better mimics the real situation. [94] Succinctly, animal models (usually mice) relies in chemically induced animals, genetically engineered mouse models (GEMM) and xenografts (patient-derived or not). Despite closely resembling human tumorigenesis, these animal models present some disadvantages namely a immune system suppression that may alter the normal tumor behavior, tumor-time development, relation cost-effectiveness, and ethical issues related [95]. Conventional 2D models consist of a monolayer of a specific cell line growing on a solid, impermeable and adherent surface of a culture flask, which appears to be a poor model to study the complexity of tumor-stroma interactions, tumor heterogeneity and key signaling pathways. However, cellular monolayers are still largely used for screening cytotoxicity. During the last years, three-dimensional (3D) models bypassed some disadvantages of monolayer models and are being recognized as valuable tools to evaluate the anticancer potential of new therapy drugs. These models have became more precise in predicting drug efficacy in primary tumors once they are more informative than the conventional 2D models [94].

1.3.1. Characteristics of 3D cellular models

Three-dimensional (3D) cellular models have been developed in the past four decades in order to fill the gap between conventional 2D monolayers and animal models [94]. Its potential relies in the possibility of mimicking morphological and functional features of primary human tumors. Firstly, using a 3D conformation, solid tumors can grow forming a heterogenic cellular organization due to the different exposure to oxygen and nutrients. Therefore, these models can be characterized by a proliferative cell population normally located at the periphery and hypoxic tumor cells population associated with necrotic areas located at the center of the tumor bulk. An intermediate layer of quiescent cells can be recruited to the proliferation sector. These differences are obtained with the tumor development during culture due to the difficulties of oxygen and nutrients diffusion and, the accumulation of waste metabolites, which can easily originate different signaling and molecular expressions within the tumor originating heterogeneity. Also, as the tumor growth increases, the proliferative population tends to decrease being the spheroids more rich in quiescent cells (Figure 1.9) [96], [97].

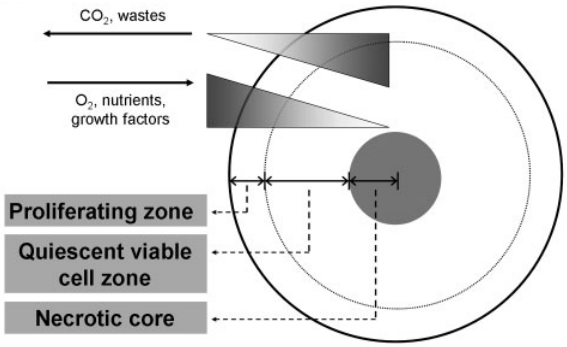

Figure 1.9 – Spheroid organizational architecture and components distribution. CO_2 and waste metabolites tend to increase from the outer to the center of the spheroid. The O_2, nutrients and growth factor disposition tends to be reverse [98].

Up to date, several 3D models were created including multicellular tumor spheroids (MCTS), tumorospheres, tissue-derived tumor spheres and organotypic multicellular spheroids. The main differences between all are related to the cells of origin and the preparation protocol [96]. Figure 1.10 summarizes the classification of 3D models and systems that are being used for their production.

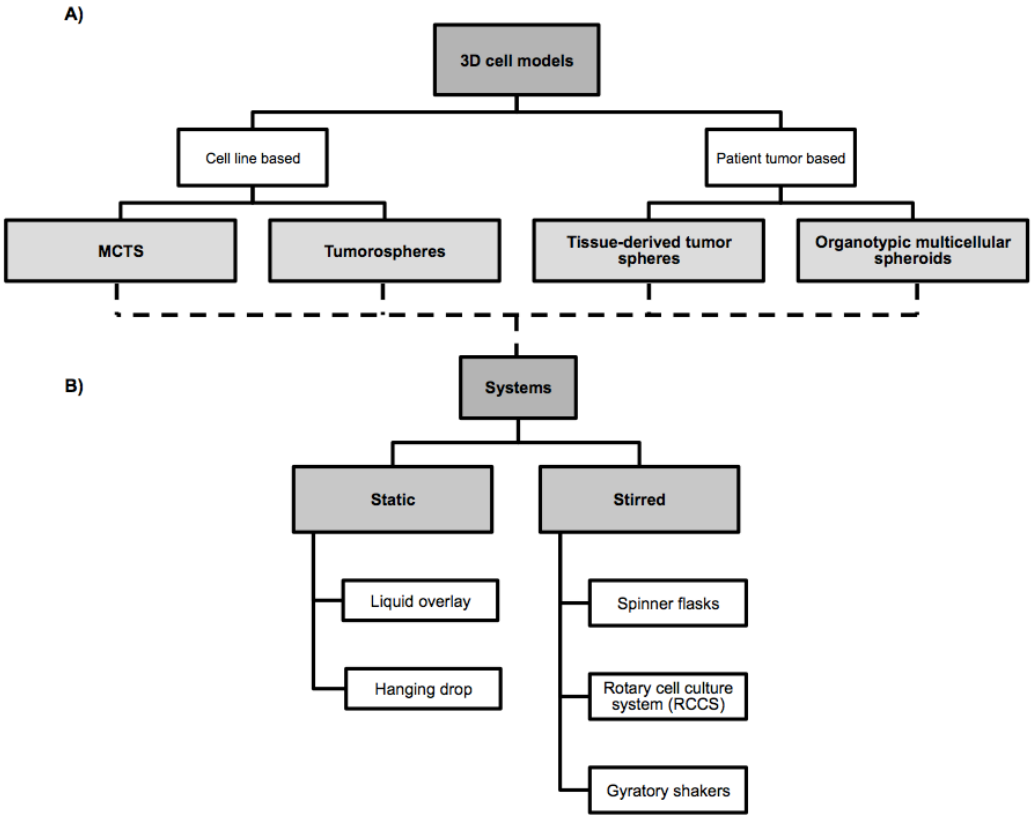

Figure 1.10 – Types of three-dimensional cell models based on cells of origin (A) and type of system that can be used for spheroids culture (B).

Sutherland et al. described MCTS for the first time in early 70s [97]. This model uses cancer cell lines, not derived from direct tumor tissue, and the spherical structure can be reached after 1-7 days of culture. There are different procedures of culturing MCTS: static (based on non-adherent surfaces)

and stirred systems (spheroids forming in suspension) [96]. The liquid overlay cultures require adhesive forces promoting cell adhesion and thus, avoiding matrix deposition. Normally, it is used agar/agarose/Matrigel®-based media that promotes cell migration to a single place where by cell-cell interactions the spheroids obtained tend to grow and increase their sizes during culture time (Figure 1.11 A) [99], [100]. Additionally, another method was developed, which does not require a non-attachment surface – the hanging drop method (Figure 1.11 B). This promotes tumor spherical aggregation through a deposit of cellular suspension in a free liquid-air interface [101].

Opposite to static methodologies, in stirred systems it is possible to obtain large-scale production of spheroids. They are the most common system for culturing MCTS and include three types: spinner flasks, rotary cell culture system (RCCS) and gyratory shakers. Spinner flasks were the first method of culturing MCTS (Figure 1.11 C) [102]. Spheroids harvested have a uniform size and diameter dependent of the inoculum density, medium composition, stirring rate and culture time. The main concern about this system is the strong shear rate hit by the spinner that may influence cells physiology [98], [103]. To overcome this problem, RCCS were created by NASA. It is the best revolutionary system in tissue engineering. Also, it is capable of simulate microgravity and mixes the cellular suspension using hydrodynamic forces diminishing the turbulence comparing to spinner flasks (Figure 1.11 D). Thus, using low shear forces the obtained spheroids have larger sizes and bigger differentiation of morphology and phenotype. The use of multiple types of cell lines is also possible using scaffolds, mainly microcarrier beads [100], [104]–[106]. Gyratory shakers are very similar to spinner flasks differing only in the origin of stirring. Cellular inoculum is added to a Erlenmeyer that rotate not by magnetic stirring but by a gyratory rotation incubator [100].

Additionally, bioreactors can be combined with scaffolds (Figure 1.11 E) [107]. Scaffold systems use microcapsules of cellulose-based membranes that are easily disrupted by enzymatic reactions. Collagen/alginate-based membranes, synthetic polymers, or hydrogels shells can be also used [100], [108], [109]. Scaffolds of microcarrier beads are innovative tools in 3D models. It does not required spontaneous cellular aggregation but it is a vehicle for adhesion promotion. The pioneer advantage relies on the possibility of growing different cell lines close to each other (as tumor, endothelial and stromal cells), promoting a tumor environment similar to *in vivo*. The beads are generally use in bioreactors [100], [104], [110].

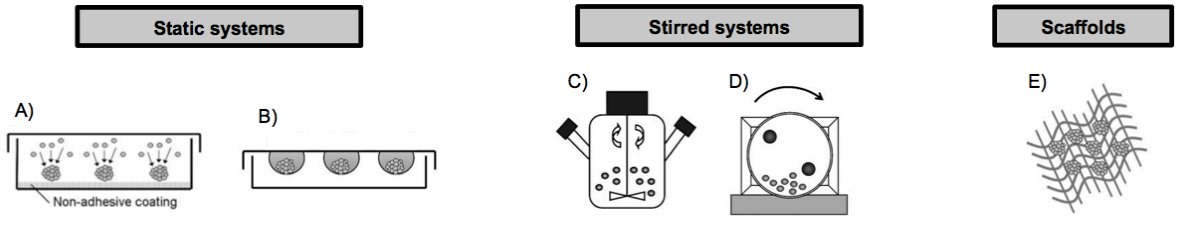

Figure 1.11 – Main systems use for 3D cell culture: liquid overlay (A); hanging drop (B); spinner flask (C); rotary cell culture system (C); scaffolds use in bioreactors (E) (adapted from [98]).

Tumorospheres are models of CSC culture and expansion derived from cell lines or rarely through the dissociated cancer tissue into a cellular suspension [96]. On this cellular suspension, cells with stemness phenotype (section 1.1.5) can be isolated. For sphere formation, cells are cultured in low density and low-adherent conditions with “stem cell medium” – absence of fetal bovine serum and supplemented with growth factors that promote stem cell growth – hence, avoiding cellular aggregation and promoting the development of the spheroid from one single cell [96], [111]. Tumorospheres were firstly described using brain tumor cells, and thus classified as neurospheres [111], and there has been a development of tumorospheres from a wide range of solid tumors including breast (mammospheres [112]), colon (colospheres [43] or colonospheres), lung, prostate, ovarian and pancreas [96]. This spheres can be cultured in static or stirred systems [113]. In addition, tissue-derived tumor spheres and organotypic multicellular spheroids use cancer tissue and not cell lines for culturing. In the first case, the tumor is partially dissociated and the new spheroids are normally formed using static systems and suspension systems with “stem cell medium” [114], [115]. The organotypic multicellular spheroids require culturing *ex vivo* fragments of the tumors until they reach a circular form using non-adherent surface systems, normally in agar-based media. The spheroids tend to grow in 2-5 or 12-18 days [96], [116].

In terms of conclusion, 3D models are the next generation for tumor biology studies since they can accurately behave as the parental tissue. Invasive behavior, tumor-stromal interactions, tumor heterogeneity are the main factors that originate a realistic model. For cancer models, scaffolds and bioreactors are the systems that better improve the diversity and capacity of the culture [103], [106]. However, it is important to mention that all the models have their advantages and disadvantages (summarized in Table 1.5) and the most adequate system must be chosen according to the aim of the study [96], [98], [100].

Table 1.5 – Advantages and disadvantages of culture systems [98], [100].

	Advantages	**Disadvantages**
Static Systems	Cheap Simple to perform Rapid and easy to screening	Small-scale production Spheroid size and shape not controlled (only in liquid overlay)
Stirred Systems	Large-scale production Simple to culture Better cell differentiation Better cell morphology Dynamism in culture conditions	Specific equipment required Large amount of reagents required (medium) Spheroid size and number not controlled Cell sensitivity to shear forces (only in spinner flasks) Expensive (only in RCCS)

1.3.2. 3D cell models for colorectal cancer

In CRC, 3D models have been used not only for studying tumor biology in terms of development, invasiveness and migration, but also to evaluate the effect of drugs and natural extracts. The models are based both in tumor-patient derived cells and cell lines.

There are more than 70 colorectal cancer cell lines described, that represent different types of primary CRC, according to their genetic background. The most frequent cell lines used are: Caco-2, COLO 320, LoVo, HCT15, HCT116, HT29, SW48, and SW480 [117]. Up to now, most of the CRC studies that applied 3D cell model used non-adherent surfaces systems based mostly in ultra-low attachment plates, agar-coated plates and hanging drop method (Table 1.6).

Table 1.6 – Resume of recent work using CRC spheroids for study whether tumor biology or effect of compounds.

3D cell model	Cell line Type of cell	System utilized	Application/Therapy	Ref.
MCTS **Tumorospheres**	Caco-2 COLO201 COLO 205 HCT116 HT29 LoVo SW1222 SW480 SW620	Liquid overlay	Bamboo effect CRC characterization Chemo-resistance Curcumin effect on CSCs Dasatinib effect on CSCs Nigericin effect on EMT Silibinin effect on stemness Stemness markers	[65], [118]–[127]
Tissue-derived tumor spheres **Organotypic multicellular spheroids**	$CD133^+$ $CD133^+/CD29^+/CK20^-$ $CD44^+$ Patient-tumor	Liquid overlay	CRC characterization Chemo-resistance Role of Aurora-A Stemness markers	[43], [114]–[116], [128]–[131]

1.3.3. HT29 cell line-derived spheroids

During the last years, the host laboratory (Nutraceuticals & Delivery Group of iBET – Oeiras, Portugal) has been collaborating with Animal Cell Technology Unit of iBET (Oeiras, Portugal) aiming at developing MCTS of CRC cell lines that can be used as a pre-clinical model for the evaluation of new natural compounds with chemotherapeutic potential [88], [132], [133]. More specifically, this model was produced by culturing HT29 cell line under stirred conditions using bioreactors (spinner vessels). HT29 cell spheroids culturing has been only reported in static systems where it forms a spherical-shape aggregate when comparing to other colon cancer cell lines [134].

To develop a stirred method it is important to fulfill certain parameters: reproducibility, predictability, effectiveness and also be an affordable method [135]. HT29 spheroids grow in three stages: aggregation, compaction and growth. In the aggregation phase (first 24 hours of culture), cellular density is maintained with the presence of clusters with different sizes and single cells, originating a

heterogenic population. From day 2 to day 3 of culture, spheroid density decreases, spheroid diameter remains and cellular concentration increases, suggesting spheroid fusion – compaction phase. From day 3 onwards the number of spheroids stabilized and there is only an increase of size during the time of culture corresponding to growth phase [132].

At day 7 of culture the spheroids acquire a stratified population (section 1.3.1, Figure 1.9) with a compacted cellular layer at the periphery and less cellular compaction at the center of the spheroids. This compaction is correlated with the increasing of cell-cell adhesion marker E-cadherin at the periphery of spheroids. Another epithelial marker is CK18, which detection is lost along the culture time. The apoptotic/necrotic region described in 3D models is also present in HT29 cell spheroids by the loss of f-actin and the presence of cleaved CK18 at the spheroid center. The loss of central E-cadherin and CK18, the presence of nuclear β-catenin and expression of Vimentin at day 12 of culture was identified in these spheroids suggesting a dedifferentiation process associated with invasiveness and possible EMT (section 1.1.4). Moreover, this HT29 cell aggragates present a positive staining of CD44 for both monolayer and spheroids confirming the presence of stemness profile in colon cancer [88], [132], [133]. Figure 1.12 shows some of the immunofluorescence staining performed with HT29 spheroids collected at different days of culture and it can be seen a well-stratified population with the presence of an apoptotic/necrotic core simulating *in vivo* tumor progression and phenotypes. However, further biomarkers should be analyzed aiming the characterization of this model in terms of stemness and self-renewal abilities and evaluate if it can be considered as a promising tool to evaluate the effect of new compounds on targeting CSC population.

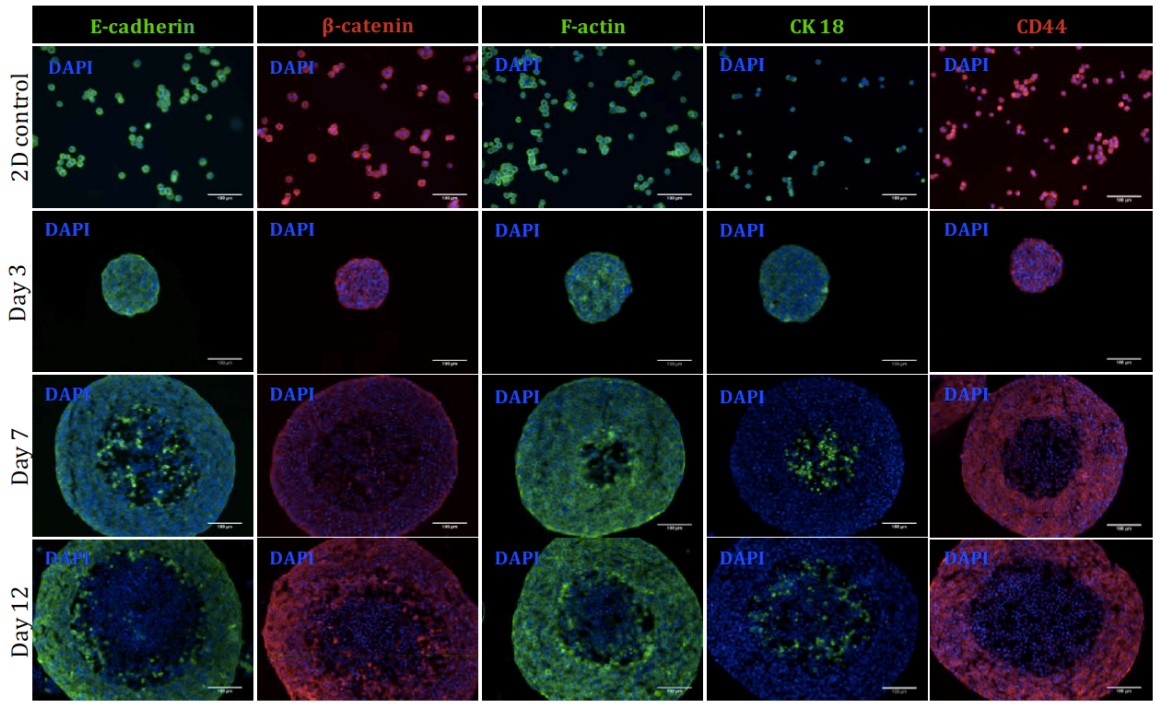

Figure 1.12 – Immunofluorescence markers use for characterization of HT29 cell spheroids cultured by stirred system [132].

1.4. Aim of the Thesis

Even though there are studies reporting the anticancer potential of citrus bioactive compounds on human cancer cells, there is no information regarding their activity on CSCs. As described above, CSCs have been recognized to be responsible for tumor initiation, chemo-resistance and relapse being considered a promising target for cancer prevention and therapy. Within this context, the aim of this thesis was to evaluate if PMFs derived from orange peels were able to target CSCs using a 3D model of colorectal cancer. The work was organized in three main steps as described in Figure 1.13.

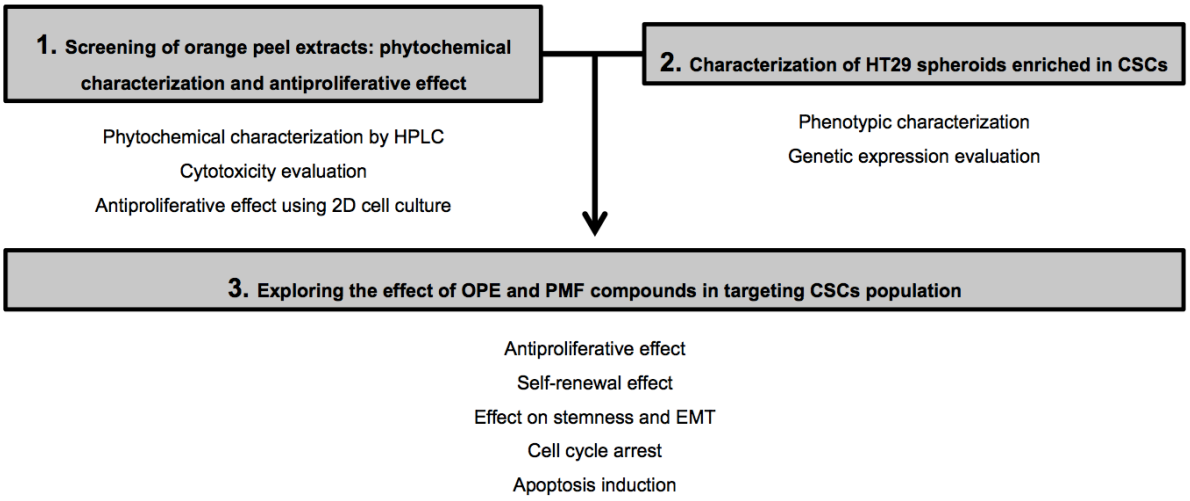

Figure 1.13 – Work plan for the present thesis organized in three main tasks.

In the first part of this project, phytochemical-rich extracts derived from orange peels and produced by supercritical fluid technology were screened and characterized in terms of PMF composition and antiproliferative effect using HT29 cell line. The aim was to identify the PMFs responsible for the bioactive effect and to evaluate the interactions between all the main components of orange peel extract.

In the second part of this thesis, the 3D cell model already developed by the host laboratory using HT29 cell line cultured in stirred conditions was characterized for CSCs population. More specifically, HT29 cell spheroids collected at different time points were subjected to a phenotypic characterization and gene expression evaluation in order to analyze the stemness and self-renewal characteristics of the 3D cell model.

Finally, the most promising extract selected from Part 1 was tested on HT29 aggregates characterized in Part 2 in order to evaluate the effect of citrus bioactive compounds in i) inhibiting cell proliferation and ii) targeting key signaling pathways related to stemness and self-renewal characteristics of CSCs population in this 3D cell model.

The present thesis was integrated in the project “OrangeCTheraphy: Chemotherapeutic effect of citrus bioactive compounds – evaluation for targeting human colorectal cancer stem cells”, funded by iNOVA4Health – Advancing Precision Medicine, a research program focused on translational

medicine. This project is composed by a multidisciplinary team from iBET (Nutraceuticals & Delivery Group and Animal Cell Technology Unit) and IPOLFG (Colon Pathology Study Group).

2. Experimental Procedures

2.1. Natural Extracts

The host laboratory (Nutraceuticals & Delivery Group of iBET – Oeiras, Portugal), kindly obtained the orange extract for the present study. Initially, the residues (peels) of orange were collected, lyophilized for 3 days, smashed and stiffed. Once gathered all the raw material, the extraction was performed using supercritical fluid extraction (SFE) (CO_2 supercritical – green technology) as described by *Toledo-Guillén et al* [68]. Three extractions were made using diverse CO_2/EtOH ratio as summarized in the Table 2.1.

Table 2.1 – Extraction conditions used to obtain natural orange peel extract (OPE). For all the extracts were used Portuguese oranges, being OPE 1 and OPE 2 obtained from the same raw material.

Orange Extract	Pressure (bar)	Temperature (K)	% CO_2/EtOH	Fraction collected (min)
OPE 1			80/20	0-15
OPE 2	250	318.15	50/50	0-15
OPE 3			80/20	0-30

The products obtained from the extractions were concentrated by rotary evaporator. Then, were dissolved in absolute ethanol at a concentration of 150 mg extract/mL and stored at -20ºC.

2.1.1. *In Vitro* Digestion

In order to evaluate the phytochemical alterations during digestion of OPE, an assay that mimics human digestion was executed. This assay is divided in three phases: oral, gastric and intestinal, as described by *Minekus et al*. [136]. The oral phase was skipped since it is predicted that this nutraceutical should be taken orally by drinking therefore it was not submitted to oral enzymes.

Briefly, the OPE (initial volume of 2.5 mL) was adjusted to a pH 7.0 (with NaOH 5 M) and a mixture of 1 mL of pepsin (2000 U/mL in the final mixture), $CaCl_2$ and simulated gastric fluid (SGF) (solution rich in electrolytes) was added. This solution was adjusted to pH 3.0 (with HCl 5 M) and incubated at 37ºC in a water bath with shaking, which simulates gastric digestion. After 2 hours, 2.5 mL of the solution was removed and stored at -20ºC and the remaining volume was subjected to simulation of intestinal digestion with the addition of simulated intestinal fluid (SIF), 5 mL of Pancreatin (100 U/mL in the final mixture), 1880 µL of bile salts (10 mM in the final mixture) and $CaCl_2$. The solution was adjusted to pH 7.0 (with NaOH 5 M). The 37ºC water bath incubation with shaking for 2 hours was repeated. Finally, the proteases were inactivated by Pefabloc® (10 µL/mL, Sigma-Aldrich, USA) and the solution collected in centrifuge tubes for protein purification (Amicon, Merck) in a 40 minutes centrifugation at maximum speed (Miikro 220R, Hettich Zentrifugen, Germany). Sample was filtered with acetate cellulose 0.2 µm sterile filter and stored at -20ºC resulting in 18.75 mg extract/mL final concentration.

2.2. Phytochemical Characterization

2.2.1. High Performance Liquid Chromatography (HPLC) for phenolic content analysis

Analytical Group of iBET (Oeiras, Portugal) performed all analytical HPLC studies of PMF content in orange peel extracts as previously described by *Serra et al*. and *Bravo et al*. [137], [138].

A Surveyor apparatus with a diode array detector (Thermo Finnigan-Surveyor, CA, USA) and an electrochemical detector (Dionex ED40) was used. PMF content of the extracts were determined by analyzing the peak area at 320 nm – through the data acquisition system, Chromquest 4.0 (Thermo Finnigan-Surveyor, CA, USA) – and comparing with the calibration curve of each compound (0.1-100 mg/L). Final results were expressed as milligrams of nobiletin, tangeretin, sinensetin or scutellarein tetramethylether per gram of dry extract.

2.3. Cell-based Assays

These assays were performed at Nutraceuticals & Delivery Group of iBET (Oeiras, Portugal).

2.3.1. Cell culture

Two human colon cancer cells lines were used, HT29 (ATCC, USA) and Caco-2 (DSMZ, Germany) cell lines.

HT29 and Caco-2 were cultivated in RPMI-1640 medium supplemented with 10% (v/v) heat-inactivated fetal bovine serum (FBS). Caco-2 was also supplemented with 1% (v/v) penicillin-streptomycin. Growth medium and supplements were obtained from Gibco (by Life Technologies, USA). Cell lines were monitored daily and split once or twice a week when reach ≈80-90% confluence in 75/175 cm^2 culture flasks until a maximum of fifty passages. The cells were incubated at 37ºC, in a humidified atmosphere of 5% CO_2.

2.3.2. Reagents

Standard compounds were purchased from Extrasynthese (Genay, France). Stock solutions of nobiletin (24.85 mM), tangeretin (8 mM), sinensetin (26.86 mM) and scutellarein tetramethylether (29.21 mM) were prepared in dimethyl sulfoxide (DMSO) (Sigma-Aldrich, USA) and stored at 4ºC. 5-fluorouracil was obtained by Sigma-Aldrich (USA). The stock solution at 50 mM concentration in distillated water was stored at -20ºC. For the cell-based assays, the reagents were diluted in culture medium (RPMI medium supplemented with 0.5% (v/v) FBS. In all experiments, a control was included were cells were incubated with DMSO/distillated water. The final solvent concentrations were maintained at 1.0%-1.5% and 25% (v/v), respectively.

OPE was obtained as described at section 2.1. In all experiments, a control was included in which cells were incubated with absolute ethanol in a final concentration of 5% (v/v).

2.3.3. Cytotoxicity assay

To evaluate the *in vitro* cytotoxicity of the extracts and standard compounds, Caco-2 cell line was used. Although this cell line is originated from a human colon adenocarcinoma, when cultured under special conditions, may lead to a monolayer growth of cells with characteristics resembling mature enterocytes which is achieved after 7 days of seeding. Hence, this model may mimic the intestinal barrier [139], [140].

The assay was performed as described by *Serra et al.* [64] with slight modifications. At density of $2x10^4$ cell/well, cells were seeded in 96-well culture plates (Falcon™, Thermo Fisher Scientific Inc.).

Medium was changed every 48 hours. After 8 days of culture, cells were treated with a range of OPE, PMFs, 5-FU concentrations, or DMSO/EtOH/distillated water solvent controls. In addition, blank control samples were included, corresponding to culture medium alone. Incubation was carried out for 4h at 37ºC with 5% CO_2. Therefore, cells were washed two times with warm PBS in order to avoid possible interferences of the samples color (specially OPE). Cytotoxicity evaluation was performed using PrestoBlue® Viability Reagent (Molecular Probes, Invitrogen, USA) in 1:20 dilution in culture medium and incubated for 1 hour at 37ºC with 5% CO_2. Fluorescence was quantified by measurement at 560 nm excitation and 590 nm emission using a microplate reader (FLx800, BioTek Instruments, USA). Triplicates were performed at each condition and the results shown as percentage of living cells relatively to the control cells using GraphPad Prism 6 (GraphPad Software, Inc., CA).

2.3.4. Antiproliferative assay using 2D cell culture system

The antiproliferative assays were performed using HT29 cell line at its exponential phase of growth as described by *Serra et al*. [141].

Briefly, cells were seeded at a density of $1x10^4$ cells/well in 96-well culture plates and were allowed to attach for 37ºC with 5% CO_2. After 24h, the medium was replaced with a range of OPE, PMFs, 5-FU concentrations, or DMSO/EtOH/distillated water controls and, the blank control samples (with only culture medium). Cells were allowed to proliferate for 24 or 72 hours at 37ºC with 5% CO_2. After that, cells were washed two times with warm PBS in order to avoid possible interferences of the samples color (specially OPE). Cell viability was assessed using PrestoBlue® Viability Reagent (Molecular Probes, Invitrogen, USA) in 1:20 dilution in culture medium and incubated for 2 hours at 37ºC with 5% CO_2. Fluorescence was quantified as described in section 2.3.3. Triplicates were performed for each condition and the results were shown as percentage of living cells in relation to the control cells. EC50 values (the concentration of sample necessary to decrease 50% of cell population) were calculated through dose-response curves using GraphPad Prism 6 (GraphPad Software, Inc., CA). The study of synergistic effects between standard compounds was performed using Compusyn software (ComboSyn, Inc.) where interaction are classified as combination index (CI) expressed as additive ($0.90 < CI < 1.10$), synergistic (< 1) and antagonistic (> 1) [142], [143].

2.3.5. 3D cell culture system – spheroids culture and formation

For the 3D cell culture system, a 125 mL spinner flask was used (Corning, NY, USA) being previously subjected to a silanization process with dimethyldiclhlorosilane (Merck 8.034452, Germany). This process provides hydrophobic surfaces to the spinner, thus avoiding cells attachment.

The culture was performed as described by *Silva* (2013) [88], [132]. Briefly, cells were grown in 175 cm^2 culture flasks until 90% confluence and then detached with trypsin-EDTA (0.25%). $2.5x10^5$ cells/mL were placed in the spinner flask together with culture medium (RPMI supplemented with 10% FBS). The system included a magnetic stirrer, and the culture was maintained for 12 days at 37ºC with 5% CO_2. The process was monitored at different times. The culture started with only 60% of the medium final volume (100mL) and the remaining was added after 6 hours. The stirring rate was initially 40 rpm, gradually increasing for 50 and 60 rpm after 8 and 28 hours, respectively. At day 4, the first medium exchange was performed (50% of the spinner flask volume) and this process was repeated daily to analyze spheroids diameter in a microscope (Leica DMIRB, Germany).

2.3.6. Antiproliferative assay using 3D cell culture system

Antiproliferative assay was performed at day 7 of the 3D cell culture using spheroids with approximately 500 µm of diameter.

As described in a previous work [132], a density of approximately 5 spheroids/well were seeded in 96-well culture plates and cell viability assessed adding 10 µL of PrestoBlue®. This step was essential to calculate the number of cells per well and thus take in account any spheroids size discrepancies. After 2 hours incubation at 37ºC with 5% CO_2, plates were centrifuged (SIGMA 3K15, Sigma Laborzentrifugen, Germany) for 5 minutes at 200 g, the supernatant was transferred to a black-96-well plate and fluorescence intensity measured. OPE, PMFs, 5-FU concentrations, DMSO/EtOH/distillated water controls and, the blank control samples were diluted in culture medium, added to each well and incubated for 24 and 72 hours at 37ºC with 5% CO_2. After that, the supernatant was removed and the spheroids viability measured with PrestoBlue® in 1:10 dilution for 2 hours at 37ºC with 5% CO_2. The fluorescence was measured as described in section 2.3.3.

The assay was performed in 6 replicates of each sample concentration in at least three independent experiments. The results were expressed in terms of percentage of living cells, in relation with control cells (spheroids incubated with only culture medium) using the following equation:

$$Cell\ viability\ (\%) = \frac{\frac{FI\ ratio\ (of\ treated\ cells)_{24/72h}}{FI\ ratio\ (of\ treated\ cells)_{0h}}}{\frac{FI\ ratio\ (of\ average\ control\ cells)_{24/72h}}{FI\ ratio\ (of\ average\ control\ cells)_{0h}}} \times 100 \qquad \textbf{Equation 1}$$

Where FI_{0h} is the fluorescence intensity obtained before the incubation of spheroids with the compounds and $FI_{24/72h}$ is the fluorescence intensity obtained after 24 and 72 hours incubation of spheroids.

EC50 values were calculated through dose-response curves using GraphPad Prism 6 (GraphPad Software, Inc., CA).

2.3.7. Soft agar colony forming unit assay

This assay allows the study of the capacity of HT29 cell line in forming colonies based in a semi-solid support. The cellular suspension used resulted of detachment of the 2D cell culture, or through HT29 spheroids dissociation from day 7 of culture. In addition, controls were made by dissociation of spheroids with 4 and 12 days of culture.

First, the bottom layer was obtained by mixing 1.2% low-melting agarose (Lonza, Rockland ME, USA) with 2x RPMI medium with 20% (v/v) FBS at a ratio of 1:1 resulting in a 0.6% growth medium solution. Afterwards, 2 mL of this solution was pipetted in each well of a 6-well culture plate (Falcon™, Thermo Fisher Scientific Inc.). To avoid bubble formation, the mixture was spread uniformly by slowly rotating the plates and then allowed to rest for 1-4 hours at room temperature in a sterile laminar flow hood until complete solidification of the bottom layers. The cellular suspension was adjusted to $1x10^3$ cell/mL in 0.3% low-melting agarose diluted in PBS (1:1 ratio) and was transferred 2 mL/well. The studied compounds and respective concentrations were added directly to this layer. The plates were cultured at 37ºC in 5% CO_2 humidified atmosphere for 14 days. The medium was renewed by adding 100 µL/well of RPMI/10% FBS twice a week. The colony formation was monitored at day 7 and 14 of culture. At the end, the number of colonies visible for the human eye was counted and photographed (Leica DMIRB/DFC295, Germany). Images were treated on Macromanager 1.4.22 and ImageJ 1.47v (National Institutes of Health, USA) software. The experiments were independently performed at least two times. The results were expressed in number of colonies relatively to the control cells or according to the plate efficiency equation:

$$Plate\ efficiency\ (\%) = \frac{number\ of\ colonies}{total\ cell\ number} \times 100 \quad \textbf{Equation 2}$$

2.3.8. Aldefluor assay by Fluorescence-activated cell sorting (FACS) analysis

This assay allowed the study of one of the putative CSCs markers through the isolation of cells with high aldehyde dehydrogenase (ALDH) enzymatic activity.

Initially, 50 HT29 cell spheroids with 7 days of culture were placed per well in a 6-well culture plate with the compounds previously diluted in culture medium (RPMI with 0.5% FBS) at final volume of 2 mL. Blank and solvent controls were also performed.

For this assay, the Aldefluor™ kit (STEMCELL Technologies Inc.) was used, following manufacturer's instructions [144]. Briefly, after 24h at 37ºC with 5% CO_2, spheroids were collected from the 6-well plates, together with one sample of the spinner flask (from days 4, 7 and 12 of culture) and spheroids dissociation was promoted by several steps of 5 minutes at 200 g centrifugation (Miikro 220R, Hettich Zentrifugen, Germany) and trypsin-EDTA (0.25%). In addition, a sample from 2D cell culture was harvested by trypsin-EDTA from a 75 cm^2 culture flask. Then, a density of $5x10^5$ cells/mL were re-suspended in Aldefluor assay reagent (containing ALDH1 substrate – BAAA, 1 µmol/L per $1x10^6$ cells) and kept in a 37ºC humidified atmosphere with 5% CO2 for 30 min. Allowing the establishment of

sorting gates, a negative control for each sample was prepared - aliquot with the same reagents where it was extra-added 2.5 µL of a specific ALDH inhibitor, DEAB. After that, samples were centrifuged at 200 g for 5 min, the supernatant removed and added 250 µL of Aldefluor assay buffer, which allows ALDH-positive cells to arrest the product result from ALDH activity with BAAA. Hence, only viable ALDH1-positive cells were identified. Cells were analyzed by flow cytometer CyFlow® Space (Partec, Germany) and data measured by using FloMax 3.0 software (Partec, Germany) and analyzed by Flowing 2.5 software (Turko Centre for Biotechnology, Finland). Each experiment was independently repeated at least two times.

2.4. Genetic-based Assays

These assays were performed at Colon Pathology Study Group of IPOLFG (Lisbon, Portugal).

2.4.1. RNA extraction and cDNA synthesis

In order to evaluate variations in HT29 cell spheroids genetic expression, two different experiments were performed: the study along the culture growth (day 4, 7 and 12) and the study of the effect of OPE and PMFs in each culture time. For the first experiment, a sample of 1 mL was taken directly from the spinner flask in the defined culture days. For the second experiment, 50 HT29 spheroids were plated per well in a 6-well plate for 72h with OPE (EC50 concentration adjusted according to the tumor size/culture day) and PMFs (individually and the mixture of the four in the same concentrations present in the OPE tested) diluted in RPMI/0.5% (v/v) FBS. The respective DMSO and EtOH controls were included. Spheroids were collected, centrifuged 5 minutes at 200 g (Miikro 220R, Hettich Zentrifugen, Germany) and, cellular lysis was performed by addition of 600 μL of lysis buffer (RNEasy mini kit, QIAGEN, USA) with the help of mechanical cellular disruption with a syringe. The samples were stored at -80ºC. Total RNA was extracted using RNeasy mini kit (Quiagen, USA) according to manufacturer's instructions [145]. At the end, RNA concentration was spectrophotometrically measured at an optical density of 260 nm in NanoDrop 2000 (Thermo Scientific, USA).

For the cDNA synthesis, a RT-PCR was performed using reagents from Invitrogen (USA). Briefly, a first mixture was made containing RNA (with a final concentration of 30 ng/μL or 22.5 ng/μL), 0.5 μL of random primers and, H_2O with DEPC until final volume of 7.75 μL/tube. The hybridization was made at 70ºC for 10 min in the Veriti 96-well thermal cycler (Applied Biosystems, CA, USA). Then, samples were put in ice and 12.25 μL/tube of second mixture added (holding 4 μL of buffer 5x, 4 μL of dNTPs, 2 μL DTT, 0.75 μL RNAse out, 1 μL Super Script, 0.5 μL H_2O). The RT-PCR continued with the following conditions: annealing at 42ºC for 1h and, extension at 70ºC for 15 min. At the end, samples were diluted in sterile water at final concentration of 6.25 ng/μL at kept at -20ºC.

2.4.2. Quantitative reverse transcription-polymerase chain reaction (RT-qPCR)

This technique allows having a qualitative and quantitative analysis of DNA due to the binding of a fluorescence probe (SYBR Green I) to the double stranded DNA molecule. Thus, in each sample, the fluorescence is proportional to the amount of DNA amplified and the quantification is relative since is calculated by normalizing data using an endogenous gene control – GAPDH (housekeeping gene).

Briefly, 2 μL of cDNA was amplified with Power SYBR® Green Quantitative PCR MasterMix (Applied Biosystems, CA, USA) or Kapa SYBR® Fast Universal qPCR kit (Kapa Biosystems, MA, USA) according to the conditions optimized for each primer (Table 2.2). Reactions were carried out in ABI Prism 7900HT Sequence Detection System (Applied Biosystems, CA, USA) with the following conditions: initial denaturation at 50ºC for 2 min, 40 cycles of denaturation and annealing (95ºC for 15 sec followed by 60ºC for 1 min) and, finally a dissociation stage at 95ºC for 15 sec followed by 60ºC

and 95ºC for 15 sec each. Each experiment was done in triplicates. All data were directly normalized to the expression levels detected for GAPDH, subsequently indirectly normalized relatively to the 2D sample (samples from the first experiment) and the solvent control (samples from the second experiment).

Table 2.2 – List of primers and respective concentration used for RT-qPCR assays.

Primer	Concentration (pmol/µL)	qPCR kit
AXIN2	3.5	Applied Biosystems
BIRC5	5	Applied Biosystems
CD44	5	Kapa Biosystems
CD44V6A	10	Kapa Biosystems
CDH1	5	Applied Biosystems
CNNA2	5	Kapa Biosystems
CTNNB1	10	Applied Biosystems
EGR1	5	Kapa Biosystems
EPCAM	3.5	Applied Biosystems
GLI1	10	Kapa Biosystems
LGR5	7.5	Kapa Biosystems
p21	5	Kapa Biosystems
PROM1	3	Kapa Biosystems
SNAI1	5	Applied Biosystems
SOX9	5	Applied Biosystems
VIM	5	Kapa Biosystems

3. Results and Discussion

With the crescent worry about Earth planet and the ecosystems there has been an increasing of green technologies in every sector. In this field, the valorization of food industry residues has been recognized due to new value added compounds that might be applied in nutrition, health and cosmetics industries. In particular, orange peel represents a huge waste residue from food industry corresponding to more than 15.6 million metric ton/year [146]. Due to its higher content in flavonoids, namely PMFs [69], [74], the development of green technologies that are able to isolate these bioactive compounds from its source is very attractive. Among all extraction processes, supercritical fluid extraction (SFE) is recognized as a highly selective technology for natural products using less time for extraction and replacing toxic organic solvents for green ones [141]. Additionally, this method has been reported to be efficient for the selective extraction of PMFs from citrus products [68]. Importantly, previous work developed by the host laboratory showed that PMF-rich extracts derived from orange peels and produced using supercritical fluid extraction with CO_2 and EtOH as co-solvent (20% v/v) were able to inhibit colorectal cancer cell growth [88], [132]. Once there is no information regarding the effect of citrus extracts in CSCs, the present work aiming at evaluating the application of orange peel extracts, obtained in Part 1, in characterized 3D HT29 colorectal cell model (Part 2) in order to evaluate the effect of phytochemicals in targeting CSCs population of the HT29 cell spheroids (Part 3).

3.1. Screening of orange peel extracts: phytochemical characterization and antiproliferative effect

In the first part of this work, orange peel extracts produced by SFE using different co-solvent percentages (80%CO_2/20%EtOH – OPE 1 and 50%CO_2/50%EtOH – OPE 2) were characterized in terms of phytochemical content and antiproliferative effect aiming at understanding the effect of type of solvent on the recovery of bioactive compounds from citrus wastes. Figure 3.1 shows the phenolic profiles of both extracts obtained by HPLC-DAD-UV and as it can be seen, similar phenolic composition was obtained for both samples.

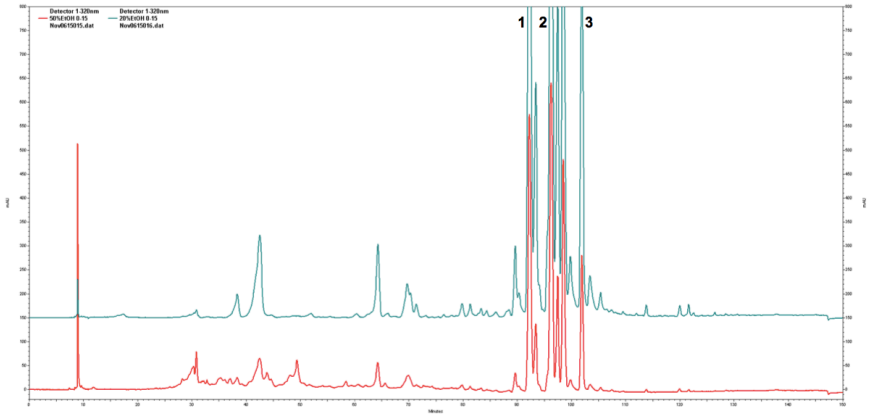

Figure 3.1 – HPLC chromatograms of OPE1 (blue) and OPE 2 (red) recorded at 320 nm. Legend: 1 – sinensetin; 2 – nobiletin; 3 – tangeretin.

The PMF content was determined using the peak areas of the chromatogram recorded at 320 nm and results showed that OPE 1 presented two times more PMF content than OPE 2 (Table 3.1) suggesting that the percentage of ethanol in this extraction influenced the selectivity for PMFs. Therefore, in this study, 20% of EtOH allowing the production of orange extracts with higher content in nobiletin, sinensetin and tangeretin. Supporting this hypothesis, using higher percentages of ethanol in SFE has been described to promote the extraction of more polar compounds decreasing the selectivity for the extraction of the compounds of interest – PMFs [141].

Table 3.1 – PMF content of orange peel extracts and EC50 values obtained.

Extracts	**CO_2-EtOH ratio**	**Nobiletin** (mg PMF/g extract)	**Sinensetin** (mg PMF/g extract)	**Tangeretin** (mg PMF/g extract)	**EC50 values** (mg extract/mL)
OPE 1	80-20	20.20	16.89	7.89	0.574 ± 0.135
OPE 2	50-50	11.78	9.50	2.57	1.175 ± 0.078

The antiproliferative effect of these extracts was evaluated using a HT29 cell monolayer and the dose-response curves are shown in Figure 3.2. OPE 1 showed higher antiproliferative effect (EC50 = 0.574 ± 0.135 mg extract/mL) than OPE 2 (EC50 = 1.175 ± 0.078 mg extract/mL). These results are in accordance with PMF content of extracts. In fact, all the PMFs identified, namely nobiletin, sinensetin and tangeretin, have been reported to have antiproliferative effect in several cancer cell lines, including HT29 cell line [74], [85].

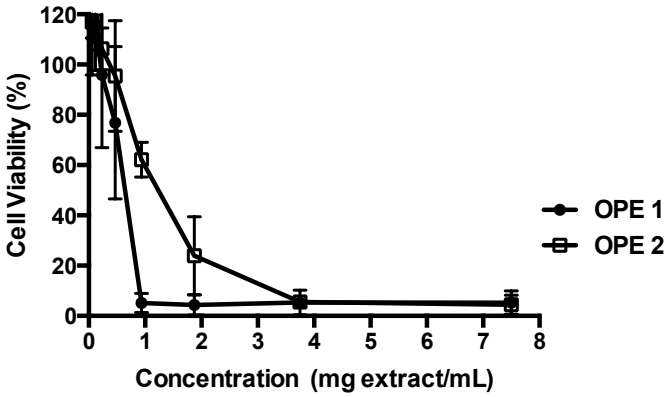

Figure 3.2 – Antiproliferative effect of OPE 1 and OPE 2 after 24h incubation on HT29 monolayer. Results were mean ± SD (n=3).

Using the same extraction protocol (section 2.1), however starting from different raw material, OPE 3 was obtained. This extract had similar concentrations of sinensetin and nobiletin and, less content of tangeretin (Tables 3.1 and 3.2).

Table 3.2 – PMF content of orange peel extracts (OPE 3) and EC50 value obtained.

Extracts	**CO_2-EtOH ratio**	**Nobiletin** (mg PMF/g extract)	**Sinensetin** (mg PMF/g extract)	**Tangeretin** (mg PMF/g extract)	**Scutellarein tetramethylether** (mg PMF/g extract)	**EC50 values** (mg extract/mL)
OPE 3	80-20	19.76	17.36	3.88	10.80	0.348 ± 0.041

OPE 3 showed strong antiproliferative activity even compared with OPE 1 obtaining smaller EC50 value (0.348 ± 0.041 mg extract/mL) (Table 3.2). This might be due to the differences of tangeretin concentrations. Moreover, the increased time of fraction collected in OPE 3 comparing to OPE 1 might also influence the concentration of PMFs. Region of growth, type of soil, time of harvest and many other factors influence the composition of the oranges, thus it is normal to obtain extracts with differences in their content [147].

A chromatogram peak area highlighted in all OPE chromatographic profiles for having an higher peak area than tangeretin (Figures 3.1 and 3.4 A) was identified in OPE 3 (Table 3.2) as scutellarein tetramethylether by HPLC-DAD-UV, a PMF that has been reported with hemostatic, anti-inflammatory and antiproliferative activities [74], [147]–[149]. Moreover, OPE exhibited antiproliferative activity in a time- and dose-dependent manner. When HT29 cell line was incubated with OPE 3 for 72h, a decrease of EC50 value was observed (Figure 3.3).

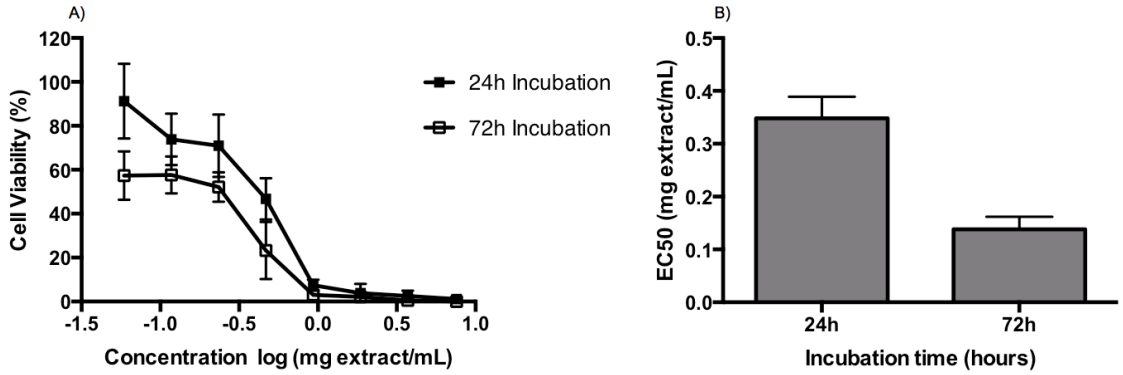

Figure 3.3 – Antiproliferative activity of OPE 3 with two different times of incubation using HT29 cell line (A). Results were mean ± SD (at least n=2). EC50 values obtained (mean ± SD) (B).

Aiming at evaluating if the metabolites presented higher antiproliferative potential than the original extract, OPE 3 was submitted to an *in vitro* digestion, step using a standardized protocol with the simulation of gastric and intestinal enzymatic digestion as described at section 2.1.1. The phenolic composition and the antiproliferative effect were compared for both samples and results are present in Figure 3.4.

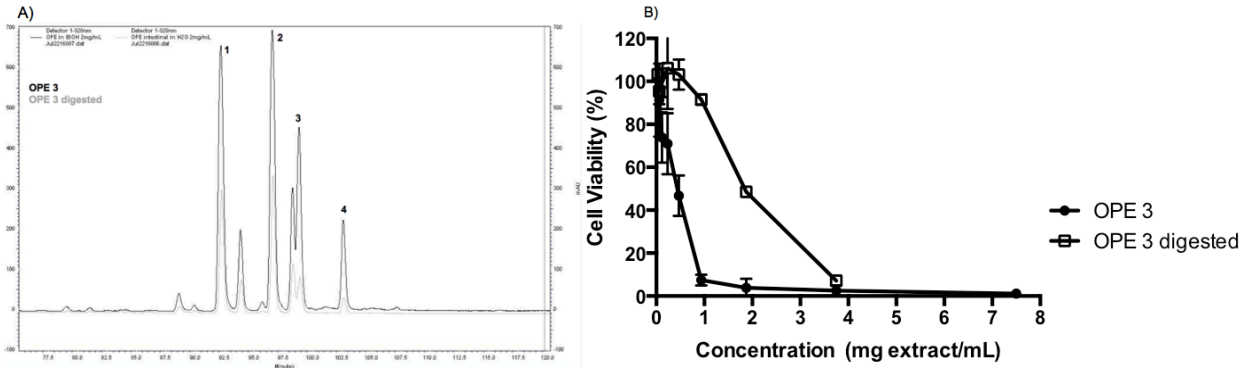

Figure 3.4 – HPLC chromatograms of OPE 3 (black) and its gastrointestinal digested sample (grey), both at concentration of 2 mg sample/mL (recorded at 320 nm). Legend: 1 – sinensetin; 2 – nobiletin; 3 – scutellarein tetramethylether; 4 – tangeretin (A). Antiproliferative activity of OPE 3 and its digested sample in HT29 colon cancer cell line with 24h of incubation. Results in mean ± SD (n=3) (B).

When analyzing the phenolic profiles of samples collected by HPLC-DAD-UV at 320 nm, it was possible to observe that similar profiles were obtained for both OPE 3 and OPE 3 digested. However, OPE 3 showed higher PMF content indicated by the highest peaks intensity and thus, to reduced cell viability. In fact, this effect was observed for all PMFs identified namely sinensetin, nobiletin, scutellarein tetramethylether and tangeretin.

It is important to note that in this work, *in vitro* digestion did not originate new compounds (through biotransformation of PMFs) as described by other authors [91], [150], [151]. Instead, there was a decreased of PMFs content. Sinensetin, nobiletin, tangeretin and scutellatein tetramethylether showed smaller chromatogram peaks indicating lower concentration compared to OPE 3. The digestion performed in this work only applied the action of gastrointestinal enzymes. Published studies, included the intestinal microbiota as they used animal models (mice ingested the compounds and urine and feces were analyzed). As a result, intestinal bacteria flora might play a crucial role in the biotransformation of PMFs compounds, as it was already described that interactions with it originated metabolites (demethylated and hydroxylated derivate with the flavonoid structure preserved (Appendix A)) with health benefits [150]–[153]. Once there are studies supporting the efficiency of metabolites derived from nobiletin and tangeretin, further studies most be done in this area specially to understand the role of intestinal microflora and its application.

Literature reported the stronger inhibitory effect of metabolites comparing to the compounds of origin in colon cancer cell lines [151]–[154]. As Figure 3.4 B shows the antiproliferative effect was lower in OPE 3 digested (EC50 = 1.831 ± 0.106 mg extract/mL) being related to the degradation of PMFs as

observed in Figure 3.4 A. Moreover, these results confirmed the effectiveness of the inhibition of cellular proliferation by the presence of the PMFs identified although in lower concentrations.

In summary, OPE 3 showed to be the extract with the highest antiproliferative effect and promising anticancer potential, thus being selected for further studies with pure compounds aiming at determining the effect of each constituent and interaction of the main bioactive compounds in the sample. It is important to mention that for orange extracts cytotoxicity assays in Caco-2 cell line were performed, and the values of EC50 were not cytotoxic in this cell model (Appendix B).

In addition to the effect of OPE, the PMFs herewith identified were also tested in combination aiming at understanding their contribution at the OPE. The interactions between compounds were analyzed (Appendix C) by Compusyn software. In Figure 3.5 is represented the antiproliferative activity of all combinations, present in equivalent concentrations that were tested in the extract.

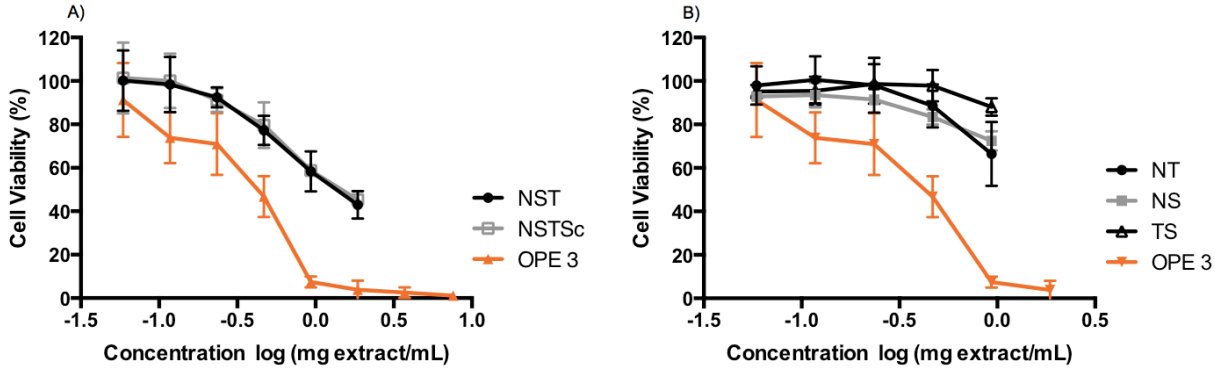

Figure 3.5 – Antiproliferative effects of the mixture of three (NST) and the four PMFs (NSTSc) (A) and the mixture of two PMFs (NT/NS/TS) (B) present in OPE 3. Incubation time of 24h using HT29 cell model. Results were expressed in mean ± SD (n=3). Legend: N = nobiletin; S = sinensetin; T = tangeretin; Sc = scutellarein tetramethylether.

Among mixtures of three (EC50 = 1.356 ± 0.193 mg extract/mL) and the four (EC50 = 1.438 ± 0.226 mg extract/mL) compounds, there were no differences in their effect on HT29 proliferation showing that scutellarein tetramethylether did not influence cell proliferation (Figure 3.5 A). In fact, Compusyn analysis (Appendix C) showed no tendency in the combinations using this PMF. Therefore, to combine two compounds, only sinensetin, nobiletin and tangeretin were tested where combinations NT, NS and TS showed weak antiproliferative effect (Figure 3.5 B) with no EC50 values calculated.

Appendix C describes all the data related to the Compusyn analysis where the evaluation of interactions between PMFs, showed to be more antagonistic for NT combination (CI >> 1), more synergistic for TS (CI values: 0.7877, 0.2908, 0.4603) and all antagonistic, additive and synergistic for NS combination (CI values: 1.7432, 1.2638, 0.9552, 0,5913). Testing several possible combinations with three compounds (namely nobiletin, sinensetin and tangeretin), higher CI values were obtained when adding tangeretin to the combination NS, promoting antagonistic interactions. In contrary, adding sinensetin to the combination of NT promoted synergism and nobiletin induced additive effect whereas antagonism or synergism. It is important to mention that once it was not possible to obtain

cellular viability values below the EC50, the analysis by Compusyn software was not totally efficient. Together, dose-response curves and Compusyn data might suggest the possibility of the presence of other compounds as terpenes (frequent compounds in citrus fruit [69]) that might have effect on proliferation and/or interact with these PMFs in order to potentiate their effect [61], [154]. Especially, monoterpenes are a common compound in *Citrus sinensis* [155] with anticancer activity documented in HT29 colon cancer cells [156].

To better understand the individual impact of each PMF and its potential interactions, and analysis of cell viability with pure PMF compounds was also performed (Figure 3.6) where none of the compounds showed higher or similar antiproliferative effect comparing to OPE 3.

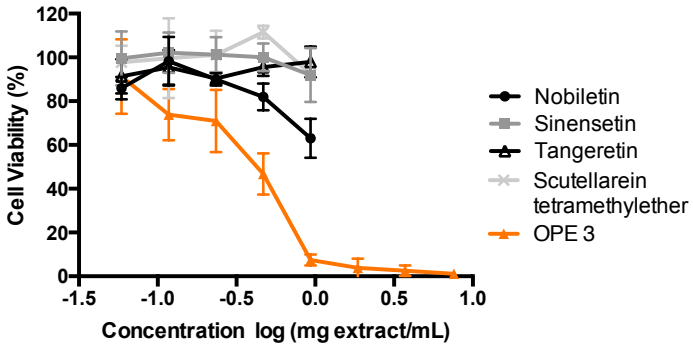

Figure 3.6 – Antiproliferative effect of standard PMFs compared to OPE 3 activity using HT29 cell line with 24h incubation (at least n=2 – results were mean ± SD).

Tangeretin showed weaker proliferative activity and nobiletin the stronger, which might be correlated to their concentration at the extract (Tables 3.2). Comparing nobiletin with sinensetin and scutellarein tetramethylether, which concentrations were at the same order of magnitude (Table 3.2), nobiletin continued to be the compound with higher antiproliferative activity. This might be explained by their chemical structure (Appendix A), since the absence of C-8 methoxyl in this class of compounds (in sinensetin and scutellarein tetramethylether) had been reported to negatively affect the antiproliferative activity [157]. Moreover, presence of methoxyl groups at the A-ring (in the case of nobiletin and tangeretin) enhanced the antiproliferative activity of the PMFs [158].

It is important to note that all the concentrations tested for PMFs were lower than those evaluated for OPE 3 due to the solubility of these compounds (concentration log -0.03 corresponding to concentrations above 0.96 mg extract/mL equivalents of OPE, the crystallization occurs interfering with the cell viability assay). Solubility problems with PMFs have already been reported [72]. Hence, the maximum concentrations tested for each compounds were: 43.70 µM for sinensetin, 46.05 µM for nobiletin, 9.76 µM for tangeretin and 29.58 µM for scutellarein tetramethylether.

PMFs are known by their anticancer properties [74]. The effect of sinensetin, nobiletin, tangeretin and scutellarein tetramethylether had been shown on several cell lines: breast, prostate and melanoma, lung, colon and gastric [74], [85], [159]–[162]. For the concentrations here tested, specially nobiletin and tangeretin (for which more data were found) showed comparable cellular viability percentages

with the literature [85], [160]. Studies previously described lower EC50 values for tangeretin followed by nobiletin, sinensetin and scutellarein tetramethylether [74], [157]. In this work, nobiletin was the PMF that probably most contributed for the OPE 3 effect due to its concentration however, it is needed the combination of more PMFs to reach the OPE 3 effect, Therefore, NST and NSTSc combinations showed high antiproliferative activity in HT29 cell monolayer although not effective as OPE 3, confirming the presence of other compounds at the extract. Additionally, cytotoxicity evaluation was performed in Caco-2 cell line showing no effect on the concentrations tested in HT29 cell line model (Appendix B).

3.2. Characterization of HT29 spheroids enriched in CSCs

Three dimensional cell models are complex and effective models for studying tumor biology [96]. Here, using 3D cell model of HT29 cell line previously developed by the host laboratory, cancer stemness was evaluated by gene expression analysis of stemness markers along different times of culture. The capacity of tumor self-renewal was analyzed using soft agar colony forming unit assay. Additionally, HT29 cell spheroids were also characterized relatively to the involvement of key signaling pathways and EMT by gene expression analysis of representative markers. The selection of the markers was based on the literature (sections 1.1.2-1.1.5) being the key factors or the most frequent markers applied to evaluate stemness and EMT characteristics.

3.2.1. Analysis of cancer stemness markers

The contribution of cancer stem cells fraction was evaluated in HT29 cell spheroids. Along the culture of the spheroids, samples were collected at days 4, 7 and 12, where HT29 cell spheroids have been reported to have different sizes associated with different cellular organization and composition [88], [132]. Spheroids dissociation was performed as described in sections 2.3.8 and 2.4.1. Biomarkers assessed were *PROM1*, *LGR5, CD44, CD44V6* and *SOX9* (by RT-qPCR) and ALDH (by flow cytometry). Results were compared with the 2D sample.

Figure 3.7 represents gene expression of several stemness markers where stemness characteristics appears to increase from the monolayer cells to day 4 of 3D culture, especially *CD44* and *PROM1* (encodes for CD133 gene). Along the culture, expression of stemness markers decreased on day 7, except for *SOX9*, although, *CD44*, *PROM1* and *SOX9* maintained their overexpression compared to 2D cells. From day 7 to 12 of culture, expression of *CD44* and *PROM1* increases again but *LGR5*, *SOX9* and *CD44V6A* expression levels maintained low or similar to the 2D culture.

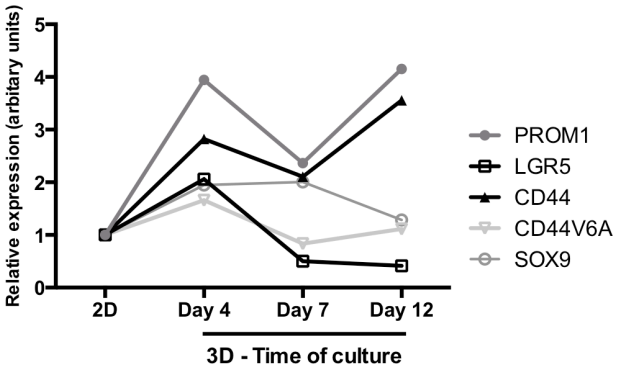

Figure 3.7 – Relative expression of stemness markers along HT29 cell culture. Results were normalized relatively to the HT29 monolayer and experiment performed in triplicate using RT-qPCR.

This analysis allowed observing the differences during time of culture and even the differences between cell monolayer and the 3D architecture and globally, the 3D cellular aggregation increased stemness expression. CD44 and CD133 were considered for a long time as the most representative markers for CSCs. The expression of these markers in colon cancer cells has been associated with higher tumorigenicity [44], [46]. $CD133^{+}$ and $CD44^{+}$ cells might be the populations responsible for

tumor initiating in HT29 culture. The increased expression of these markers during the first four days of culture suggested a superior cellular aggregation and proliferation activity of these populations relatively to the others. Conversely, the previous work described similar expression of CD44 in 2D and day 3 spheroids by FACS [132]. The spheroids architecture changed at day 7 of culture, where a stratified cell population and a necrotic/apoptotic center was observed [132]. These changes might be the reason for the somehow decreased expression of stemness markers, although in the case of *PROM1* and *CD44* this may be not relevant as they continue overexpressed. *LGR5* increased expression was found in primary and metastatic colon tumors [49]. In this work, an increased expression on day 4 features the stemness profile of HT29, however, there is a decrease in the others days of culture. CSCs population is also considered as responsible for tumor relapse through its dedifferentiation followed by EMT and metastasis [50]. Previous work from host laboratory hypothesized the possibility of HT29 spheroids undergo EMT at day 12 (section 1.3.3) [132]. Moreover, high expression of CD133 and CD44 has been associated with metastatic stage in HCT116 colon cell line [46]. These evidences might explain the higher expression of *CD44* and *PROM1* at day 12 comparing to day 7 of culture.

Additionally, the presence of $ALDH^+$ cells, also indicative of stemness, was evaluated in the HT29 culture. As Figure 3.8 shows, the HT29 cell line was rich in ALDH positive cells. There was a slight increase of $ALDH^+$ population from 2D to 3D (days 4 and 7 of culture). However, a significant ($P \leq 0.05$) decrease was observed on HT29 cell spheroids collected at day 12 of culture. The decrease in day 12 is in agreement with the decrease observed in gene expression for *LGR5* and *SOX9* at this time point.

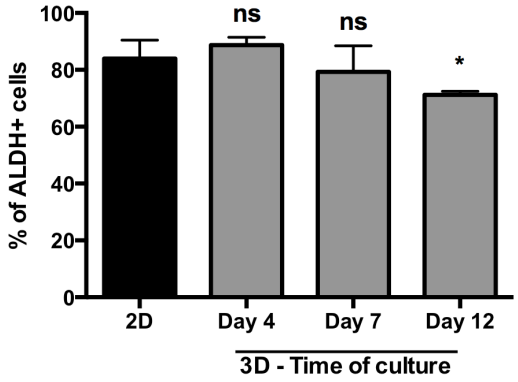

Figure 3.8 – Percentage of $ALDH^+$ cells in 2D and 3D HT29 models. Results were obtained by ALDEFLUOR assay and were expressed as mean ± SD of two independent experiments. The significant differences are expressed in asterisks (ns $P>0.05$; * $P\leq0.05$) by one-way ANOVA analysis for comparisons with 2D.

Since results showed high percentage of $ALDH^+$ cell in 2D and 3D models, HT29 cell line might be characterized by ALDH-rich phenotype. Nonetheless, it was previously described higher tumorigenicity in $CD44^+/CD133^+$ colon cells with association to $ALDH^+$ phenotype than the negative [47]. Also, previous work with this model revealed that HT29 cell spheroids have a high proliferative rate at day 12 of culture due to the presence of $CD44^+$ phenotype by immunofluorescence (section 1.3.3, Figure

1.12) [132]. Thus, it suggests the possibility of ALDH expression being related to the overexpression of CD44 and PROM1 (Figure 3.7).

CD44, *CD133* and ALDH appear to contribute for the CSCs-enriched population of the HT29 cell aggregates. These results are in agreement with existing literature that demonstrated the presence of CD44, CD133 and ALDH enriched populations in HT29 cell spheroids [134]. Nevertheless, as mentioned in section 1.1.5 and by these results, tumor heterogeneity and complexity requires a set of markers to characterized the stem population. These results showed that only one marker is not sufficient, especially ALDH, to accomplish this characterization. These three markers together with *LGR5* create a good set for characterize the HT29 CSCs population in CRC once each one reflects different functions related to stemness (section 1.1.5, Table 1.2).

3.2.2. Evaluation of capacity of self-renewal

Self-renewal is an essential property of CSCs [163], and it is described by the ability of originate one or two stem cells by symmetrical or asymmetrical cell division. This mechanism allows the tumor to maintain the CSCs population and it is measured by the cell capacity of spheroid formation [164]. In order to evaluate this property, HT29 cell spheroids at days 4,7 and 12 of culture were dissociated as described in section 2.3.7 and then isolated cells introduced in an agarose-based matrix and the capacity of forming secondary tumor colonies observed. Figure 3.9 shows the number of colonies obtained with cells from each day of spheroid culture and results were compared with 2D model.

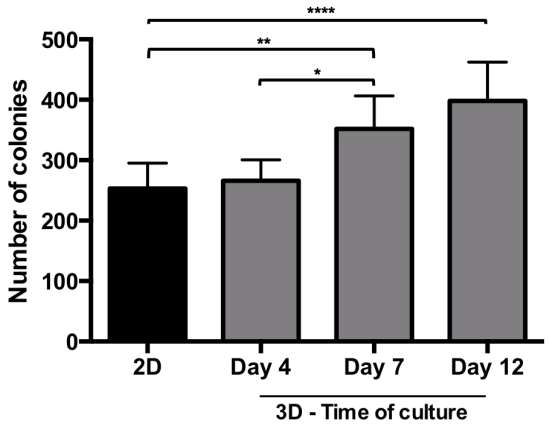

Figure 3.9 – Capacity of HT29 spheroids forming secondary tumors (colonies) through soft agar colony forming unit assay. After 14 days, the resulting visible colonies were counted and expressed in mean ± SD (at least n=2). The letter labels on the histogram indicate the statistical significant differences according to one-way ANOVA for multiple comparisons (* P≤0.05; ** P≤0.01; **** P≤0.0001).

All the samples were capable of forming large number of colonies (200 – 450), morphologically similar in shape and size. Plate efficiency was calculated (Table 3.3) showing resemblances in the same order of magnitude with studies using HT29 cells [65]. Colony formation number increased significantly when used cells from days 7 and 12 of 3D culture. Studies have been reported the association of stemness markers with the capability of cell forming colonies where $ALDH^+$ HT29 cells were capable of forming colonies in contrast to $ALDH^-$ cells [165], the silencing of Lgr5 formed less and smaller spheroid colonies [165] and the presence of $CD133^+/CD44^+$ phenotype is recognized to enhance tumorigenicity [44]. Consequently, the increased capability of forming colonies confirmed the highly rich CSCs phenotype of HT29 cell line. Moreover, it suggests that the capability of growing colonies appear to be associated with the presence of a rich cell population in *CD44* and *CD133*, more than ALDH and *LGR5* considering their decrease at day 12 of culture (section 3.2.1, Figures 3.7 and 3.8) and the fact that it has been shown not to influence negatively the number of colonies formed, as described by *Chen et al*. [165].

Table 3.3 – Plate efficiency of HT29 cells expressed in mean ± SD.

HT29 cell model		Plate efficiency (%)
2D		12.65 ± 2.11
3D model	**Day 4**	13.30 ± 1.72
	Day 7	17.59 ± 2.74
	Day 12	19.90 ± 3.22

3.2.3. Involvement of key signaling pathways and EMT

The results of the expression of markers for cell adhesion, invasion, EMT and Wnt signaling pathways (by RT-qPCR) are shown in Figures 3.10, 3.11 and 3.12. In general, there was an increase in gene expression for most of the markers on day 4 of culture followed by a decrease during the next days to similar expression levels as observed in the 2D sample. However, *SNAI1* and *AXIN2* genes maintained overexpressed and the expression of *GLI1* and *EGR1* is almost lost.

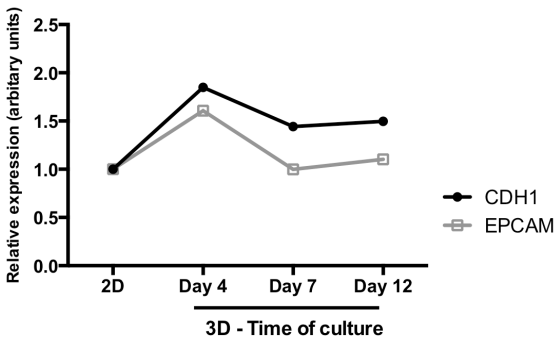

Figure 3.10 – Relative expression of epithelial markers using RT-qPCR. Results were normalized relatively to the HT29 cell monolayer and experiment performed in triplicate.

One of the first steps of EMT is the loss of E-cadherin (encoded by *CDH1* gene) [26]. Here, its slight higher expression (*CDH1* gene) at day 4 relatively to days 7/12 (Figure 3.10) might be due to the presence of a bigger cellular aggregation comparing to the other days where the apoptotic/necrotic core promotes lower compaction, as previously described [132]. The cellular density at the spheroids promoted E-cadherin expression, although it was not highly overexpressed once its regulator *SNAI1* (it inhibits *CDH1*) was activated (Figure 3.11), down-regulating E-cadherin [163]. EPCAM is an important epithelial and cell adhesion marker whose overexpression contributes to tumor progression and it is a common feature at CRC [167]. As a cell adhesion marker its expression follows the expression of *CDH1*, confirming the just mentioned cell adhesion considerations about the spheroid culture. Although its expression normally keeps up the CD44 expression [52], in this cancer model it was not possible to demonstrate. Data demonstrated that *EPCAM* expression did not vary between 2D and 3D cells.

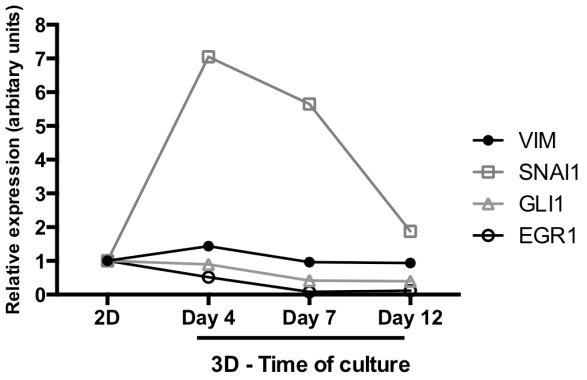

Figure 3.11 – Relative expression of EMT markers using RT-qPCR. Results were normalized relatively to the HT29 monolayer and experiment performed in triplicate.

Loosing the epithelial phenotype, tumor cells tend to replace it by a mesenchymal one. The most known mesenchymal marker studied in several tumors is Vimentin, which expression is inversely associate to the lost of E-cadherin [168]. As depicted in Figure 3.11, *VIM* (encoding Vimentin) expression slightly increased at day 4 of culture and maintained the expression levels similar to the monoculture for the following days. This may be discrepant with what *Silva* (2013) described once at

day 3 of culture did not find expression of the mesenchymal marker [132]. Since RT-qPCR analysis was performed at day 4 of culture, a day after *Silva* (2013) analyzed, the HT29 cell spheroids could start already expressing Vimentin. Moreover, although it was expected an overexpression during the culture, reflecting the evolution of tumor to an invasive stage, this was not observed. Indeed, Vimentin expression levels in 2D and 3D cell culture appeared to be similar, however further analysis must be performed to complement this information. E-cadherin-Vimentin relation may not be so linear as it was expected, in fact, in some 3D cell models was detected the presence of Vimentin and no significant expression of E-cadherin in mono- and co-cultures [169]. Another EMT marker is Snail, a transcription factor that regulates EMT and downregulates E-cadherin that recently has been associated to CSCs activities, as $CD44^+$ HT29 cells had been reported with higher expression of this marker than $CD44^-$ cells [163]. In agreement, the increased expression of *SNAI1* in day 4, relatively to the 2D culture, resembles that of *CD44* (section 3.2.1, Figure 3.7). Regarding *EGR1* and *GLI1*, these markers showed a slightly decrease expression relatively to the 2D cell culture. The role of Egr1 has been along disputing once is considered tumor suppressor (in breast and lung cancer) or promoter (prostate and gastric cancer). In colon cancer had been reported as an apoptosis inhibitor and tumor growth developer, and also its expression is proportional to tumor stage development [170], [171]. Therefore its expression is not consensual. Gli1 is a transcription factor associated to Hedgehog signaling. This molecular pathway has been reported in epithelial colon cancer cells as one of the pathways associated to metastatic behavior due to the upregulation of Gli1 [172], plus it has been described with strong signaling in HT29 cell lines [173]. However, other studies showed its downregulation associated to Wnt signaling stimulus and cell proliferation [174]. Therefore, despite the low expression levels of *VIM*, *GLI1* and *EGR1* are somehow concordant with each other. The meaning of this expression signature should be further studied and should be confirmed.

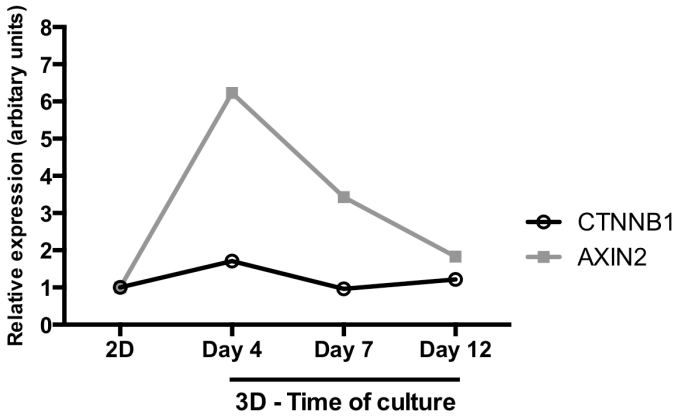

Figure 3.12 – Relative expression of Wnt signaling markers using RT-qPCR. Results were normalized relatively to the HT29 monolayer and experiment performed in triplicate.

In fact, analyzing Wnt signaling pathway markers (Figure 3.12) *CTNNB1* (encoded β-catenin gene) expression increased at day 4 of culture as well as *AXIN2* but in this case showing a higher increase relatively to the cell monolayer. Wnt signaling pathway activation and high β-catenin levels are associated to tumor initiation and progression [27]. The *AXIN2* increase, as a direct Wnt/β-catenin

target gene, is compatible with the increase of *CTNNB1* expression. In fact, Axin2 overexpression is a common feature in CRC [175]. Additionally, increased levels of Axin2 are associated with low cell proliferation and higher levels of Snail, contributing to differentiation and EMT [175]. Indeed, the increase in *AXIN2* expression at day 4 cell spheroids relatively to the 2D cell culture resembled that of *SNAI1* (Figure 3.11).

To conclude, Table 3.4 summarizes the results described in section 3.2 comparing the expression levels of all markers evaluated.

Table 3.4 – Cell markers expression levels along the culture of HT29 cell spheroids relatively to the cell monolayer expression. Legend: 0 = similar expression; +/ - = high/low expression; + + / - - = very high/low expression; + + + / - - - = extremely high/low expression.

Biomarkers		**Cell spheroids expression levels**		
		Day 4	**Day 7**	**Day 12**
Stemness	**CD133 (*PROM1*)**	+ + +	+	+ + +
	CD44	+ +	+	++
	ALDH	0	0	0
	LGR5	+	-	-
	SOX9	+	+	0
	CD44V6A	+	0	0
Epithelial / Cell-cell adhesion	**E-cadherin (*CDH1*)**	+	0	0
	EPCAM	+	0	0
EMT	***VIM***	0	0	0
	SNAI1	+ + +	+ + +	+
	EGR1	-	- - -	- - -
	GLI1	0	-	-
Wnt signaling pathway	**β-catenin (*CTNNB1*)**	+	0	0
	AXIN2	+ + +	+ +	+

Overall, these data complement the results obtained previously by *Silva* (2013) [132]. The relevant alterations were observed between day 4 and days 7/12 showing to be a multistage model. HT29 cell aggregates were mostly characterized by a stemness character than EMT. Along 12 days of culture, the aggregates showed differences related to stemness but it was shown that the culture was enriched in CSCs being the cancer population highly rich in *CD44*, *CD133* and ALDH positive cells. Additionally, increasing expression of *CD44* and *PROM1* resulted in higher self-renewal capacity

where sphere cells from days 7/12 of culture showed higher capacity of forming secondary colonies comparing to monolayer cells. Relatively to the EMT, the acquisition of this character was not a characteristic feature of this HT29 3D cell model. Indeed Vimentin and E-cadherin expressions did not differ inversely and *GLI1* and *EGR1* showed a slight decrease. The absence of the predictable expression signature may indicate the possibility of the HT29 cell spheroids had a partial EMT. This process has been recently described as the presence of both epithelial and mesenchymal phenotypes at the invasive front of the tumor [176]. Partial EMT confers higher plasticity to the cells being also associated with a higher stemness profile [177]. In agreement, *Silva* (2013) described the not fully absence of cell adhesion markers as E-cadherin and CK18 [132]. Results from this work observed the presence of both Vimentin and E-cadherin and, more importantly the overexpression of *AXIN2* and Snail (*SNAI1*) showed to be directly involved in EMT and stemness processes [178]. Given that, HT29 cell spheroids may reflect a model with partial EMT associated to a highly rich stem cell population. This fact makes the model a promising tool for the evaluation of potential anticancer drugs in order to avoid tumor relapse. This poorly differentiated population tends to develop a more aggressive phenotype [122], [179] being more immuno-resistant and chemo-tolerant, thus having higher survival rates [180]. Important to mention, the complexity of the markers needed to characterize the tumors reflects the heterogeneity of CSCs population. Thus, each one cannot be seen individually. All markers make part of a highly genetic network and therefore are always important to take into account their interactions to better understand the biology of cancer.

Specifically for the markers that did not showed differences from 2D to 3D cultures, further analysis specially to HT29 cell monolayer, should be performed quantifying the expression levels. Suggestions fall into flow cytometry or immunoblotting approaches. Moreover, as RT-qPCR was only performed using one culture from 2D and 3D HT29 models, additional cultures must be monitored in order to confirm the partial EMT hypothesis. Also, to analyze the possibility of tumor progression to an invasive and metastatic stage, the culture should be monitored for a longer time.

3.3. Exploring the effect of OPE and PMF compounds in targeting CSCs population

In this section, OPE 3 selected from Part 1 and the main PMF compounds identified were tested in the HT29 cell spheroids characterized in Part 2 for CSCs population aiming at evaluating i) antiproliferative effect; ii) inhibition of self-renewal ability; iii) influence in gene expression, including stemness, EMT, and cell cycle markers. Day 7 spheroids were chosen to performed the assays once previous work already identified the resemblances with *in vivo* tumors due to their structural complexity and stratified population [88], [132], [133]. Moreover, in the present study (section 3.2) spheroids collected at this day of culture presented highly rich population with stemness properties. Only for the genetic expression assessment it was used HT29 cell spheroids with several days of culture.

3.3.1. Antiproliferative activity

The antiproliferative effect of OPE 3 was evaluated on HT29 cell spheroids collected at day 7 of culture using different incubation times – 24h and 72h. Dose-responses curves obtained are demonstrated in Figure 3.13 A showing that OPE 3 inhibited cell proliferation of HT29 cell spheroids in a time- and dose-dependent manner. The antiproliferative effect was improved with 72h incubation being the EC50 value two times lower (EC50 = 1.182 ± 0.071 mg extract/mL). EC50 value of OPE 3 incubated for 24h was 2.188 ± 0.999 mg extract/mL. Longer exposure time might contribute to enhance the access of OPE 3 to the tumor bulk leading to a more effective treatment. Similar results were obtained by *Silva* (2013) where EC50 values were two times lower with the increasing of OPE incubation time [132].

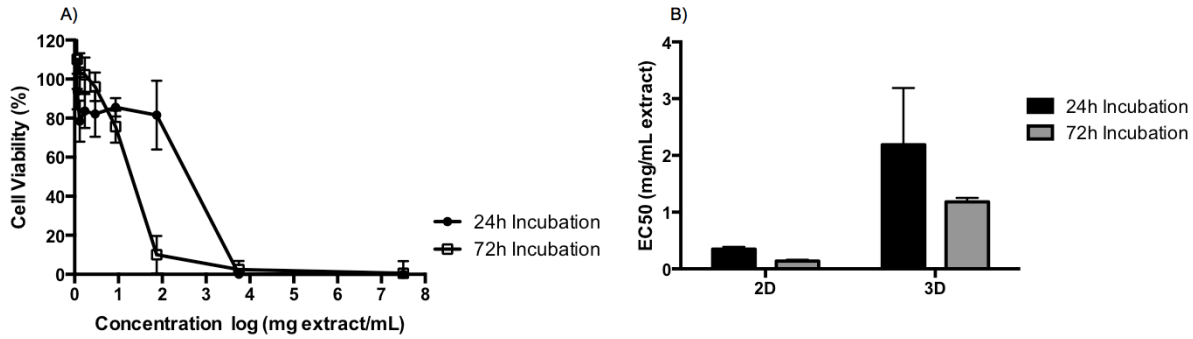

Figure 3.13 – Dose-response curves of OPE 3 at 24h and 72h incubation using HT29 cell spheroids (results were mean ± SD (at least n=3 with hexaplicates)) (A). Comparing EC50 values of 2D and 3D HT29 culture at different incubation times (mean ± SD) (B).

It is important to highlight that when compared with the results obtained in 2D culture (Figure 3.13 B), EC50 values for the HT29 cell aggregates for 24h and 72h exposure are six and eight times higher, respectively. The higher concentration of extract needed to decrease 50% of the cell population may reflect the existence of a higher cellular compaction hindering the diffusion of OPE 3 to all HT29 cells. Also, as already described, HT29 cell spheroids population showed resistant characteristics due to the gene expression alterations related to stemness and EMT (section 3.2) [134].

For the PMFs evaluation, only the combinations of three and four PMFs were assessed once showed higher antiproliferative activity in HT29 cell monolayer (section 3.1). Being the 72h exposure time more effective for OPE 3, it was the time chosen to treat the HT29 cell spheroids with the PMFs. Figure 3.14 shows the relation between OPE 3 and the PMFs where, the mixture of four PMFs (NSTSc) showed similar profile to the OPE 3 effect, demonstrating bigger antiproliferative effect than the combination NST.

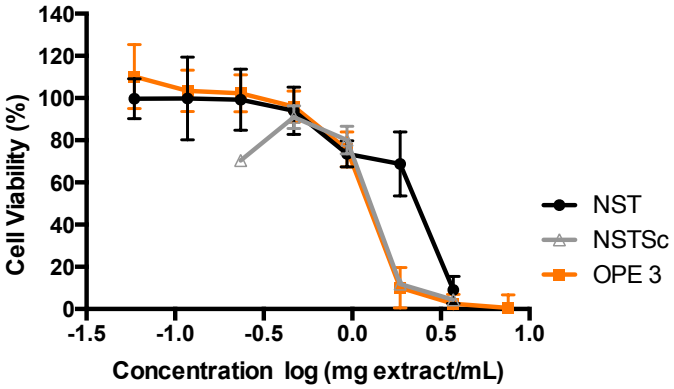

Figure 3.14 – Dose-response curves of the mixture of three (NST) and the mixture of the four PMFs (NSTSc) present in OPE 3. Results were expressed in mean ± SD (at least three independent experiments performed in hexaplicates). Legend: N = nobiletin; S = sinensetin; T = tangeretin; Sc = scutellarein tetramethylether.

Each dose-response curves EC50 values were calculated by GraphPad 6.0 software as Table 3.5 shows. The differences of EC50 values between NST and NSTSc might be influenced by the increasing of incubation time (in HT29 cell monolayer EC50 values were not different), which might influence the activity of the compounds, being the activity of scutellarein tetramethylether more evident. Although these findings, the possible existences of terpenes in the natural extract interfering positively should not be discard.

Table 3.5 – EC50 values of OPE 3 and the mixtures of PMFs determined using 3D model (72h incubation).

Phytochemicals	**EC50** (mg extract/mL)
OPE 3	1.182 ± 0.071
NST	2.048 ± 0.233
NSTSc	1.240 ± 0.144

3.3.2. Inhibition of self-renewal ability

Aiming at assessing the effect of OPE 3 and the PMFs (Figure 3.15) on self-renewal capability of HT29 cells, soft agar colony forming unit assay was performed as described in section 2.3.7 using day 7 cell spheroids. As in the antiproliferative assay, OPE 3 inhibited the growth of colonies in a dose-dependent manner (Figure 3.15 A). At the highest concentration, which was equivalent to EC50 value obtained with HT29 monolayer, it was not observed the formation of colonies. At the other concentrations, colonies formed had mostly smaller diameters than the control. In Figure 3.15 B, results showed higher colony inhibition percentage for NST (52.5 ± 3.5%) and NSTSc combination (55.8 ± 7.1 %) although with no differences between both demonstrating that scutellarein tetramethylether did not influence the colony formation in the mixture. However, the inhibition was far away from the obtained with OPE 3, which highlights the presence of another components at the extract. Additionally, the three isolated PMFs and TS combination showed no effect and, NS and NT combinations showed weak capacity in inhibiting colonies formation at the concentrations present in 0.35 mg extract/mL of OPE 3.

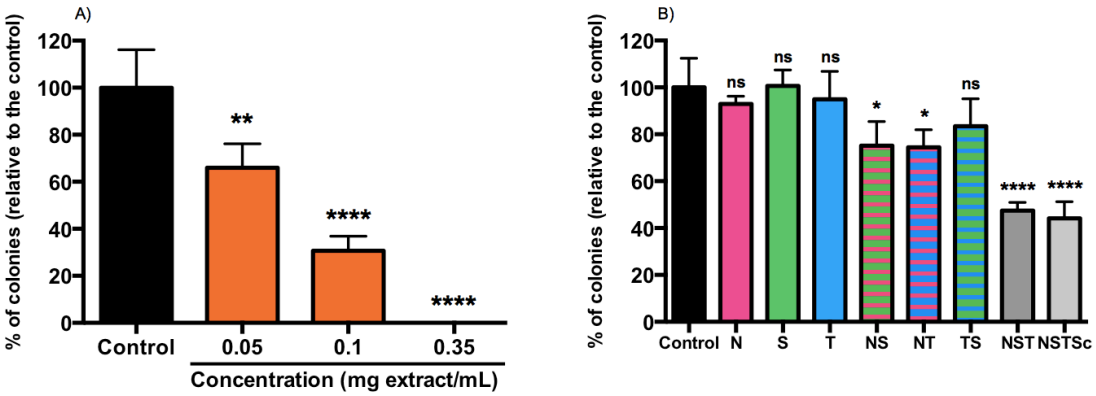

Figure 3.15 – Percentage of colonies formed after treatment with OPE 3 (A) and PMFs with concentration equivalent to 0.35 mg extract/mL (B). Results were mean ± SD in percentage relatively to the control (without treatment) during 14 days (n=3). The asterisks represent the statistical significant differences according to one-way ANOVA for multiple comparisons relatively to the control (ns P>0.05; * P≤0.05; ** P≤0.01; **** P≤0.0001). Legend: N = nobiletin 17.11 μM; S = sinensetin 16.24 μM; T = tangeretin 3.63 μM; Sc = scutellarein tetramethylether 10.99 μM.

Once different concentration of PMFs preclude the chance of comparing them and conclude which bioactive compound contributes to suppress self-renewal capability, another approach was performed where all four PMFs were tested at the same concentration as in Figure 3.16.

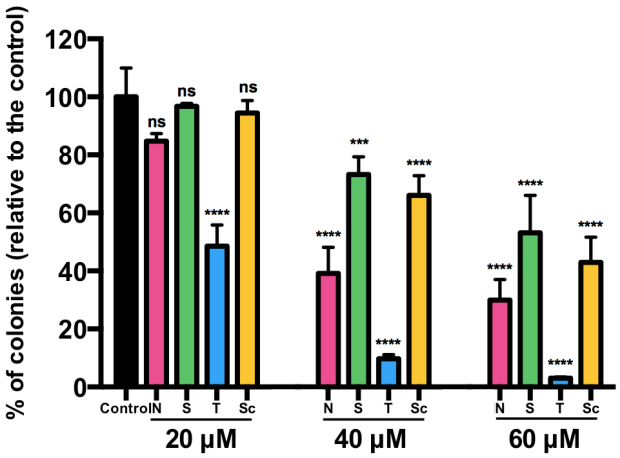

Figure 3.16 – Ability of PMFs to inhibit colonies formation. Results were mean ± SD (n=3). The asterisks represent the statistical significant differences according to one-way ANOVA for multiple comparisons relatively to untreated cells (ns P>0.05; *** P≤0.001; **** P≤0.0001). Legend: N = nobiletin; S = sinensetin; T = tangeretin; Sc = scutellarein tetramethylether.

Figure 3.16 can give two different conclusions. First, when comparing different concentrations for the same compound it was possible to observe that the treatments for all PMFs inhibited colony formation in a dose-dependent manner. Secondly, in each concentration, sinensetin and scutellarein tetramethylether showed less effect than nobiletin and tangeretin. Among all PMFs, tangeretin was the phenolic compound that demonstrated the highest and more prominent effect followed by nobiletin. In fact, with concentration of 40 µM, tangeretin was capable of inhibiting 90.3 ± 1.5% of colonies formation, a higher percentage that the obtained with NST (total of PMFs of 36.98 µM) or NSTSc (total of 47.97 µM). In addition, to obtain similar colony formation inhibition as with NST and NSTSc, it was only needed 20 µM of tangeretin (inhibition of 51.45 ± 7.33%), which shows high effectiveness of this PMF with half of the molarity of the mixtures. Relatively to the other PMFs and mixtures, tangeretin could be a favorable polymethoxylated compound for targeting CSCs since at lower dosages, demonstrated a significant effect on self-renewal inhibition of HT29 cells.

In summary, treatment with OPE 3 and PMFs showed to be dose-dependent. Moreover the concentration of PMFs equivalent to OPE 3 did not have an effective effect. Other studies had also shown no inhibition of colony formation when cells were treated with the standard compounds [65]. Specifically related to PMFs, nobiletin and tangeretin showed weak effect in inhibiting colony formation in lung cancer cell lines, although, this study used monolayer cells with different type of treatment [160]. Nobiletin and mainly tangeretin were able to suppress colon cancer cells colony formation using lower concentrations. Taken together, the results suggested that phytochemical extract rich in tangeretin might have great potential in chemotherapy targeting colon CSCs population.

3.3.3. Inhibition of aldehyde dehydrogenase activity by Aldefluor assay

Before the analysis of the gene expression of HT29 cell spheroids when treated with OPE and its bioactive compounds, a preliminary approach was performed aiming at understanding the influence of the samples in stemness, directly in ALDH$^+$ population. Day 7 cell spheroids were assessed as described in section 2.3.8. The results are presented in Figure 3.17.

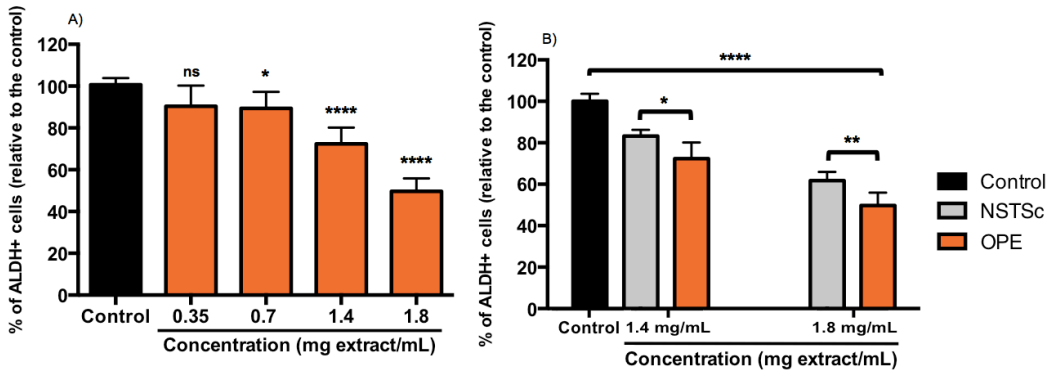

Figure 3.17 – Effect of OPE 3 in ALDH$^+$ cell population (A) and comparing the effect of NSTSc combination with OPE at the ALDH$^+$ population (B). Results were mean ± SD (at least n=2). The asterisks represent the statistical significant differences according to one-way ANOVA for multiple comparisons relatively to untreated cells (ns P>0.05; * P≤0.05; ** P≤0.01 *** P≤0.001; **** P≤0.0001). Legend: NSTSc = combination of nobiletin, sinensetin, tangeretin and scutellarein tetramethylether; OPE = orange peel extract.

As shown in Figure 3.17 A, there was a significant effect of OPE 3 in decreasing the ALDH$^+$ HT29 population in a dose-dependent manner. When the mixture NSTSc was tested at the same concentrations presented in 1.4 mg extract/mL and 1.8 mg/extract/mL OPE 3 (Figure 3.17 B), the effect was statistical different from the OPE 3, which confirms the presence of other compounds in the extract inhibiting ALDH$^+$ population. Table 3.6 resumes the inhibition obtained from both samples (NSTSc and OPE 3), where differences between OPE 3 and the mixture were about 10% inhibition.

Table 3.6 – Effect of OPE 3 and the combination NSTSc on reducing ALDH$^+$ population in HT29 cell spheroids. Results were in mean ± SD.

% of ALDH$^+$ HT29 population inhibition		
Concentration	**1.4 mg extract/mL**	**1.8 mg extract/mL**
OPE 3	27.75 ± 7.76	50.35 ± 6.20
NSTSc	16.75 ± 3.03	38.22 ± 4.16

The standard PMFs were also tested at equivalent concentration of 1.8 mg extract/mL of OPE 3 showing no effect (data not shown). In fact, a reduction of ALDH$^+$ cells were only observed for 100 µM of each compound, and for all the compounds similar effects were observed as Figure 3.18 shows. However, tangeretin showed higher inhibition rate of 19.98 ± 6.61% comparing with the average of the

other three PMFs – 14.69 ± 5.40%. Additional studies could be done in this area with higher concentration in order to determine significant differences between PMFs.

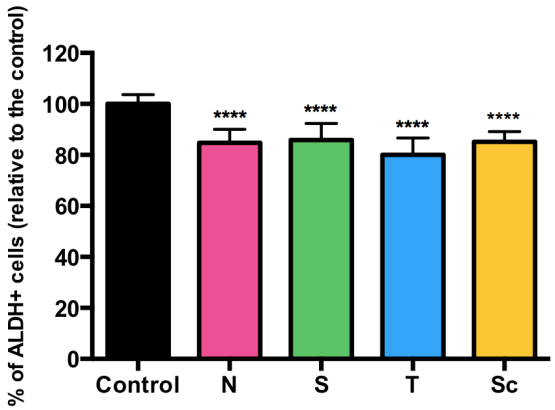

Figure 3.18 – Effect of isolated PMFs in suppressing ALDH$^+$ population using HT29 cell spheroids. Results were mean ± SD (n=3). The asterisks represent the statistical significant differences according to one-way ANOVA for multiple comparisons relatively to untreated cells (**** P≤0.0001). Concentration tested were 100 μM for each PMF. Legend: N = nobiletin; S = sinensetin; T = tangeretin; Sc = scutellarein tetramethylether.

Aldehyde dehydrogenase activity has been associated with the stemness character of the tumor contributing for chemo- and radioresistance. Inhibitors of ALDH activity had been reported from synthetic drugs to phytochemicals as isoflavones and terpenoids [181]. Some chemopreventive compounds, as curcumin, piperine and sulforaphane, had already been reported with the effect in the stemness marker ALDH associated mainly to breast cancer. These studies had 50-90% ALDH$^+$ population suppression with very low treatment dosage (1-20 μM) [182], [183].

3.3.4. Influence on the expression of markers of cancer stemness, EMT, cell cycle and key signaling pathways

The influence of treatments with phytochemical extract and its bioactive compounds on cancer stemness, EMT, cell cycle and key signaling pathways was also assessed by the RT-qPCR analysis of specific markers for days 4,7 and 12 of HT29 cell spheroids culture. For OPE 3 treatment, the concentration approximately of EC50 values corresponding with the size of the culture (data not shown) was tested, being 0.25, 1 and 1.5 mg extract/mL, respectively. The treatment of day 7 cell spheroids was firstly performed as showed in Figure 3.19.

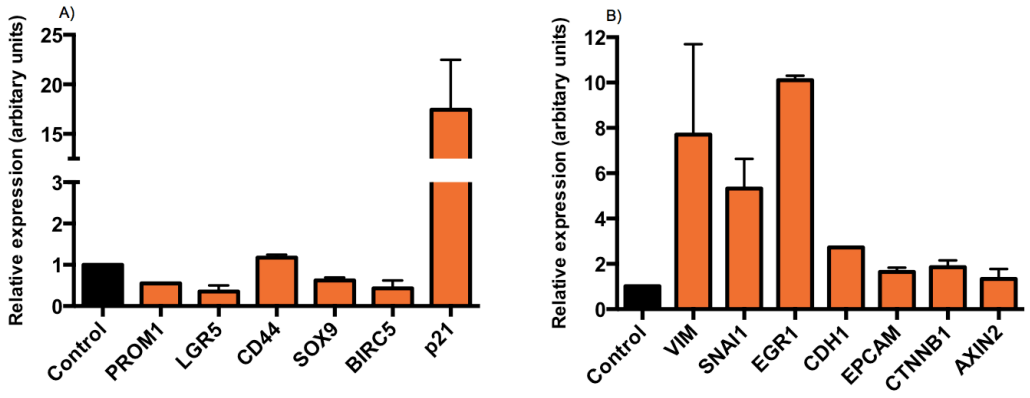

Figure 3.19 – Relative expression of specific markers using RT-qPCR for stemness (*PROM1, LGR5, CD44*, *SOX9*) apoptosis (*BIRC5*) and cell cycle (*p21*) (A); EMT (*VIM, SNAI1*), invasion (*EGR1*), epithelial/cell adhesion (*CDH1, EPCAM*), and Wnt signaling (*CTNNB1, AXIN2*) (B) markers. It was used day 7 of HT29 cell spheroids treated with OPE 3 for 72h. Each expression level was normalized relatively to the solvent control. Results were mean ± SD with at least n=2.

As Figure 3.19 A shows, in the presence of OPE 3 the stemness markers (*PROM1*, *LGR5*, *SOX9*) tend to decrease their expression with the exception of *CD44*, which did not alter. These data are in accordance with the previously postulated once the treatment was capable of decreasing $ALDH^+$ population (section 3.3.3) and being the self-renewal capability intrinsically related with stemness [50], reduction of these markers may associate to an inhibition of colony formation (section 3.3.2). Moreover, although there is no literature reporting the effectiveness of citrus extracts, other phytochemicals have been reporting to reduce CSCs population on colon cancer lines [184].

BIRC5 is an apoptotic marker responsible for preventing apoptosis by caspases-3 and 7 inhibition [185]. Decrease of the marker has been pointing the increase of apoptosis phenomenon by inhibition of cell growth and metastasis [186]. In this work, *p21*, which overexpression is referred to G1/S cell arrest [187], increased highly following OPE treatment. Thus, OPE 3 clearly induced apoptosis and promoted G1/S cell arrest (Figure 3.19 A). Although data are not consistent with G2/M cell arrest assessed by *Silva* (2013) [132], this might be explained by the increasing of concentration and incubation time with the orange extract in the present work (previously was 0.63 mg extract/mL for 24h). Up to now, tangeretin and nobiletin have been shown the most promising results in self-renewal inhibition and antiproliferative activity, respectively. Moreover, these compounds have been described as inducers of G1 cell cycle arrest [85], thus suggesting that OPE 3 capacity of inducing cell cycle arrest might be due to the presence of these two PMFs compounds.

EMT markers (Figure 3.19 B) did not show a decreased of expression, in contrary, the OPE 3 treatment increased EMT and invasion markers with high expression levels of *VIM*, *SNAI1* and *EGR1*. Nevertheless, E-cadherin (*CDH1*), and *EPCAM* are overexpressed contributing to cell adhesion. Therefore, treatment with OPE 3 was capable of reduce the stemness, inducing cell cycle arrest and apoptosis. However, it promoted EMT, which may lead to tumor aggressiveness.

In addition, as mentioned above, OPE 3 was also applied to spheroids of days 4 and 12 of culture their corresponding EC50 values (Figure 3.21).

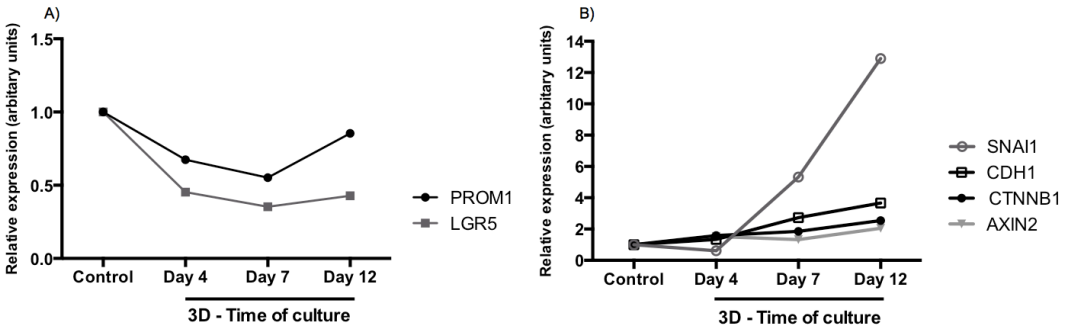

Figure 3.20 – Relative expression of specific markers using RT-qPCR for stemness (*PROM1, LGR5*) (A) and EMT (*SNAI1*), epithelial/cell adhesion (*CDH1*) and Wnt signaling (*CTNNB1, AXIN2*) markers (B). It was used days 4, 7 and 12 of HT29 spheroids treated with OPE 3 for 72h. Each expression level was normalized relatively to the solvent control. Results were performed in triplicates.

The expression of stemness markers decreased more with the treatment of spheroids from day 7 followed by day 4 and 12. Also, the reduction was more pronounced in *LGR5* than in *PROM1* expressions (Figure 3.20 A). Relatively to EMT (Figure 3.20 B), at day 4 spheroids, *SNAI1* expression decreased, *CDH1* maintained and the *CTNNB1* and *AXIN2* slightly increased. All markers increased for spheroids from days 7 and 12. These data allowed comparing how tumor samples in different stages of growth of 3D culture behave towards orange extract treatment. It is clear that although OPE 3 induced *SNAI1* expression promoting EMT, it reduced stemness character at spheroids from days 7 and 12. Yet, spheroids from day 4 were affected at both stemness and EMT profiles.

As the action of OPE 3 appeared to differ for the three culture times and not proportional, a question was raised based on the concentrations used: although it was applied different concentrations according to the spheroids size, may this influence the response to treatment? For that, cell aggregates from day 7 of culture were treated with three OPE 3 concentrations (0.25, 1 and 1.5 mg extract/mL). Also, HT29 cell spheroids from days 4, 7 and 12 of culture were treated with OPE 3 at 1 mg extract/mL. Figure 3.21 shows the results.

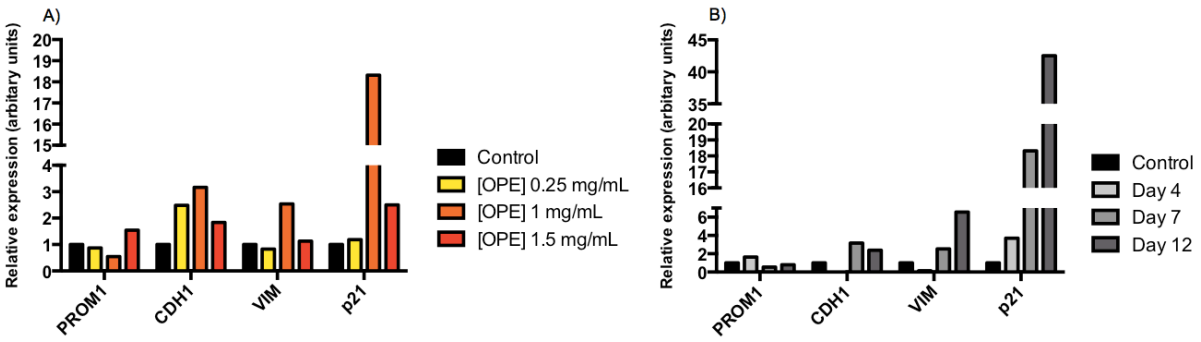

Figure 3.21 – Comparing the relative expression of specific markers using RT-qPCR and different concentrations treatments using day 7 spheroids (A). Comparing the relative expression of specific markers using RT-qPCR and treatment of 1 mg extract/mL of OPE 3 to days 4,7, and 12 spheroids (B). Treatment was performed with 72h incubation, and expression levels were normalized relatively to the solvent control using triplicates by RT-qPCR.

As Figure 3.21 A shows, concentration of 0.25 mg extract/mL did not affect stemness and cell cycle (*PROM1* and *p21* maintained) but increased epithelial character (augmentation of *CDH1*). At 1 mg extract/mL of OPE 3, stemness was decreased, partial EMT was manifested, and G1/S cell arrest was highly promoted in accordance with Figure 3.19. At the highest concentration, stemness (*PROM1*) was stimulated similarly to cell adhesion (*CDH1*) and cell cycle arrest (*p21*). These results might lead to conclude that the concentration of natural extract influenced the response, however, increasing levels of concentrations not always represented stronger and proportional effect. The fact that 1 mg extract/mL stimulates mesenchymal markers and 1.5 mg extract/mL stimulates stemness markers might be due to a negative feedback phenomenon. Indeed, drug dosage is always important when a specific effect is pretended. Every compound has the right dose for the compensatory response, however, when exceeded negative reactions might occur [188]. The excellent response by the spheroids towards OPE 3 treatment would be a reduction of stemness and mesenchymal properties and increasing of epithelial character creating impact on tumor aggressiveness and invasiveness behaviors and also leading to a possible tumor relapse [11]. Therefore, it is possible that OPE 3 concentration between 0.25-1 mg extract/mL may have the impact expected in day 7 HT29 cell spheroids.

Applying the same concentration for different culture time spheroids led also to dissimilar expression responses (Figure 3.21 B). For day 4 spheroids, OPE 3 promoted mainly stemness. Both epithelial and mesenchymal markers were increased at day 7 HT29 cell spheroids where *VIM* expression tended to increase more at day 12 spheroids. Stemness was only reduced positively at day 7 spheroids with a decreased of *PROM1* expression. Cell cycle arrest was promoted along culture time. Taken together with Figure 3.21 A data, the results reflected the notion of the importance of concentration to obtain the perfect effect on colon cancer tumors. The discrepancies obtained here together with the fact that at different culture time the gene expression altered (section 3.2), suggested that the optimal concentration of OPE 3 should probably be decided regarding tumor size and stage. Wide range of tumors including CRC, have already some therapy selection based on TNM staging system and in presence of specific biomarkers [189]. Although, the methodology initially applied

(Figure 3.20) is logical, further studies must be developed in order to determine the optimal concentration for each culture time where stemness and EMT are affected. As referred in section 3.2, spheroids differed from day 4 to days 7/12 which was reflected in the treatment with OPE 3: between days 7 and 12 of culture gene expression might vary according to the concentration tested once cell spheroids have similar characteristics however, between days 4 and 7, the time of culture was the major factor influencing (more different phenotypes).

Although there is no literature reporting the effectiveness of citrus extracts reducing CSCs population, inducing cell cycle arrest and apoptosis and, suppressing differentiation, others phytochemicals have been reporting in these fields. Especially, curcumin, resveratrol, sulforaphane and genistein reported their action on colon cancer stem cell population [184], [190]–[192]. Plus, recently it has been described a natural extract from bamboo leaves contributing to downregulation of Wnt signaling, especially β-catenin levels and upregulation of CK20 leading to a reduction of stemness and a development of an epithelial phenotype using HT29 cell line [65].

Additionally, PMFs compounds were also tested in day 7 HT29 cell spheroids in a preliminary approach as presented in Figure 3.22. The objectives were mainly to understand the influence of each compound and the relation between the mixtures of the four PMFs at the extract. The concentrations tested were regarding to the PMFs content correspondent in 1 mg extract/mL of OPE 3.

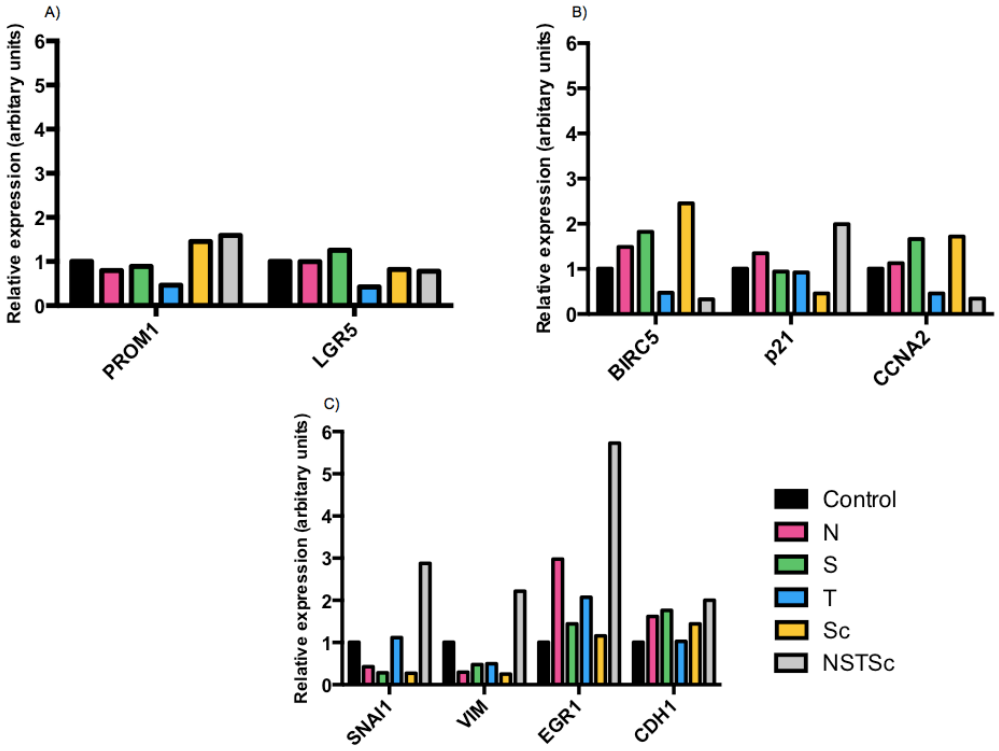

Figure 3.22 – Relative expression of specific markers using RT-qPCR for stemness (*PROM1, LGR5*) (A); apoptosis (*BIRC5*) and cell cycle (*p21, CCNA2*) (B); EMT (*SNAI1, VIM*), invasion (*EGR1*) and epithelial/cell adhesion (*CDH1*) (C) markers. It was used day 7 HT29 spheroids treated with PMFs for 72h. Each expression level was normalized relatively to the solvent control. Results were performed in triplicates. Legend: N = nobiletin; S = sinensetin; T = tangeretin; Sc = scutellarein tetramethylether.

Comparing the mixture of four PMFs with the isolated compounds, the mixture did not have effect on reducing CSCs population. In contrary, *PROM1* expression level slightly increases as in scutellarein tetramethylether treatment. Only tangeretin showed to be capable of reducing this population (Figure 3.22 A). Thus, tangeretin effect might be suppressed in the mixture of PMFs by the presence of other compounds. Relatively to the apoptotic marker (Figure 3.22 B), *BIRC5*, there was a relevant decreasing of expression for NSTSc and tangeretin predicting the apoptotic induction in HT29 cell spheroids, being the tangeretin effect in discordance with literature reported in HT29 cell line [85]. Different concentrations used or time points may explain these differences. Moreover the apoptotic induction by NSTSc was mainly due to the presence of tangeretin. Levels of *p21* and *CCNA2* (cyclin A2 gene) are intrinsically connected. In fact, polyphenol compounds were described as having effect of G1/S cell arrest by a increase of p21 and a decrease of cyclin A2 levels [193]. Here, it was observed G1/S arrest when HT29 cell spheroids were treated with NSTSc. Maintenance of *p21* expression and downregulation of *CCNA2* at treatment with tangeretin suggested G2/M phase arrest (Figure 3.22 B). Inversely, literature reported the G1 cell arrest and the absence of apoptosis in HT29 cell treated with nobiletin and tangeretin [85]. This might be correlated with different concentrations applied, and more importantly the application at monolayer cells or at 3D cell model (which has been seen that might have differences in gene expression – section 3.2). Data from Figure 3.19 suggested G1 cell cycle arrest being promoted by the major presence of nobiletin and tangeretin. However, data from Figure 3.22 confirmed that it was only NSTSc treatment that arrest the cell cycle at G1 phase as OPE 3, suggesting that it was the presence of the four compounds together that influenced cell cycle arrest.

In addition, the mixture promoted the increasing of partial EMT profile (Figure 3.22 C), with increasing of Snail (*SNAI1*), Vimentin (*VIM*), *EGR1* and E-cadherin (*CDH1*) markers. This tendency was identical when the HT29 spheroids were treated with OPE 3 (Figure 3.19), which suggested that these expression levels were due to the presence of these compounds and not others not yet identified. Nonetheless, differences in gene expression were higher when cell spheroids were treated with OPE 3, which might be due to the presence of other compounds potentiating the effect. Conversely, standard PMFs originated a decrease of EMT phenotype – *SNAI1* (excepted in tangeretin treatment where its expression was maintained) and Vimentin. In the invasion marker (*EGR1*), sinensetin and scutellarein tetramethylether showed to keep the expression level of the marker while the other compounds promoted invasion. Finally, *CDH1* expression was induced by all PMFs except tangeretin that did not affect it. Therefore, the different PMFs contributed differently to the effect on HT29 spheroids. The most promising compound appeared to be tangeretin once contributed for reduction of stemness, apoptosis and EMT (excepted *EGR1* marker) and, cell cycle arrest. Secondarily, scutellarein tetramethylether, highly contributed for decrease the EMT phenotype (Snail and Vimentin) and avoid the increasing of invasion (*EGR1*). Thus, this compound appears to be a promising tool in cancer treatment field. To finish, the increasing of invasion and EMT and, decreasing of stemness at the spheroids treated with the mixture and OPE 3 might be explained by the antagonist interaction between PMFs (section 3.1) in addition with the possibility of PMFs concentration might exceeded the compensatory effect.

Overall, these preliminary data allowed understanding the importance of choosing correctly the concentration for the expected effect. The mixture of four PMFs showed resemblance with the OPE 3 effect except in reducing stemness, which might suggest that the presence of other compounds at the extract might interfere contributing itself for the effect or potentiating PMFs. Otherwise, antagonistic effects showed in the present work (section 3.1) between the PMFs may also contribute to this phenomenon. Additionally, further studies should be performed as confirming the actual experiment, new concentrations tested, multiple PMFs combination at the same concentration as in the extract as also in different concentrations. It is important to mention that it has not been yet reported a complex study of gene expression using a phytochemical and its bioactive compounds, therefore, these data represent preliminary findings that have prompt orange peel extract and the PMFs as a promising therapeutic tools in CRC.

3.3.5. Combination of 5-fluorouracil and orange peel extract

Chemotherapy drugs are normally associated to the development of toxicity by normal cells and side effects along several organ systems. Therefore, new approaches had been improved using dietary phytochemicals as adjuvants in cancer therapy, thus diminishing the toxicity of the treatment and acquiring the same or even better results in eliminating cancer cells [194].

With the aim to determine if orange peel extracts together with a chemotherapy drug contribute for the elimination of cancer cells, it was combined OPE 3 with one of the most frequent drugs using for CRC treatment – 5-fluorouracil. Important to mention that 5-FU did not show cytotoxicity in Caco-2 cell model for the concentrations tested, moreover, the literature confirmed for higher incubation time no effect [195]. Figure 3.23 shows the results obtained.

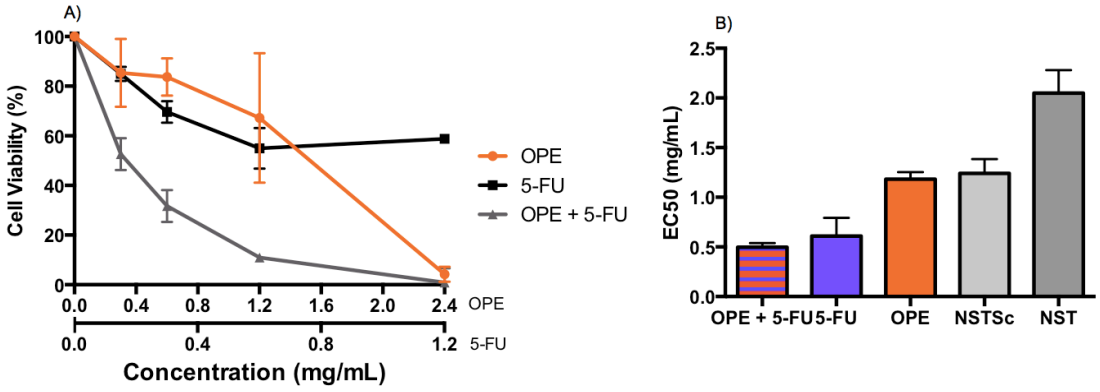

Figure 3.23 – Antiproliferative activity of orange peel extract, 5-fluorouracil and the combination of the two compounds (OPE + 5-FU) (A). Incubation time of 72h using HT29 spheroid model. Results were expressed in mean ± SD (n=3). Comparing EC50 values obtained (mean ± SD) (B). Legend: 5-FU = 5-fluorouracil; OPE = orange peel extract; N = nobiletin; S = sinensetin; T = tangeretin; Sc = scutellarein tetramethylether.

The 5-FU showed smaller EC50 value (Figure 3.23 B) than OPE 3, however, cellular viability did not achieved values under 50%. The chemical drugs are design to have a plateau effect not leading to total cellular death [194]. Then, it was normal that after 0.5 mg/mL of 5-FU the cell viability was maintained. Comparing the response of the individual samples with the combination of two (Figure 3.23 A), OPE+5-FU showed higher antiproliferative effect than the isolated samples. When the OPE+5-FU was capable of eliminating 50% of the population, both OPE and 5-FU did not have antiproliferative effect (cell viability approximately of 100%). Thus, EC50 value for the combination of OPE and 5-FU was 0.4975 ± 0.042 mg/mL corresponding roughly to 0.3317 mg/mL of OPE 3 with 0.1658 mg/ml of 5-FU. Several polyphenols and terpenes had shown in *in vivo* and *in vitro* models to potentiate the effect of chemotherapeutical drugs mainly in leukemia, colon, lung, pancreas and breast cancer [194], [196]. In CRC, curcumin if the most commonly polyphenol studied showing synergistic interaction with 5-fluorouracil and dasatinib by sensitizing colon cancer cells, enhancing apoptosis and inhibiting metastasis [197], [198]. Also, combinations of resveratrol with oxaplatin, and EGCG with sulindac showed promising anticancer effect than the compounds separately [199], [200].

Moreover, it was analyzed the interaction between the compounds using Compusyn software as explained in section 2.3.4. Table 3.7 summarized the combination index for the concentrations tested.

Table 3.7 - Combination Index values resulting of the interactions between OPE 3 and 5-FU. Data obtained by Compusyn software resulting of the compilation of the antiproliferative percentages.

Concentration (mg/mL)		**Combination Index (CI)**
[OPE]	[5-FU]	**OPE + 5-FU**
2.40	1.20	0.3106
1.20	0.60	0.5204
0.60	0.30	0.5248
0.30	0.15	0.4645

According to Chou et al. [143] a CI inferior to 1 is considered synergism, but there are different gradients being the range 0.3-0.7 considered real synergism. Therefore and according with the data obtained, the interaction of orange peel extract with 5-FU led to synergism being the cellular proliferation highly inhibited. These results are favorable data to open a deeper research in this field. The OPE+5-FU combination might be a promising chemotherapeutic tool. Thus, the research might start with the same approach development during this work with OPE 3. Moreover, studies with nanodelivery systems might be develop for a target delivery of the compounds at the tumor. The encapsulation of dietary compounds with anticancer drugs might enhance the compound cellular distribution, solubility and bioavailability of the phytochemicals and, reduce also the cytotoxicity of the drug [196]. Then, the treatment will be specific to release in the target zone (tumoral), which appear to be an interesting approach for both OPE and the combination of it with antitumoral drugs.

4. Conclusion

In the present thesis the effect of a phytochemical rich extracts derived from orange peels in targeting colorectal cancer stem cells was investigated. Even though there are several studies reporting the anticancer properties of citrus fruits, this is the first demonstration of the activity of orange polymethoxylated flavones in modulating a specific cell population responsible for tumor initiation, relapse and resistance to chemotherapy.

The orange extract was obtained by high-pressure technology that showed to be a highly selective extraction process for the isolation of polymethoxylated flavones from orange residues. When using CO_2:EtOH (80:20% v/v) as extraction solvent, a PMF-rich extract was obtained presenting high antiproliferative effect in HT29 cell line. The potential anticancer effect was also demonstrated in a 3D model of HT29 cell spheroids, which showed resemblances to the *in vivo* tumor, mimicking avascular microregions. Importantly, the orange peel extract demonstrated to be effective in reducing cancer stemness biomarkers and self-renewal capacity in 3D spheroids. Moreover, the extract induced apoptosis and cell cycle arrest in G1/S phase and acted synergistically with 5-fluorouracil, diminishing the chemo-cytotoxicity associated to this drug. Nobiletin, sinensetin, tangeretin and scutellarein tetramethylether were the main polymethoxylated flavones presented in the orange peel extract and although their combination is necessary to inhibit cancer cell proliferation, tangeretin was pointed as the main contributor in targeting CSCs population.

The 3D cell models of colorectal cancer used in this work proved to be a valuable pre-clinical model to obtain well-stratified tumor samples enriched in CSCs. Also, it allowed the evaluation of the chemotherapeutic potential of a dietary phytochemical extract and its bioactive molecules. Future studies will focus on the evaluation of structure-activity relationship of citrus bioactive compounds as to evaluate its impact on CSC metabolism.

5. References

[1] "Cancer Facts and Statistics | American Cancer Society." [Online]. Available: http://www.cancer.org/research/cancerfactsstatistics/. [Accessed: 04-Jan-2016].

[2] J. Ferlay, E. Steliarova-Foucher, J. Lortet-Tieulent, S. Rosso, J. W. W. Coebergh, H. Comber, D. Forman, and F. Bray, "Cancer incidence and mortality patterns in Europe: Estimates for 40 countries in 2012," *Eur. J. Cancer*, vol. 49, no. 6, pp. 1374–1403, Apr. 2013.

[3] A. Jemal, F. Bray, M. M. Center, J. Ferlay, E. Ward, and D. Forman, "Global cancer statistics," *CA. Cancer J. Clin.*, vol. 61, no. 2, pp. 69–90, Mar. 2011.

[4] T. R. Harrison, E. Braunwald, and D. L. Kasper, *Harrison's principles of internal medicine*. New York: McGraw-Hill, 2005.

[5] M. Ponz de Leon and L. Roncucci, "The cause of colorectal cancer," *Dig. Liver Dis.*, vol. 32, no. 5, pp. 426–439, Jun. 2000.

[6] W. C. Willett, M. J. Stampfer, G. A. Colditz, B. A. Rosner, and F. E. Speizer, "Relation of Meat, Fat, and Fiber Intake to the Risk of Colon Cancer in a Prospective Study among Women," *N. Engl. J. Med.*, vol. 323, no. 24, pp. 1664–1672, Dec. 1990.

[7] M.D. Randall W. Burt, M.D. James A. DiSario, and P. D. and Lisa Cannon-Albright, "GENETICS OF COLON CANCER: Impact of Inheritance on Colon Cancer Risk," *Annu. Rev. Med.*, vol. 46, no. 1, pp. 371–379, 1995.

[8] S. L. (Stanley L. Robbins, R. S. Cotran, and Kumar, Vinay, *Patologia [de] Robbins & Cotran: Bases Patológicas das Doenças*. Rio de Janeiro (RJ): Elsevier, 2010.

[9] M. Fleming, S. Ravula, S. F. Tatishchev, and H. L. Wang, "Colorectal carcinoma: Pathologic aspects," *J. Gastrointest. Oncol.*, vol. 3, no. 3, pp. 153–173, Sep. 2012.

[10] R. R. Seeley, T. D. Stephens, P. Tate, and R. R. Seeley, *Anatomy & physiology*, 6th ed. Boston: McGraw-Hill, 2003.

[11] M. Todaro, M. G. Francipane, J. P. Medema, and G. Stassi, "Colon Cancer Stem Cells: Promise of Targeted Therapy," *Gastroenterology*, vol. 138, no. 6, pp. 2151–2162, May 2010.

[12] A. G. Vaiopoulos, I. D. Kostakis, M. Koutsilieris, and A. G. Papavassiliou, "Colorectal Cancer Stem Cells," *STEM CELLS*, vol. 30, no. 3, pp. 363–371, Mar. 2012.

[13] E. R. Fearon and B. Vogelstein, "A genetic model for colorectal tumorigenesis," *Cell*, vol. 61, no. 5, pp. 759–767, Jun. 1990.

[14] A. Walther, E. Johnstone, C. Swanton, R. Midgley, I. Tomlinson, and D. Kerr, "Genetic prognostic and predictive markers in colorectal cancer," *Nat. Rev. Cancer*, vol. 9, no. 7, pp. 489–499, Jul. 2009.

[15] A. Leslie, F. A. Carey, N. R. Pratt, and R. J. C. Steele, "The colorectal adenoma–carcinoma sequence," *Br. J. Surg.*, vol. 89, no. 7, pp. 845–860, Jul. 2002.

[16] C. Fanali, D. Lucchetti, M. Farina, M. Corbi, V. Cufino, A. Cittadini, and A. Sgambato, "Cancer stem cells in colorectal cancer from pathogenesis to therapy: Controversies and perspectives," *World J. Gastroenterol. WJG*, vol. 20, no. 4, pp. 923–942, Jan. 2014.

[17] R. Fodde, R. Smits, and H. Clevers, "APC, Signal transduction and genetic instability in colorectal cancer," *Nat. Rev. Cancer*, vol. 1, no. 1, pp. 55–67, Oct. 2001.

[18] L. Novellasdemunt, P. Antas, and V. S. W. Li, "Targeting Wnt signaling in colorectal cancer. A Review in the Theme: Cell Signaling: Proteins, Pathways and Mechanisms," *Am. J. Physiol. Cell Physiol.*, vol. 309, no. 8, pp. C511–521, Oct. 2015.

[19] D. Colussi, G. Brandi, F. Bazzoli, and L. Ricciardiello, "Molecular Pathways Involved in Colorectal Cancer: Implications for Disease Behavior and Prevention," *Int. J. Mol. Sci.*, vol. 14, no. 8, pp. 16365–16385, Aug. 2013.

[20] T. C. G. A. Network, "Comprehensive molecular characterization of human colon and rectal cancer," *Nature*, vol. 487, no. 7407, pp. 330–337, Jul. 2012.

[21] S. Ogino, K. Nosho, K. Shima, Y. Baba, N. Irahara, G. J. Kirkner, A. Hazra, I. De Vivo, E. L. Giovannucci, J. A. Meyerhardt, and C. S. Fuchs, "p21 Expression in Colon Cancer and Modifying Effects of Patient Age and Body Mass Index on Prognosis," *Cancer Epidemiol. Biomark. Prev. Publ. Am. Assoc. Cancer Res. Cosponsored Am. Soc. Prev. Oncol.*, vol. 18, no. 9, pp. 2513–2521, Sep. 2009.

[22] D. Pinto, A. Gregorieff, H. Begthel, and H. Clevers, "Canonical Wnt signals are essential for homeostasis of the intestinal epithelium," *Genes Dev.*, vol. 17, no. 14, pp. 1709–1713, Jul. 2003.

[23] R. Kalluri and R. A. Weinberg, "The basics of epithelial-mesenchymal transition," *J. Clin. Invest.*, vol. 119, no. 6, pp. 1420–1428, Jun. 2009.

[24] A. F. Chambers, A. C. Groom, and I. C. MacDonald, “Metastasis: Dissemination and growth of cancer cells in metastatic sites,” *Nat. Rev. Cancer*, vol. 2, no. 8, pp. 563–572, Aug. 2002.
[25] E. W. Thompson and D. F. Newgreen, “Carcinoma Invasion and Metastasis: A Role for Epithelial-Mesenchymal Transition?,” *Cancer Res.*, vol. 65, no. 14, pp. 5991–5995, Jul. 2005.
[26] J. P. Thiery, “Epithelial-mesenchymal transitions in tumour progression,” *Nat. Rev. Cancer*, vol. 2, no. 6, pp. 442–454, Jun. 2002.
[27] T. Brabletz, A. Jung, and T. Kirchner, “β-Catenin and the morphogenesis of colorectal cancer,” *Virchows Arch.*, vol. 441, no. 1, pp. 1–11, Apr. 2002.
[28] M. A. Nieto, “The snail superfamily of zinc-finger transcription factors,” *Nat. Rev. Mol. Cell Biol.*, vol. 3, no. 3, pp. 155–166, Mar. 2002.
[29] Y. Kang and J. Massagué, “Epithelial-Mesenchymal Transitions: Twist in Development and Metastasis,” *Cell*, vol. 118, no. 3, pp. 277–279, Aug. 2004.
[30] S. Vega, A. V. Morales, O. H. Ocaña, F. Valdés, I. Fabregat, and M. A. Nieto, “Snail blocks the cell cycle and confers resistance to cell death,” *Genes Dev.*, vol. 18, no. 10, pp. 1131–1143, May 2004.
[31] K. Yokoyama, N. Kamata, R. Fujimoto, S. Tsutsumi, M. Tomonari, M. Taki, H. Hosokawa, and M. Nagayama, “Increased invasion and matrix metalloproteinase-2 expression by Snail-induced mesenchymal transition in squamous cell carcinomas,” *Int. J. Oncol.*, vol. 22, no. 4, pp. 891–898, Apr. 2003.
[32] C. Kudo-Saito, H. Shirako, T. Takeuchi, and Y. Kawakami, “Cancer Metastasis Is Accelerated through Immunosuppression during Snail-Induced EMT of Cancer Cells,” *Cancer Cell*, vol. 15, no. 3, pp. 195–206, Mar. 2009.
[33] M. A. Huber, N. Kraut, and H. Beug, “Molecular requirements for epithelial–mesenchymal transition during tumor progression,” *Curr. Opin. Cell Biol.*, vol. 17, no. 5, pp. 548–558, Oct. 2005.
[34] L. Larue and A. Bellacosa, “Epithelial–mesenchymal transition in development and cancer: role of phosphatidylinositol 3′ kinase/AKT pathways,” *Oncogene*, vol. 24, no. 50, pp. 7443–7454, 2005.
[35] C. Aguilar-Gallardo and C. Simón, “Cells, stem cells, and cancer stem cells,” *Semin. Reprod. Med.*, vol. 31, no. 1, pp. 5–13, Jan. 2013.
[36] R. A. Burrell, N. McGranahan, J. Bartek, and C. Swanton, “The causes and consequences of genetic heterogeneity in cancer evolution,” *Nature*, vol. 501, no. 7467, pp. 338–345, Sep. 2013.
[37] T. Reya, S. J. Morrison, M. F. Clarke, and I. L. Weissman, “Stem cells, cancer, and cancer stem cells,” *Nature*, vol. 414, no. 6859, pp. 105–111, Nov. 2001.
[38] P. Dalerba, R. W. Cho, and M. F. Clarke, “Cancer Stem Cells: Models and Concepts,” *Annu. Rev. Med.*, vol. 58, no. 1, pp. 267–284, 2007.
[39] P. Chu, D. J. Clanton, T. S. Snipas, J. Lee, E. Mitchell, M.-L. Nguyen, E. Hare, and R. J. Peach, “Characterization of a subpopulation of colon cancer cells with stem cell-like properties,” *Int. J. Cancer*, vol. 124, no. 6, pp. 1312–1321, Mar. 2009.
[40] P. Dalerba, S. J. Dylla, I.-K. Park, R. Liu, X. Wang, R. W. Cho, T. Hoey, A. Gurney, E. H. Huang, D. M. Simeone, A. A. Shelton, G. Parmiani, C. Castelli, and M. F. Clarke, “Phenotypic characterization of human colorectal cancer stem cells,” *Proc. Natl. Acad. Sci. U. S. A.*, vol. 104, no. 24, pp. 10158–10163, Jun. 2007.
[41] I. Ma and A. L. Allan, “The role of human aldehyde dehydrogenase in normal and cancer stem cells,” *Stem Cell Rev.*, vol. 7, no. 2, pp. 292–306, Jun. 2011.
[42] L. Du, H. Wang, L. He, J. Zhang, B. Ni, X. Wang, H. Jin, N. Cahuzac, M. Mehrpour, Y. Lu, and Q. Chen, “CD44 is of Functional Importance for Colorectal Cancer Stem Cells,” *Clin. Cancer Res.*, vol. 14, no. 21, pp. 6751–6760, Nov. 2008.
[43] L. Ricci-Vitiani, D. G. Lombardi, E. Pilozzi, M. Biffoni, M. Todaro, C. Peschle, and R. De Maria, “Identification and expansion of human colon-cancer-initiating cells,” *Nature*, vol. 445, no. 7123, pp. 111–115, Jan. 2007.
[44] K. Wang, J. Xu, J. Zhang, and J. Huang, “Prognostic role of CD133 expression in colorectal cancer: a meta-analysis,” *BMC Cancer*, vol. 12, p. 573, 2012.
[45] N. Haraguchi, M. Ohkuma, H. Sakashita, S. Matsuzaki, F. Tanaka, K. Mimori, Y. Kamohara, H. Inoue, and M. Mori, “CD133+CD44+ Population Efficiently Enriches Colon Cancer Initiating Cells,” *Ann. Surg. Oncol.*, vol. 15, no. 10, pp. 2927–2933, Jul. 2008.
[46] K. Chen, F. Pan, H. Jiang, J. Chen, L. Pei, F. Xie, and H. Liang, “Highly enriched CD133+CD44+ stem-like cells with CD133+CD44high metastatic subset in HCT116 colon cancer cells,” *Clin. Exp. Metastasis*, vol. 28, no. 8, pp. 751–763, Jul. 2011.
[47] E. H. Huang, M. J. Hynes, T. Zhang, C. Ginestier, G. Dontu, H. Appelman, J. Z. Fields, M. S. Wicha, and B. M. Boman, “Aldehyde Dehydrogenase 1 Is a Marker for Normal and Malignant

Human Colonic Stem Cells (SC) and Tracks SC Overpopulation during Colon Tumorigenesis," *Cancer Res.*, vol. 69, no. 8, pp. 3382–3389, Apr. 2009.
[48] A.-M. Baker, T. A. Graham, G. Elia, N. A. Wright, and M. Rodriguez-Justo, "Characterization of LGR5 stem cells in colorectal adenomas and carcinomas," *Sci. Rep.*, vol. 5, p. 8654, Mar. 2015.
[49] H. Uchida, K. Yamazaki, M. Fukuma, T. Yamada, T. Hayashida, H. Hasegawa, M. Kitajima, Y. Kitagawa, and M. Sakamoto, "Overexpression of leucine-rich repeat-containing G protein-coupled receptor 5 in colorectal cancer," *Cancer Sci.*, vol. 101, no. 7, pp. 1731–1737, Jul. 2010.
[50] E. C. Anderson, C. Hessman, T. G. Levin, M. M. Monroe, and M. H. Wong, "The Role of Colorectal Cancer Stem Cells in Metastatic Disease and Therapeutic Response," *Cancers*, vol. 3, no. 1, pp. 319–339, Jan. 2011.
[51] "Treatment of colon cancer, by stage." [Online]. Available: http://www.cancer.org/cancer/colonandrectumcancer/detailedguide/colorectal-cancer-treating-by-stage-colon. [Accessed: 20-Sep-2016].
[52] I. Herrmann, P. A. Baeuerle, M. Friedrich, A. Murr, S. Filusch, D. Rüttinger, M. W. Majdoub, S. Sharma, P. Kufer, T. Raum, and M. Münz, "Highly Efficient Elimination of Colorectal Tumor-Initiating Cells by an EpCAM/CD3-Bispecific Antibody Engaging Human T Cells," *PLoS ONE*, vol. 5, no. 10, Oct. 2010.
[53] N. Barker and H. Clevers, "Mining the Wnt pathway for cancer therapeutics," *Nat. Rev. Drug Discov.*, vol. 5, no. 12, pp. 997–1014, Dec. 2006.
[54] D. Hanahan and R. A. Weinberg, "Hallmarks of Cancer: The Next Generation," *Cell*, vol. 144, no. 5, pp. 646–674, Mar. 2011.
[55] H. Greenlee, "Natural Products for Cancer Prevention," *Semin. Oncol. Nurs.*, vol. 28, no. 1, pp. 29–44, Feb. 2012.
[56] E. T. Hawk, "Colorectal Cancer Prevention," *J. Clin. Oncol.*, vol. 23, no. 2, pp. 378–391, Jan. 2005.
[57] M. Pericleous, D. Mandair, and M. E. Caplin, "Diet and supplements and their impact on colorectal cancer," *J. Gastrointest. Oncol.*, vol. 4, no. 4, pp. 409–423, Dec. 2013.
[58] R. H. Liu, "Dietary Bioactive Compounds and Their Health Implications," *J. Food Sci.*, vol. 78, no. s1, pp. A18–A25, Jun. 2013.
[59] Y.-J. Surh, "Cancer chemoprevention with dietary phytochemicals," *Nat. Rev. Cancer*, vol. 3, no. 10, pp. 768–780, Oct. 2003.
[60] W.-Y. Huang, Y.-Z. Cai, and Y. Zhang, "Natural Phenolic Compounds From Medicinal Herbs and Dietary Plants: Potential Use for Cancer Prevention," *Nutr. Cancer*, vol. 62, no. 1, pp. 1–20, Dec. 2009.
[61] R. H. Liu, "Potential Synergy of Phytochemicals in Cancer Prevention: Mechanism of Action," *J. Nutr.*, vol. 134, no. 12, p. 3479S–3485S, Dec. 2004.
[62] P. Fresco, F. Borges, C. Diniz, and M. p. m. Marques, "New insights on the anticancer properties of dietary polyphenols," *Med. Res. Rev.*, vol. 26, no. 6, pp. 747–766, Nov. 2006.
[63] N. G. Amado, D. Predes, M. M. Moreno, I. O. Carvalho, F. A. Mendes, and J. G. Abreu, "Flavonoids and Wnt/β-catenin signaling: potential role in colorectal cancer therapies," *Int. J. Mol. Sci.*, vol. 15, no. 7, pp. 12094–12106, 2014.
[64] A. A. M. Ana Teresa Serra, "Processing cherries (Prunus avium) using supercritical fluid technology. Part 2. Evaluation of SCF extracts as promising natural chemotherapeutical agents," *J. Supercrit. Fluids*, vol. 55, no. 3, pp. 1007–1013, 2011.
[65] S. J. Min, J. Y. Lim, H. R. Kim, S.-J. Kim, and Y. Kim, "Sasa quelpaertensis Leaf Extract Inhibits Colon Cancer by Regulating Cancer Cell Stemness in Vitro and in Vivo," *Int. J. Mol. Sci.*, vol. 16, no. 5, pp. 9976–9997, 2015.
[66] H. Mukhtar and N. Ahmad, "Green tea in chemoprevention of cancer," *Toxicol. Sci. Off. J. Soc. Toxicol.*, vol. 52, no. 2 Suppl, pp. 111–117, Dec. 1999.
[67] S. K. Jaganathan, M. V. Vellayappan, G. Narasimhan, and E. Supriyanto, "Role of pomegranate and citrus fruit juices in colon cancer prevention," *World J. Gastroenterol. WJG*, vol. 20, no. 16, pp. 4618–4625, Apr. 2014.
[68] Toledo-Guillén, A.R., Higuera-Ciapara, I., García-Navarrete, G., Fuente, J.C. de la, "Extraction of Bioactive Flavonoid Compounds from Orange (Citrus sinensis) Peel Using Supercritical CO2," *Spec Abstr J Biotechnol 2010 150S S1–S576*.
[69] S. Li, C.-Y. Lo, and C.-T. Ho, "Hydroxylated Polymethoxyflavones and Methylated Flavonoids in Sweet Orange (Citrus sinensis) Peel," *J. Agric. Food Chem.*, vol. 54, no. 12, pp. 4176–4185, Jun. 2006.

[70] G. K. Jayaprakasha, P. S. Negi, S. Sikder, L. J. Rao, and K. K. Sakariah, “Antibacterial activity of Citrus reticulata peel extracts,” *Z. Für Naturforschung C J. Biosci.*, vol. 55, no. 11–12, pp. 1030–1034, Dec. 2000.
[71] O. Benavente-García and J. Castillo, “Update on uses and properties of citrus flavonoids: new findings in anticancer, cardiovascular, and anti-inflammatory activity,” *J. Agric. Food Chem.*, vol. 56, no. 15, pp. 6185–6205, Aug. 2008.
[72] S. Li, M.-H. Pan, C.-Y. Lo, D. Tan, Y. Wang, F. Shahidi, and C.-T. Ho, “Chemistry and health effects of polymethoxyflavones and hydroxylated polymethoxyflavones,” *J. Funct. Foods*, vol. 1, no. 1, pp. 2–12, Jan. 2009.
[73] N. E. Rawson, C.-T. Ho, and S. Li, “Efficacious anti-cancer property of flavonoids from citrus peels,” *Food Sci. Hum. Wellness*, vol. 3, no. 3–4, pp. 104–109, Sep. 2014.
[74] J. A. Manthey and N. Guthrie, “Antiproliferative Activities of Citrus Flavonoids against Six Human Cancer Cell Lines,” *J. Agric. Food Chem.*, vol. 50, no. 21, pp. 5837–5843, Oct. 2002.
[75] P. Qiu, H. Guan, P. Dong, S. Li, C.-T. Ho, M.-H. Pan, D. J. McClements, and H. Xiao, “The p53, Bax and p21 dependent inhibition of colon cancer cell growth by 5-hydroxy polymethoxyflavones,” *Mol. Nutr. Food Res.*, vol. 55, no. 4, pp. 613–622, Apr. 2011.
[76] P. Qiu, P. Dong, H. Guan, S. Li, C.-T. Ho, M.-H. Pan, D. J. McClements, and H. Xiao, “Inhibitory effects of 5-hydroxy polymethoxyflavones on colon cancer cells,” *Mol. Nutr. Food Res.*, vol. 54 Suppl 2, pp. S244–252, Jul. 2010.
[77] L. Wang, J. Wang, L. Fang, Z. Zheng, D. Zhi, S. Wang, S. Li, C.-T. Ho, and H. Zhao, “Anticancer Activities of Citrus Peel Polymethoxyflavones Related to Angiogenesis and Others,” *BioMed Res. Int.*, vol. 2014, 2014.
[78] W. Wang, L. Heideman, C. S. Chung, J. C. Pelling, K. J. Koehler, and D. F. Birt, “Cell-cycle arrest at G2/M and growth inhibition by apigenin in human colon carcinoma cell lines,” *Mol. Carcinog.*, vol. 28, no. 2, pp. 102–110, Jun. 2000.
[79] H. J. Park, M.-J. Kim, E. Ha, and J.-H. Chung, “Apoptotic effect of hesperidin through caspase3 activation in human colon cancer cells, SNU-C4,” *Phytomedicine*, vol. 15, no. 1–2, pp. 147–151, Jan. 2008.
[80] T. Tanaka, T. Tanaka, M. Tanaka, T. Kuno, T. Tanaka, T. Tanaka, M. Tanaka, and T. Kuno, “Cancer Chemoprevention by Citrus Pulp and Juices Containing High Amounts of β-Cryptoxanthin and Hesperidin, Cancer Chemoprevention by Citrus Pulp and Juices Containing High Amounts of β-Cryptoxanthin and Hesperidin,” *BioMed Res. Int. BioMed Res. Int.*, vol. 2012, 2012, p. e516981, Nov. 2011.
[81] C.-S. Lai, S. Li, C. B. Liu, Y. Miyauchi, M. Suzawa, C.-T. Ho, and M.-H. Pan, “Effective suppression of azoxymethane-induced aberrant crypt foci formation in mice with citrus peel flavonoids,” *Mol. Nutr. Food Res.*, vol. 57, no. 3, pp. 551–555, Mar. 2013.
[82] A. Lentini, C. Forni, B. Provenzano, and S. Beninati, “Enhancement of transglutaminase activity and polyamine depletion in B16-F10 melanoma cells by flavonoids naringenin and hesperitin correlate to reduction of the in vivo metastatic potential,” *Amino Acids*, vol. 32, no. 1, pp. 95–100, Jan. 2007.
[83] H. M. Song, G. H. Park, H. J. Eo, J. W. Lee, M. K. Kim, J. R. Lee, M. H. Lee, J. S. Koo, and J. B. Jeong, “Anti-Proliferative Effect of Naringenin through p38-Dependent Downregulation of Cyclin D1 in Human Colorectal Cancer Cells,” *Biomol. Ther.*, vol. 23, no. 4, pp. 339–344, Jul. 2015.
[84] P. Totta, F. Acconcia, S. Leone, I. Cardillo, and M. Marino, “Mechanisms of Naringenin-induced Apoptotic Cascade in Cancer Cells: Involvement of Estrogen Receptor a and ß Signalling,” *IUBMB Life*, vol. 56, no. 8, pp. 491–499, Aug. 2004.
[85] K. L. Morley, P. J. Ferguson, and J. Koropatnick, “Tangeretin and nobiletin induce G1 cell cycle arrest but not apoptosis in human breast and colon cancer cells,” *Cancer Lett.*, vol. 251, no. 1, pp. 168–178, Jun. 2007.
[86] K. KAWABATA, A. MURAKAMI, and H. OHIGASHI, “Nobiletin, a Citrus Flavonoid, Down-Regulates Matrix Metalloproteinase-7 (matrilysin) Expression in HT-29 Human Colorectal Cancer Cells,” *Biosci. Biotechnol. Biochem.*, vol. 69, no. 2, pp. 307–314, Jan. 2005.
[87] R. Suzuki, H. Kohno, A. Murakami, K. Koshimizu, H. Ohigashi, M. Yano, H. Tokuda, H. Nishino, and T. Tanaka, “Citrus nobiletin inhibits azoxymethane-induced large bowel carcinogenesis in rats,” *BioFactors*, vol. 21, no. 1–4, pp. 111–114, Jan. 2004.
[88] Silva, Inês, Bento da Silva, Bronze, Maria, Alves, Paula, Duarte, Catarina, Brito, Catarina, and Serra, Ana Teresa, “Exploring the anti-tumoral effect of citrus polymethoxylated flavones using a 3D cell model of colorectal cancer,” submitted 2016.
[89] M.-H. Pan, W.-J. Chen, S.-Y. Lin-Shiau, C.-T. Ho, and J.-K. Lin, “Tangeretin induces cell-cycle G1 arrest through inhibiting cyclin-dependent kinases 2 and 4 activities as well as elevating Cdk

inhibitors p21 and p27 in human colorectal carcinoma cells," *Carcinogenesis*, vol. 23, no. 10, pp. 1677–1684, Oct. 2002.
[90] Y. Ting, Y.-S. Chiou, M.-H. Pan, C.-T. Ho, and Q. Huang, "In vitro and in vivo anti-cancer activity of tangeretin against colorectal cancer was enhanced by emulsion-based delivery system," *J. Funct. Foods*, vol. 15, pp. 264–273, May 2015.
[91] J. Zheng, M. Song, P. Qiu, P. Dong, X. Cai, and H. Xiao, "Biotransformation of citrus polymethoxyflavones in rats and mice (1044.22)," *FASEB J.*, vol. 28, no. 1 Supplement, p. 1044.22, Apr. 2014.
[92] J. Zheng, M. Song, P. Dong, P. Qiu, S. Guo, Z. Zhong, S. Li, C.-T. Ho, and H. Xiao, "Identification of novel bioactive metabolites of 5-demethylnobiletin in mice," *Mol. Nutr. Food Res.*, vol. 57, no. 11, pp. 1999–2007, Nov. 2013.
[93] O. of the Commissioner, "The Drug Development Process." [Online]. Available: http://www.fda.gov/ForPatients/Approvals/Drugs/default.htm. [Accessed: 18-Aug-2016].
[94] S. Constant, S. Huang, L. Wiszniewski, and C. Mas, "Colon Cancer: Current Treatments and Preclinical Models for the Discovery and Development of New Therapies," in *Drug Discovery*, H. El-Shemy, Ed. InTech, 2013.
[95] M. Cekanova and K. Rathore, "Animal models and therapeutic molecular targets of cancer: utility and limitations," *Drug Des. Devel. Ther.*, vol. 8, pp. 1911–1922, Oct. 2014.
[96] L.-B. Weiswald, D. Bellet, and V. Dangles-Marie, "Spherical Cancer Models in Tumor Biology," *Neoplasia*, vol. 17, no. 1, pp. 1–15, Jan. 2015.
[97] R. M. Sutherland, "Cell and environment interactions in tumor microregions: the multicell spheroid model," *Science*, vol. 240, no. 4849, pp. 177–184, Apr. 1988.
[98] R.-Z. Lin and H.-Y. Chang, "Recent advances in three-dimensional multicellular spheroid culture for biomedical research," *Biotechnol. J.*, vol. 3, no. 9–10, pp. 1172–1184, Oct. 2008.
[99] J. M. Yuhas, A. P. Li, A. O. Martinez, and A. J. Ladman, "A simplified method for production and growth of multicellular tumor spheroids," *Cancer Res.*, vol. 37, no. 10, pp. 3639–3643, Oct. 1977.
[100] J. B. Kim, "Three-dimensional tissue culture models in cancer biology," *Semin. Cancer Biol.*, vol. 15, no. 5, pp. 365–377, Oct. 2005.
[101] J. M. Kelm, N. E. Timmins, C. J. Brown, M. Fussenegger, and L. K. Nielsen, "Method for generation of homogeneous multicellular tumor spheroids applicable to a wide variety of cell types," *Biotechnol. Bioeng.*, vol. 83, no. 2, pp. 173–180, Jul. 2003.
[102] R. M. Sutherland, W. R. Inch, J. A. McCredie, and J. Kruuv, "A multi-component radiation survival curve using an in vitro tumour model," *Int. J. Radiat. Biol. Relat. Stud. Phys. Chem. Med.*, vol. 18, no. 5, pp. 491–495, 1970.
[103] J. Friedrich, R. Ebner, and L. A. Kunz-Schughart, "Experimental anti-tumor therapy in 3-D: Spheroids – old hat or new challenge?," *Int. J. Radiat. Biol.*, vol. 83, no. 11–12, pp. 849–871, Jan. 2007.
[104] S. R. Pollack, D. F. Meaney, E. M. Levine, M. Litt, and E. D. Johnston, "Numerical model and experimental validation of microcarrier motion in a rotating bioreactor," *Tissue Eng.*, vol. 6, no. 5, pp. 519–530, Oct. 2000.
[105] T. J. Goodwin, T. L. Prewett, D. A. Wolf, and G. F. Spaulding, "Reduced shear stress: a major component in the ability of mammalian tissues to form three-dimensional assemblies in simulated microgravity," *J. Cell. Biochem.*, vol. 51, no. 3, pp. 301–311, Mar. 1993.
[106] J. Barrila, A. L. Radtke, A. Crabbé, S. F. Sarker, M. M. Herbst-Kralovetz, C. M. Ott, and C. A. Nickerson, "Organotypic 3D cell culture models: using the rotating wall vessel to study host–pathogen interactions," *Nat. Rev. Microbiol.*, vol. 8, no. 11, pp. 791–801, Nov. 2010.
[107] D. Antoni, H. Burckel, E. Josset, and G. Noel, "Three-Dimensional Cell Culture: A Breakthrough in Vivo," *Int. J. Mol. Sci.*, vol. 16, no. 3, pp. 5517–5527, Mar. 2015.
[108] K. Alessandri, B. R. Sarangi, V. V. Gurchenkov, B. Sinha, T. R. Kießling, L. Fetler, F. Rico, S. Scheuring, C. Lamaze, A. Simon, S. Geraldo, D. Vignjević, H. Doméjean, L. Rolland, A. Funfak, J. Bibette, N. Bremond, and P. Nassoy, "Cellular capsules as a tool for multicellular spheroid production and for investigating the mechanics of tumor progression in vitro," *Proc. Natl. Acad. Sci.*, vol. 110, no. 37, pp. 14843–14848, Sep. 2013.
[109] A. Nyga, U. Cheema, and M. Loizidou, "3D tumour models: novel in vitro approaches to cancer studies," *J. Cell Commun. Signal.*, vol. 5, no. 3, pp. 239–248, Aug. 2011.
[110] R. A. Johns, A. Tichotsky, M. Muro, J. P. Spaeth, T. D. Le Cras, and A. Rengasamy, "Halothane and isoflurane inhibit endothelium-derived relaxing factor-dependent cyclic guanosine monophosphate accumulation in endothelial cell-vascular smooth muscle co-cultures independent of an effect on guanylyl cyclase activation," *Anesthesiology*, vol. 83, no. 4, pp. 823–834, Oct. 1995.

[111] S. K. Singh, I. D. Clarke, M. Terasaki, V. E. Bonn, C. Hawkins, J. Squire, and P. B. Dirks, “Identification of a Cancer Stem Cell in Human Brain Tumors,” *Cancer Res.*, vol. 63, no. 18, pp. 5821–5828, Sep. 2003.
[112] D. Ponti, A. Costa, N. Zaffaroni, G. Pratesi, G. Petrangolini, D. Coradini, S. Pilotti, M. A. Pierotti, and M. G. Daidone, “Isolation and In vitro Propagation of Tumorigenic Breast Cancer Cells with Stem/Progenitor Cell Properties,” *Cancer Res.*, vol. 65, no. 13, pp. 5506–5511, Jul. 2005.
[113] M. Serra, S. B. Leite, C. Brito, J. Costa, M. J. T. Carrondo, and P. M. Alves, “Novel culture strategy for human stem cell proliferation and neuronal differentiation,” *J. Neurosci. Res.*, vol. 85, no. 16, pp. 3557–3566, Dec. 2007.
[114] L.-B. Weiswald, S. Richon, G. Massonnet, J.-M. Guinebretière, S. Vacher, I. Laurendeau, P. Cottu, E. Marangoni, F. Nemati, P. Validire, D. Bellet, I. Bièche, and V. Dangles-Marie, “A short-term colorectal cancer sphere culture as a relevant tool for human cancer biology investigation,” *Br. J. Cancer*, vol. 108, no. 8, pp. 1720–1731, Apr. 2013.
[115] J. Kondo, H. Endo, H. Okuyama, O. Ishikawa, H. Iishi, M. Tsujii, M. Ohue, and M. Inoue, “Retaining cell-cell contact enables preparation and culture of spheroids composed of pure primary cancer cells from colorectal cancer,” *Proc. Natl. Acad. Sci. U. S. A.*, vol. 108, no. 15, pp. 6235–6240, Apr. 2011.
[116] U. Rajcevic, J. C. Knol, S. Piersma, S. Bougnaud, F. Fack, E. Sundlisaeter, K. Søndenaa, R. Myklebust, T. V. Pham, S. P. Niclou, and C. R. Jiménez, “Colorectal cancer derived organotypic spheroids maintain essential tissue characteristics but adapt their metabolism in culture,” *Proteome Sci.*, vol. 12, p. 39, Jul. 2014.
[117] D. Mouradov, C. Sloggett, R. N. Jorissen, C. G. Love, S. Li, A. W. Burgess, D. Arango, R. L. Strausberg, D. Buchanan, S. Wormald, L. O’Connor, J. L. Wilding, D. Bicknell, I. P. M. Tomlinson, W. F. Bodmer, J. M. Mariadason, and O. M. Sieber, “Colorectal Cancer Cell Lines Are Representative Models of the Main Molecular Subtypes of Primary Cancer,” *Cancer Res.*, vol. 74, no. 12, pp. 3238–3247, Jun. 2014.
[118] N. A. Dallas, L. Xia, F. Fan, M. J. Gray, P. Gaur, G. van Buren, S. Samuel, M. P. Kim, S. J. Lim, and L. M. Ellis, “Chemoresistant Colorectal Cancer Cells, the Cancer Stem Cell Phenotype, and Increased Sensitivity to Insulin-like Growth Factor-I Receptor Inhibition,” *Cancer Res.*, vol. 69, no. 5, pp. 1951–1957, Mar. 2009.
[119] H.-M. Zhou, T.-T. Dong, L.-L. Wang, B. Feng, H.-C. Zhao, X.-K. Fan, and M.-H. Zheng, “Suppression of colorectal cancer metastasis by nigericin through inhibition of epithelial-mesenchymal transition,” *World J. Gastroenterol. WJG*, vol. 18, no. 21, pp. 2640–2648, Jun. 2012.
[120] S. Kumar, K. Raina, C. Agarwal, and R. Agarwal, “Silibinin strongly inhibits the growth kinetics of colon cancer stem cell-enriched spheroids by modulating interleukin 4/6-mediated survival signals,” *Oncotarget*, vol. 5, no. 13, pp. 4972–4989, Jun. 2014.
[121] J. Nautiyal, S. S. Kanwar, Y. Yu, and A. P. Majumdar, “Combination of dasatinib and curcumin eliminates chemo-resistant colon cancer cells,” *J. Mol. Signal.*, vol. 6, p. 7, Jul. 2011.
[122] T. M. Yeung, S. C. Gandhi, J. L. Wilding, R. Muschel, and W. F. Bodmer, “Cancer stem cells from colorectal cancer-derived cell lines,” *Proc. Natl. Acad. Sci.*, vol. 107, no. 8, pp. 3722–3727, Feb. 2010.
[123] M. G. Muraro, V. Mele, S. Däster, J. Han, M. Heberer, G. Cesare Spagnoli, and G. Iezzi, “CD133+, CD166+CD44+, and CD24+CD44+ Phenotypes Fail to Reliably Identify Cell Populations with Cancer Stem Cell Functional Features in Established Human Colorectal Cancer Cell Lines,” *Stem Cells Transl. Med.*, vol. 1, no. 8, pp. 592–603, Aug. 2012.
[124] B. Wei, X.-Y. Han, C.-L. Qi, S. Zhang, Z.-H. Zheng, Y. Huang, T.-F. Chen, and H.-B. Wei, “Coaction of Spheroid-Derived Stem-Like Cells and Endothelial Progenitor Cells Promotes Development of Colon Cancer,” *PLoS ONE*, vol. 7, no. 6, Jun. 2012.
[125] R. HUANG, G. WANG, Y. SONG, Q. TANG, Q. YOU, Z. LIU, Y. CHEN, Q. ZHANG, J. LI, S. MUHAMMAND, and X. WANG, “Colorectal cancer stem cell and chemoresistant colorectal cancer cell phenotypes and increased sensitivity to Notch pathway inhibitor,” *Mol. Med. Rep.*, vol. 12, no. 2, pp. 2417–2424, Aug. 2015.
[126] Y. Li, B. Xiao, S. Tu, Y. Wang, and X. Zhang, “Cultivation and identification of colon cancer stem cell-derived spheres from the Colo205 cell line,” *Braz. J. Med. Biol. Res.*, vol. 45, no. 3, pp. 197–204, Feb. 2012.
[127] H. Dolznig, C. Rupp, C. Puri, C. Haslinger, N. Schweifer, E. Wieser, D. Kerjaschki, and P. Garin-Chesa, “Modeling Colon Adenocarcinomas in Vitro,” *Am. J. Pathol.*, vol. 179, no. 1, pp. 487–501, Jul. 2011.

[128] S. V. Shmelkov, J. M. Butler, A. T. Hooper, A. Hormigo, J. Kushner, T. Milde, R. St. Clair, M. Baljevic, I. White, D. K. Jin, A. Chadburn, A. J. Murphy, D. M. Valenzuela, N. W. Gale, G. Thurston, G. D. Yancopoulos, M. D'Angelica, N. Kemeny, D. Lyden, and S. Rafii, "CD133 expression is not restricted to stem cells, and both CD133+ and CD133– metastatic colon cancer cells initiate tumors," *J. Clin. Invest.*, vol. 118, no. 6, pp. 2111–2120, Jun. 2008.
[129] P. Cammareri, A. Scopelliti, M. Todaro, V. Eterno, F. Francescangeli, M. P. Moyer, A. Agrusa, F. Dieli, A. Zeuner, and G. Stassi, "Aurora-A Is Essential for the Tumorigenic Capacity and Chemoresistance of Colorectal Cancer Stem Cells," *Cancer Res.*, vol. 70, no. 11, pp. 4655–4665, Jun. 2010.
[130] J. E. Carpentino, M. J. Hynes, H. D. Appelman, T. Zheng, D. A. Steindler, E. W. Scott, and E. H. Huang, "Aldehyde Dehydrogenase Expressing Colon Stem Cells Contribute to Tumorigenesis in the Transition from Colitis to Cancer," *Cancer Res.*, vol. 69, no. 20, pp. 8208–8215, Oct. 2009.
[131] L.-B. Weiswald, S. Richon, P. Validire, M. Briffod, R. Lai-Kuen, F. P. Cordelières, F. Bertrand, D. Dargere, G. Massonnet, E. Marangoni, B. Gayet, M. Pocard, I. Bieche, M.-F. Poupon, D. Bellet, and V. Dangles-Marie, "Newly characterised ex vivo colospheres as a three-dimensional colon cancer cell model of tumour aggressiveness," *Br. J. Cancer*, vol. 101, no. 3, pp. 473–482, Jul. 2009.
[132] I. A. M. Silva, "Evaluation of chemotherapeutic potential of natural extracts using 3D models of colon cancer," masterThesis, Faculdade de Ciências e Tecnologia, 2013.
[133] V. E. Santo, M. F. Estrada, S. P. Rebelo, S. Abreu, I. Silva, C. Pinto, S. C. Veloso, A. T. Serra, E. Boghaert, P. M. Alves, and C. Brito, "Adaptable stirred-tank culture strategies for large scale production of multicellular spheroid-based tumor cell models," *J. Biotechnol.*, vol. 221, pp. 118–129, Mar. 2016.
[134] X. Fan, N. Ouyang, H. Teng, and H. Yao, "Isolation and characterization of spheroid cells from the HT29 colon cancer cell line," *Int. J. Colorectal Dis.*, vol. 26, no. 10, pp. 1279–1285, Jun. 2011.
[135] M. Serra, C. Brito, C. Correia, and P. M. Alves, "Process engineering of human pluripotent stem cells for clinical application," *Trends Biotechnol.*, vol. 30, no. 6, pp. 350–359, Jun. 2012.
[136] M. Minekus, M. Alminger, P. Alvito, S. Ballance, T. Bohn, C. Bourlieu, F. Carrière, R. Boutrou, M. Corredig, D. Dupont, C. Dufour, L. Egger, M. Golding, S. Karakaya, B. Kirkhus, S. Le Feunteun, U. Lesmes, A. Macierzanka, A. Mackie, S. Marze, D. J. McClements, O. Ménard, I. Recio, C. N. Santos, R. P. Singh, G. E. Vegarud, M. S. J. Wickham, W. Weitschies, and A. Brodkorb, "A standardised static in vitro digestion method suitable for food - an international consensus," *Food Funct.*, vol. 5, no. 6, pp. 1113–1124, Jun. 2014.
[137] A. T. Serra, J. Poejo, A. A. Matias, M. R. Bronze, and C. M. M. Duarte, "Evaluation of Opuntia spp. derived products as antiproliferative agents in human colon cancer cell line (HT29)," *Food Res. Int.*, vol. 54, no. 1, pp. 892–901, Nov. 2013.
[138] M. N. Bravo, S. Silva, A. V. Coelho, L. V. Boas, and M. R. Bronze, "Analysis of phenolic compounds in Muscatel wines produced in Portugal," *Anal. Chim. Acta*, vol. 563, no. 1–2, pp. 84–92, Mar. 2006.
[139] M. Rousset, "The human colon carcinoma cell lines HT-29 and Caco-2: two in vitro models for the study of intestinal differentiation," *Biochimie*, vol. 68, no. 9, pp. 1035–1040, Sep. 1986.
[140] Y. Sambuy, I. D. Angelis, G. Ranaldi, M. L. Scarino, A. Stammati, and F. Zucco, "The Caco-2 cell line as a model of the intestinal barrier: influence of cell and culture-related factors on Caco-2 cell functional characteristics," *Cell Biol. Toxicol.*, vol. 21, no. 1, pp. 1–26, Jan. 2005.
[141] A. T. Serra, I. J. Seabra, M. E. M. Braga, M. R. Bronze, H. C. de Sousa, and C. M. M. Duarte, "Processing cherries (Prunus avium) using supercritical fluid technology. Part 1: Recovery of extract fractions rich in bioactive compounds," *J. Supercrit. Fluids*, vol. 55, no. 1, pp. 184–191, Nov. 2010.
[142] T. C. Chou and P. Talalay, "Quantitative analysis of dose-effect relationships: the combined effects of multiple drugs or enzyme inhibitors," *Adv. Enzyme Regul.*, vol. 22, pp. 27–55, 1984.
[143] T.-C. Chou, "Theoretical Basis, Experimental Design, and Computerized Simulation of Synergism and Antagonism in Drug Combination Studies," *Pharmacol. Rev.*, vol. 58, no. 3, pp. 621–681, Sep. 2006.
[144] "ALDEFLUOR™ Kit." [Online]. Available: http://www.stemcell.com/en/Products/All-Products/ALDEFLUOR-Kit.aspx. [Accessed: 26-Mar-2016].
[145] "RNeasy 96 Kit - QIAGEN Online Shop." [Online]. Available: https://www.qiagen.com/us/shop/sample-technologies/rna/rna-preparation/rneasy-96-kit/#orderinginformation. [Accessed: 21-Aug-2016].

[146] A. M. Balu, V. Budarin, P. S. Shuttleworth, L. A. Pfaltzgraff, K. Waldron, R. Luque, and J. H. Clark, “Valorisation of orange peel residues: waste to biochemicals and nanoporous materials,” *ChemSusChem*, vol. 5, no. 9, pp. 1694–1697, Sep. 2012.
[147] H. Pandith, X. Zhang, S. Thongpraditchote, Y. Wongkrajang, W. Gritsanapan, and S. J. Baek, “Effect of Siam weed extract and its bioactive component scutellarein tetramethyl ether on anti-inflammatory activity through NF-κB pathway,” *J. Ethnopharmacol.*, vol. 147, no. 2, pp. 434–441, May 2013.
[148] H. Pandith, X. Zhang, J. Liggett, K.-W. Min, W. Gritsanapan, and S. J. Baek, “Hemostatic and Wound Healing Properties of Chromolaena odorata Leaf Extract,” *ISRN Dermatol.*, vol. 2013, Aug. 2013.
[149] J. Wu, K. Liu, and X. Shi, “The anti-inflammatory activity of several flavonoids isolated from Murraya paniculata on murine macrophage cell line and gastric epithelial cell (GES-1),” *Pharm. Biol.*, vol. 54, no. 5, pp. 868–881, 2016.
[150] S. E. Nielsen, V. Breinholt, C. Cornett, and L. O. Dragsted, “Biotransformation of the citrus flavone tangeretin in rats. Identification of metabolites with intact flavane nucleus,” *Food Chem. Toxicol. Int. J. Publ. Br. Ind. Biol. Res. Assoc.*, vol. 38, no. 9, pp. 739–746, Sep. 2000.
[151] C. Ma, J. Zheng, T. Warnick, S. Leschine, and H. Xiao, “Biotransformation of Polymethoxyflavones by Mouse and Human Colonic Microflora,” *FASEB J.*, vol. 27, no. 1 Supplement, pp. 1056.10–1056.10, Apr. 2013.
[152] M. Kim, N. Kim, and J. Han, “Metabolism of Kaempferia parviflora polymethoxyflavones by human intestinal bacterium Bautia sp. MRG-PMF1,” *J. Agric. Food Chem.*, vol. 62, no. 51, pp. 12377–12383, Dec. 2014.
[153] S. Li, Z. Wang, S. Sang, M.-T. Huang, and C.-T. Ho, “Identification of nobiletin metabolites in mouse urine,” *Mol. Nutr. Food Res.*, vol. 50, no. 3, pp. 291–299, Mar. 2006.
[154] R. H. Liu, “Health benefits of fruit and vegetables are from additive and synergistic combinations of phytochemicals,” *Am. J. Clin. Nutr.*, vol. 78, no. 3, p. 517S–520S, Sep. 2003.
[155] N. Tao, Y. Liu, and M. Zhang, “Chemical composition and antimicrobial activities of essential oil from the peel of bingtang sweet orange (Citrus sinensis Osbeck),” *Int. J. Food Sci. Technol.*, vol. 44, no. 7, pp. 1281–1285, Jul. 2009.
[156] K. N. Chidambara Murthy, G. K. Jayaprakasha, and B. S. Patil, “D-limonene rich volatile oil from blood oranges inhibits angiogenesis, metastasis and cell death in human colon cancer cells,” *Life Sci.*, vol. 91, no. 11–12, pp. 429–439, Oct. 2012.
[157] S. Kawaii, Y. Tomono, E. Katase, K. Ogawa, and M. Yano, “Antiproliferative Activity of Flavonoids on Several Cancer Cell Lines,” *Biosci. Biotechnol. Biochem.*, vol. 63, no. 5, pp. 896–899, 1999.
[158] S. Kawaii, T. Ikuina, T. Hikima, T. Tokiwano, and Y. Yoshizawa, “Relationship between Structure and Antiproliferative Activity of Polymethoxyflavones towards HL60 Cells,” *Anticancer Res.*, vol. 32, no. 12, pp. 5239–5244, Dec. 2012.
[159] G. Luo, X. Guan, and L. Zhou, “Apoptotic effect of citrus fruit extract nobiletin on lung cancer cell line A549 in vitro and in vivo,” *Cancer Biol. Ther.*, vol. 7, no. 6, pp. 966–973, Jun. 2008.
[160] N. Charoensinphon, “Inhibition of Lung Carcinogenesis by Polymethoxyflavones,” *Dissertations*, Sep. 2013.
[161] Y. Dong, G. Ji, A. Cao, J. Shi, H. Shi, J. Xie, and D. Wu, “[Effects of sinensetin on proliferation and apoptosis of human gastric cancer AGS cells],” *Zhongguo Zhong Yao Za Zhi Zhongguo Zhongyao Zazhi China J. Chin. Mater. Medica*, vol. 36, no. 6, pp. 790–794, Mar. 2011.
[162] N. Yoshimizu, Y. Otani, Y. Saikawa, T. Kubota, M. Yoshida, T. Furukawa, K. Kumai, K. Kameyama, M. Fujii, M. Yano, T. Sato, A. Ito, and M. Kitajima, “Anti-tumour effects of nobiletin, a citrus flavonoid, on gastric cancer include: antiproliferative effects, induction of apoptosis and cell cycle deregulation,” *Aliment. Pharmacol. Ther.*, vol. 20, pp. 95–101, Jul. 2004.
[163] W. Hwang, M. Yang, M. Tsai, H. Lan, S. Su, S. Chang, H. Teng, S. Yang, Y. Lan, S. Chiou, and H. Wang, “SNAIL Regulates Interleukin-8 Expression, Stem Cell–Like Activity, and Tumorigenicity of Human Colorectal Carcinoma Cells,” *Gastroenterology*, vol. 141, no. 1, pp. 279–291.e5, Jul. 2011.
[164] S. He, D. Nakada, and S. J. Morrison, “Mechanisms of Stem Cell Self-Renewal,” *Annu. Rev. Cell Dev. Biol.*, vol. 25, no. 1, pp. 377–406, 2009.
[165] L. Du, Y.-J. Li, M. Fakih, R. L. Wiatrek, M. Duldulao, Z. Chen, P. Chu, J. Garcia-Aguilar, and Y. Chen, “Role of SUMO activating enzyme in cancer stem cell maintenance and self-renewal,” *Nat. Commun.*, vol. 7, p. 12326, Jul. 2016.

[166] X. CHEN, B. WEI, X. HAN, Z. ZHENG, J. HUANG, J. LIU, Y. HUANG, and H. WEI, “LGR5 is required for the maintenance of spheroid-derived colon cancer stem cells,” *Int. J. Mol. Med.*, vol. 34, no. 1, pp. 35–42, Jul. 2014.
[167] S. Kuhn, M. Koch, T. Nübel, M. Ladwein, D. Antolovic, P. Klingbeil, D. Hildebrand, G. Moldenhauer, L. Langbein, W. W. Franke, J. Weitz, and M. Zöller, “A Complex of EpCAM, Claudin-7, CD44 Variant Isoforms, and Tetraspanins Promotes Colorectal Cancer Progression,” *Am. Assoc. Cancer Res.*, vol. 5, no. 6, pp. 553–567, Jun. 2007.
[168] M. E. Kidd, D. K. Shumaker, and K. M. Ridge, “The Role of Vimentin Intermediate Filaments in the Progression of Lung Cancer,” *Am. J. Respir. Cell Mol. Biol.*, vol. 50, no. 1, pp. 1–6, Jan. 2014.
[169] A. Amann, M. Zwierzina, G. Gamerith, M. Bitsche, J. M. Huber, G. F. Vogel, M. Blumer, S. Koeck, E. J. Pechriggl, J. M. Kelm, W. Hilbe, and H. Zwierzina, “Development of an Innovative 3D Cell Culture System to Study Tumour - Stroma Interactions in Non-Small Cell Lung Cancer Cells,” *PLOS ONE*, vol. 9, no. 3, p. e92511, Mar. 2014.
[170] Y.-E. Joo, “Expression of early growth response-1 in colorectal cancer and its relation to tumor cell proliferation and apoptosis,” *Oncol. Rep.*, Nov. 2013.
[171] A. Chen, J. Xu, and A. C. Johnson, “Curcumin inhibits human colon cancer cell growth by suppressing gene expression of epidermal growth factor receptor through reducing the activity of the transcription factor Egr-1,” *Oncogene*, vol. 25, no. 2, pp. 278–287, Sep. 2005.
[172] F. Varnat, A. Duquet, M. Malerba, M. Zbinden, C. Mas, P. Gervaz, and A. Ruiz i Altaba, “Human colon cancer epithelial cells harbour active HEDGEHOG-GLI signalling that is essential for tumour growth, recurrence, metastasis and stem cell survival and expansion,” *EMBO Mol. Med.*, vol. 1, no. 6–7, pp. 338–351, Sep. 2009.
[173] G. Chatel, C. Ganeff, N. Boussif, L. Delacroix, A. Briquet, G. Nolens, and R. Winkler, “Hedgehog signaling pathway is inactive in colorectal cancer cell lines,” *Int. J. Cancer*, vol. 121, no. 12, pp. 2622–2627, Dec. 2007.
[174] T. Akiyoshi, M. Nakamura, K. Koga, H. Nakashima, T. Yao, M. Tsuneyoshi, M. Tanaka, and M. Katano, “Gli1, downregulated in colorectal cancers, inhibits proliferation of colon cancer cells involving Wnt signalling activation,” *Gut*, vol. 55, no. 7, pp. 991–999, Jul. 2006.
[175] Z.-Q. Wu, T. Brabletz, E. Fearon, A. L. Willis, C. Y. Hu, X.-Y. Li, and S. J. Weiss, “Canonical Wnt suppressor, Axin2, promotes colon carcinoma oncogenic activity,” *Proc. Natl. Acad. Sci. U. S. A.*, vol. 109, no. 28, pp. 11312–11317, Jul. 2012.
[176] J. M. Lee, S. Dedhar, R. Kalluri, and E. W. Thompson, “The epithelial–mesenchymal transition: new insights in signaling, development, and disease,” *J. Cell Biol.*, vol. 172, no. 7, pp. 973–981, Mar. 2006.
[177] M. K. Jolly, B. Huang, M. Lu, S. A. Mani, H. Levine, and E. Ben-Jacob, “Towards elucidating the connection between epithelial–mesenchymal transitions and stemness,” *J. R. Soc. Interface*, vol. 11, no. 101, p. 20140962, Dec. 2014.
[178] A. G. De Herreros, S. Peiró, M. Nassour, and P. Savagner, “Snail family regulation and epithelial mesenchymal transitions in breast cancer progression,” *J. Mammary Gland Biol. Neoplasia*, vol. 15, no. 2, pp. 135–147, Jun. 2010.
[179] F. J. Rodriguez, L. J. Lewis-Tuffin, and P. Z. Anastasiadis, “E-cadherin’s dark side: possible role in tumor progression,” *Biochim. Biophys. Acta*, vol. 1826, no. 1, pp. 23–31, Aug. 2012.
[180] M. K. Jolly, M. Boareto, B. Huang, D. Jia, M. Lu, E. Ben-Jacob, J. N. Onuchic, and H. Levine, “Implications of the Hybrid Epithelial/Mesenchymal Phenotype in Metastasis,” *Front. Oncol.*, vol. 5, Jul. 2015.
[181] V. Koppaka, D. C. Thompson, Y. Chen, M. Ellermann, K. C. Nicolaou, R. O. Juvonen, D. Petersen, R. A. Deitrich, T. D. Hurley, and V. Vasiliou, “Aldehyde Dehydrogenase Inhibitors: a Comprehensive Review of the Pharmacology, Mechanism of Action, Substrate Specificity, and Clinical Application,” *Pharmacol. Rev.*, vol. 64, no. 3, pp. 520–539, Jul. 2012.
[182] Y. Li, T. Zhang, H. Korkaya, S. Liu, H.-F. Lee, B. Newman, Y. Yu, S. G. Clouthier, S. J. Schwartz, M. S. Wicha, and D. Sun, “Sulforaphane, a Dietary Component of Broccoli/Broccoli Sprouts, Inhibits Breast Cancer Stem Cells,” *Clin. Cancer Res. Off. J. Am. Assoc. Cancer Res.*, vol. 16, no. 9, pp. 2580–2590, May 2010.
[183] M. Kakarala, D. E. Brenner, H. Khorkaya, C. Cheng, K. Tazi, C. Ginestier, S. Liu, G. Dontu, and M. S. Wicha, “Targeting Breast Stem Cells with the Cancer Preventive Compounds Curcumin and Piperine,” *Breast Cancer Res. Treat.*, vol. 122, no. 3, pp. 777–785, Aug. 2010.
[184] E.-S. Scarpa and P. Ninfali, “Phytochemicals as Innovative Therapeutic Tools against Cancer Stem Cells,” *Int. J. Mol. Sci.*, vol. 16, no. 7, pp. 15727–15742, Jul. 2015.

[185] J. M. Hernandez, J. M. Farma, D. Coppola, A. Hakam, W. J. Fulp, D.-T. Chen, E. M. Siegel, T. J. Yeatman, and D. Shibata, “Expression of the Antiapoptotic Protein Survivin in Colon Cancer,” *Clin. Colorectal Cancer*, vol. 10, no. 3, pp. 188–193, Sep. 2011.
[186] H. Wang, X. Zhang, L. Wang, G. Zheng, L. Du, Y. Yang, Z. Dong, Y. Liu, A. Qu, and C. Wang, “Investigation of cell free BIRC5 mRNA as a serum diagnostic and prognostic biomarker for colorectal cancer,” *J. Surg. Oncol.*, vol. 109, no. 6, pp. 574–579, May 2014.
[187] K. Harada and G. R. Ogden, “An overview of the cell cycle arrest protein, p21WAF1,” *Oral Oncol.*, vol. 36, no. 1, pp. 3–7, Jan. 2000.
[188] A. Peper, “Aspects of the Relationship Between Drug Dose and Drug Effect,” *Dose-Response*, vol. 7, no. 2, pp. 172–192, Feb. 2009.
[189] J. A. Ludwig and J. N. Weinstein, “Biomarkers in Cancer Staging, Prognosis and Treatment Selection,” *Nat. Rev. Cancer*, vol. 5, no. 11, pp. 845–856, Nov. 2005.
[190] A. S. Jaiswal, B. P. Marlow, N. Gupta, and S. Narayan, “Beta-catenin-mediated transactivation and cell-cell adhesion pathways are important in curcumin (diferuylmethane)-induced growth arrest and apoptosis in colon cancer cells,” *Oncogene*, vol. 21, no. 55, pp. 8414–8427, Dec. 2002.
[191] P. Dandawate, S. Padhye, A. Ahmad, and F. H. Sarkar, “Novel strategies targeting cancer stem cells through phytochemicals and their analogs,” *Drug Deliv. Transl. Res.*, vol. 3, no. 2, pp. 165–182, Apr. 2013.
[192] R. Y. Odom, M. Y. Dansby, A. M. Rollins-Hairston, K. M. Jackson, and W. G. Kirlin, “Phytochemical induction of cell cycle arrest by glutathione oxidation and reversal by N-acetylcysteine in human colon carcinomacarcinoma cells,” *Nutr. Cancer*, vol. 61, no. 3, pp. 332–339, 2009.
[193] Y. J. Park, J. Wen, S. Bang, S. W. Park, and S. Y. Song, “[6]-Gingerol Induces Cell Cycle Arrest and Cell Death of Mutant p53-expressing Pancreatic Cancer Cells,” *Yonsei Med. J.*, vol. 47, no. 5, pp. 688–697, Oct. 2006.
[194] K. Sak, “Chemotherapy and dietary phytochemical agents,” *Chemother. Res. Pract.*, vol. 2012, p. 282570, 2012.
[195] K. Y. Cheah, G. S. Howarth, and S. E. P. Bastian, “Grape seed extract dose-responsively decreases disease severity in a rat model of mucositis; concomitantly enhancing chemotherapeutic effectiveness in colon cancer cells,” *PloS One*, vol. 9, no. 1, p. e85184, 2014.
[196] M. Fantini, M. Benvenuto, L. Masuelli, G. V. Frajese, I. Tresoldi, A. Modesti, and R. Bei, “In Vitro and in Vivo Antitumoral Effects of Combinations of Polyphenols, or Polyphenols and Anticancer Drugs: Perspectives on Cancer Treatment,” *Int. J. Mol. Sci.*, vol. 16, no. 5, pp. 9236–9282, Apr. 2015.
[197] J. Nautiyal, S. Banerjee, S. S. Kanwar, Y. Yu, B. B. Patel, F. H. Sarkar, and A. P. N. Majumdar, “Curcumin Enhances Dasatinib Induced Inhibition of Growth and Transformation of Colon Cancer Cells,” *Int. J. Cancer J. Int. Cancer*, vol. 128, no. 4, pp. 951–961, Feb. 2011.
[198] M. Shakibaei, A. Mobasheri, C. Lueders, F. Busch, P. Shayan, and A. Goel, “Curcumin Enhances the Effect of Chemotherapy against Colorectal Cancer Cells by Inhibition of NF-κB and Src Protein Kinase Signaling Pathways,” *PLOS ONE*, vol. 8, no. 2, p. e57218, Feb. 2013.
[199] V. Aires, E. Limagne, A. K. Cotte, N. Latruffe, F. Ghiringhelli, and D. Delmas, “Resveratrol metabolites inhibit human metastatic colon cancer cells progression and synergize with chemotherapeutic drugs to induce cell death,” *Mol. Nutr. Food Res.*, vol. 57, no. 7, pp. 1170–1181, Jul. 2013.
[200] M. Suganuma, A. Saha, and H. Fujiki, “New cancer treatment strategy using combination of green tea catechins and anticancer drugs,” *Cancer Sci.*, vol. 102, no. 2, pp. 317–323, Feb. 2011.
[201] M. Swaminathan, C. F. Chee, S. P. Chin, M. J. C. Buckle, N. A. Rahman, S. W. Doughty, and L. Y. Chung, “Flavonoids with M1 Muscarinic Acetylcholine Receptor Binding Activity,” *Molecules*, vol. 19, no. 7, pp. 8933–8948, Jun. 2014.
[202] “Pure chemical manufacturer: Extrasynthese, pure chemical for HPLC chromatography.” [Online]. Available: http://www.extrasynthese.com/. [Accessed: 22-Sep-2016].

6. Appendix

Appendix A – Structure of PMFs

Table 6.1 – Structure of the main compounds present in natural extracts of orange [210], [211].

Backbone structure of flavones	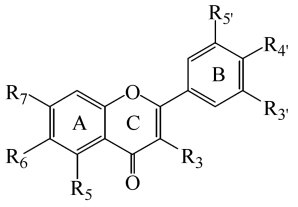
Nobiletin	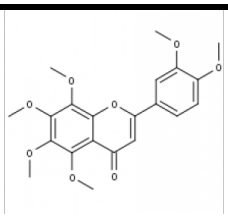
Sinensetin	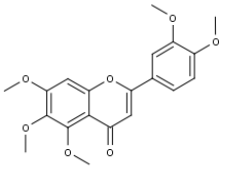
Tangeretin	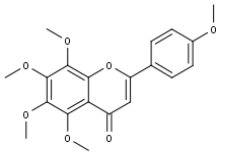
Scutellarein tetramethylether	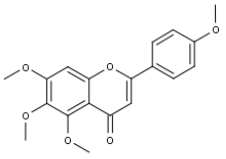

Appendix B – Cytotoxicity assay

Cytotoxicity assays were performed as described in section 2.3.3. Figure 6.1 shows the results obtained.

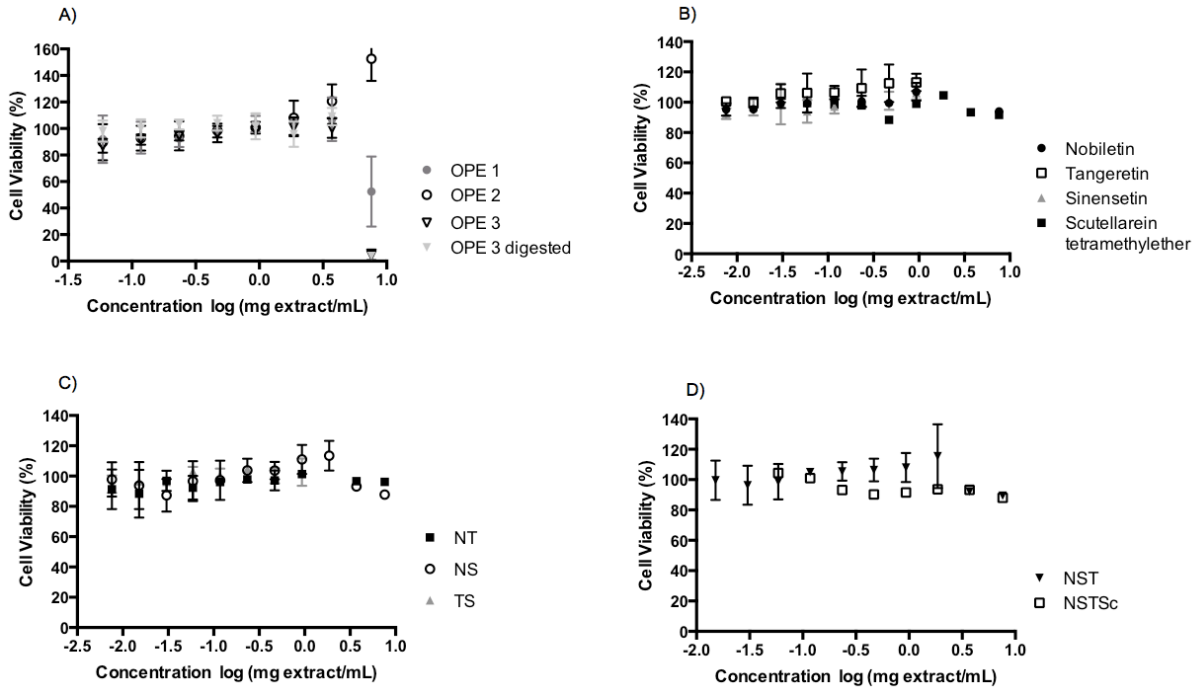

Figure 6.1 – Cytotoxicity assays using Caco-2 cell line for: A) several orange peel extracts; B) isolated PMFs; C) Combination of two PMFs; D) combination of three and four PMFs. Results were in mean ± SD (at least n=2).

OPE 1, OPE 3 and OPE 3 digested showed cytotoxicity at the highest concentration tested (7.5 mg extract/mL), however the EC50 values from the antiproliferative assays (sections 3.1 and 3.3.1) showed not having cytotoxicity in the Caco-2 cell model. PMFs did not show cytotoxicity for any concentration of each sample.

Appendix D

CI were calculated using the results from the antiproliferative assays (section 3.1) on Compusyn software and expressed as CI < 1 – synergism; CI > 1 – antagonism; 0.90 < CI < 1.10 – additive effects. Labels in green are the synergistic effect; in bold are the additive interactions; and the rest the antagonistic.

Table 6.2 – Combination Index from the combination between two PMFs. Legend: N = nobiletin; S = sinensetin; T = tangeretin; Sc = scutellarein tetramethylether.

				Combination Index (CI)		
[Nob] µM	[Sin] µM	[Tang] µM	[Scu] µM	NT	NS	TS
92.09	87.40	19.52	59.16	-	-	-
46.05	43.70	9.76	29.58	334.783	1.743	24.144
23.03	21.85	4.88	14.79	12.351	1.264	**0.709**
11.51	10.93	2.44	7.39	2.268	**0.955**	**0.291**
5.76	5.46	1.22	3.70	29.288	**0.591**	**0.460**

Table 6.3 – Combination Index from the possible combinations between three PMFs. Legend: N = nobiletin; S = sinensetin; T = tangeretin; Sc = scutellarein tetramethylether; + = compound added to a mixture of two other compounds.

				Combination Index (CI)			
[Nob] µM	[Sin] µM	[Tang] µM	[Scu] µM	NST	S+NT	T+NS	N+TS
92.09	87.40	19.52	59.16	-	-	-	-
46.05	43.70	9.76	29.58	672.270	1.384	670.387	**0.983**
23.03	21.85	4.88	14.79	57.449	**0.878**	57.076	**0.868**
11.51	10.93	2.44	7.39	3.137	**0.607**	3.504	**1.062**
5.76	5.46	1.22	3.70	1.427	**0.489**	4.851	2.924

Table 6.4 – Combination Index from the possible combinations between four PMFs. Legend: N = nobiletin; S = sinensetin; T = tangeretin; Sc = scutellarein tetramethylether; + = compound/s added to a mixture of two or three other compounds.

				Combination Index (CI)				
[Nob] µM	[Sin] µM	[Tang] µM	[Scu] µM	**NSTSc**	**NST+Sc**	**NT+S+Sc**	**NS+T+Sc**	**TS+N+Sc**
92.09	87.40	19.52	59.16	3843.920	2.019	2.759	3842.580	1.768
46.05	43.70	9.76	29.58	652.809	1.340	1.611	652.032	1.213
23.03	21.85	4.88	14.79	43.888	**1.144**	**1.082**	43.543	8.934
11.51	10.93	2.44	7.39	4.039	**0.936**	**0.705**	4.248	**1.052**
5.76	5.46	1.22	3.70	31.132	19.477	3.204	1909.490	22719.600